GENERAL ATOMIC

GA-A13510
UC-77

THORIUM UTILIZATION PROGRAM

QUARTERLY PROGRESS REPORT FOR THE PERIOD ENDING MAY 31, 1975

Prepared under
Contract AT(04-3)-167
Project Agreement No. 53
for the San Francisco Operations Office
U.S. Energy Research and Development Administration

DATE PUBLISHED: AUGUST 15, 1975

Printed in the United States of America
Available from
National Technical Information Service
U.S. Department of Commerce
5285 Port Royal Road
Springfield, Virginia 22161
Price: Printed Copy $7.60; Microfiche $2.25

DISCLAIMER

GA-A13510
UC-77

THORIUM UTILIZATION PROGRAM

QUARTERLY PROGRESS REPORT FOR THE PERIOD ENDING MAY 31, 1975

Prepared under
Contract AT(04-3)-167
Project Agreement No. 53
for the San Francisco Operations Office
U.S. Energy Research and Development Administration

GENERAL ATOMIC PROJECT 3225

DATE PUBLISHED: AUGUST 15, 1975

QUARTERLY REPORT SERIES*

GA-A13178 - June 1974 through August 1974

GA-A13255 - September 1974 through November 1974

GA-A13366 - December 1974 through February 1975

*Prior to GA-A13178, the Thorium Utilization Program was reported in the Base Program Quarterly Progress Report.

ABSTRACT

This publication is the fourth of a quarterly series presenting results of work performed under the National HTGR Fuel Recycle Program (also known as the Thorium Utilization Program) at General Atomic Company. Results of work on this program were previously included in a quarterly series on the HTGR Base Program.

The work reported includes the development of unit processes and equipment for reprocessing of High-Temperature Gas-Cooled Reactor (HTGR) fuel and the design and development of an integrated line to demonstrate the head end of HTGR reprocessing using unirradiated fuel materials. Work is also described on the evaluation of alternate techniques for fuel reprocessing to surmount possible operating problems with the reference flow sheet and the development of the conceptual design of a target recycle facility to identify the requirements of large-scale recycle of HTGR fuels.

INTRODUCTION

This report covers the work performed by General Atomic Company under U.S. Energy Research and Development Administration Contract AT(04-3)-167, Project Agreement No. 53. The work done under this project agreement is part of the program for development of recycle technology for High-Temperature Gas-Cooled Reactor (HTGR) fuels described in the "National HTGR Fuel Recycle Development Program" (ORNL 4702).

The objective of the program is to provide the necessary technology, development, engineering, and demonstration of the steps required in the economic recycle of HTGR fuels utilizing thorium as a fertile material. Work at General Atomic Company is concentrating on the development of reprocessing methods (subtask 110 of the National Program), engineering and economic studies (subtask 310), and the application of recycle technology to the conceptual design of a large-scale recycle facility (subtask 320).

The objectives of subtask 110, Reprocessing Development, are to develop the necessary technology for the construction and operation of a prototype reprocessing facility which will process irradiated fuel materials and to provide the capability for commercial recycle of HTGR fuels. The output of this subtask includes (1) definition of process flow sheets, (2) development of equipment components, and (3) definition of operating data.

The objectives of subtask 310 are to guide the development program from the viewpoint of overall recycle needs and to obtain an economical HTGR fuel recycle method for early recovery and use of bred U-233. Alternate methods and options for reprocessing and refabrication are evaluated, and recommendations are made for possible further experimental development.

The objectives of subtask 320 are to develop a conceptual design of a target-size recycle plant for the reprocessing and refabrication of HTGR fuels and to use the results developed in the preparation of this design to guide the development work. The output of this task is in the form of design criteria, reference process flow sheets, and equipment sizing for a target recycle facility.

CONTENTS

FIGURES

FIGURES (Continued)

FIGURES (Continued)

TABLES

TABLE (Continued)

1. SUMMARY

The development program for reprocessing continues to be heavily oriented toward the design and construction of a prototype head-end line. Design and procurement of the multistage crushing system, the primary and secondary fluidized bed burners, and pneumatic transport systems connecting these unit operations are continuing. Progress made in the evolution of these designs is reported.

Experimental studies have continued on pneumatic transport systems presently installed and operating and preliminary data on particle breakage is reported. Separation tests have been performed on various fuel particle mixtures including those containing broken SiC shells. Operating parameters to obtain greater than 98% separation have been defined.

The 20-cm primary burner has been operated to verify a perforated conical gas distributor design. The dense-phase pneumatic transport system for graphite fines recycle is being installed for testing during the next quarter.

Test runs were made on the 20-cm primary fluidized-bed burner that emphasized performance during the initial period of the operating cycle, during which time the high bed graphite concentration and large mean particle size impose the most severe operating conditions. The operational response of the perforated conical distributor to an increase in fresh feed size was studied. Final bed carbon burnout, product removal, and pneumatic product transport were also analyzed. All components of the dense-phase graphite fines recycle system for the 20-cm primary burner have arrived and installation is proceeding.

Preliminary results from studies of heat transfer and fluidization of primary burner material in the induction-heated 10-cm secondary burner vessel indicate a possibility that the minimum fluidization velocity of the large (>500 μm) material does not decrease with increasing temperature as predicted by standard correlations.

Ten leaching runs were made during the quarter. Runs 97 and 98 were shakedown runs of the leaching equipment after all equipment in the leaching room was rearranged as a result of installation of the evaporator stripper and the insols dryer. Runs 99 and 100 were made to check out an air-lift sampling system. Equipment problems led to the termination of Run 101 without data collection. Analytical data on runs 102, 103, 104, 105, and 106 are not complete; the results will be included in the next quarterly report.

A series of tests has been started to determine the feasibility and characteristics of using steam jet ejectors as a method of removing the product slurry from experimental and commercial dissolvers. The effect of the sparge rate on the transfer characteristics has been determined in this first set of runs.

Nine runs were made with the 12-in. solid-bowl centrifuge to determine the separation efficiency as a function of the feed rate and the rpm of the centrifuge for SiC hulls from a 1.3 specific gravity $NaNO_3$ solution. Analysis of data from the first six runs indicates that better than 99% separation efficiency can be obtained.

Eleven insols dryer runs were conducted during the quarter. The objective of these runs was shakedown testing of the insols dryer system and initial data acquisition.

Five feed adjustment runs for feed to the solvent extraction system were conducted using the batchwise mode of operation. The primary objectives of these runs were shakedown testing of the newly installed system and initial data acquisition.

Information gained from shakedown tests led to some modifications in the equipment. Analytical data obtained from successfully completed runs indicate that the system produces an acid deficient product. The first series of experimental runs will determine the effect of the steam stripping rate at a constant boiling point (135°C) on the acidity of the final product.

Eight solvent extraction tests were completed during the quarter. The flowsheets investigated relate to HTGR fuel reprocessing and the Idaho HTGR fuel reprocessing pilot plant. The data are complete for Runs 17, 18, 24, and 25 and the results of these runs are reported. The data on the other four runs are not complete as yet. The runs reported here were the first made in the expanded solvent extraction system of the pilot plant. Each of the runs used the extraction and partition flowsheet. Solvent degradation simulation studies were begun in this run series.

Construction of the control room and platform extensions for installation of the head-end reprocessing prototype line was completed. A description of this facility construction is given.

2. FUEL ELEMENT CRUSHING

2.1. UNIFRAME PROTOTYPE FUEL ELEMENT SIZE REDUCTION SYSTEM

2.1.1. Introduction

A size reduction system, designated UNIFRAME (Fig. 2-1), has been proposed for reducing spent HTGR fuel and control rod elements to a suitable feed for fluidized-bed burning to separate the fuel and graphite for subsequent fissile material recovery. The design and procurement of a full-scale prototype of this system is under way.

The UNIFRAME system comprises five major equipment items, arranged in an array that utilizes gravity flow, eliminates the need for intra-equipment material transport devices, and provides a continuous size reduction process without recycle.

The major equipment items are:

1. Primary crusher: an overhead eccentric jaw crusher for reducing the elements to ≤6-in. ring-sized fragments.

2. Secondary crusher: an overhead eccentric jaw crusher for further reduction of the fragments to ≤2-in. ring-sized fragments.

3. Tertiary crusher: a double-roll crusher for final reduction of the fragments to ≤3/16-in. ring-sized product.

4. Screener: a vibratory screener-separator for separating the acceptable product from any oversized fragments.

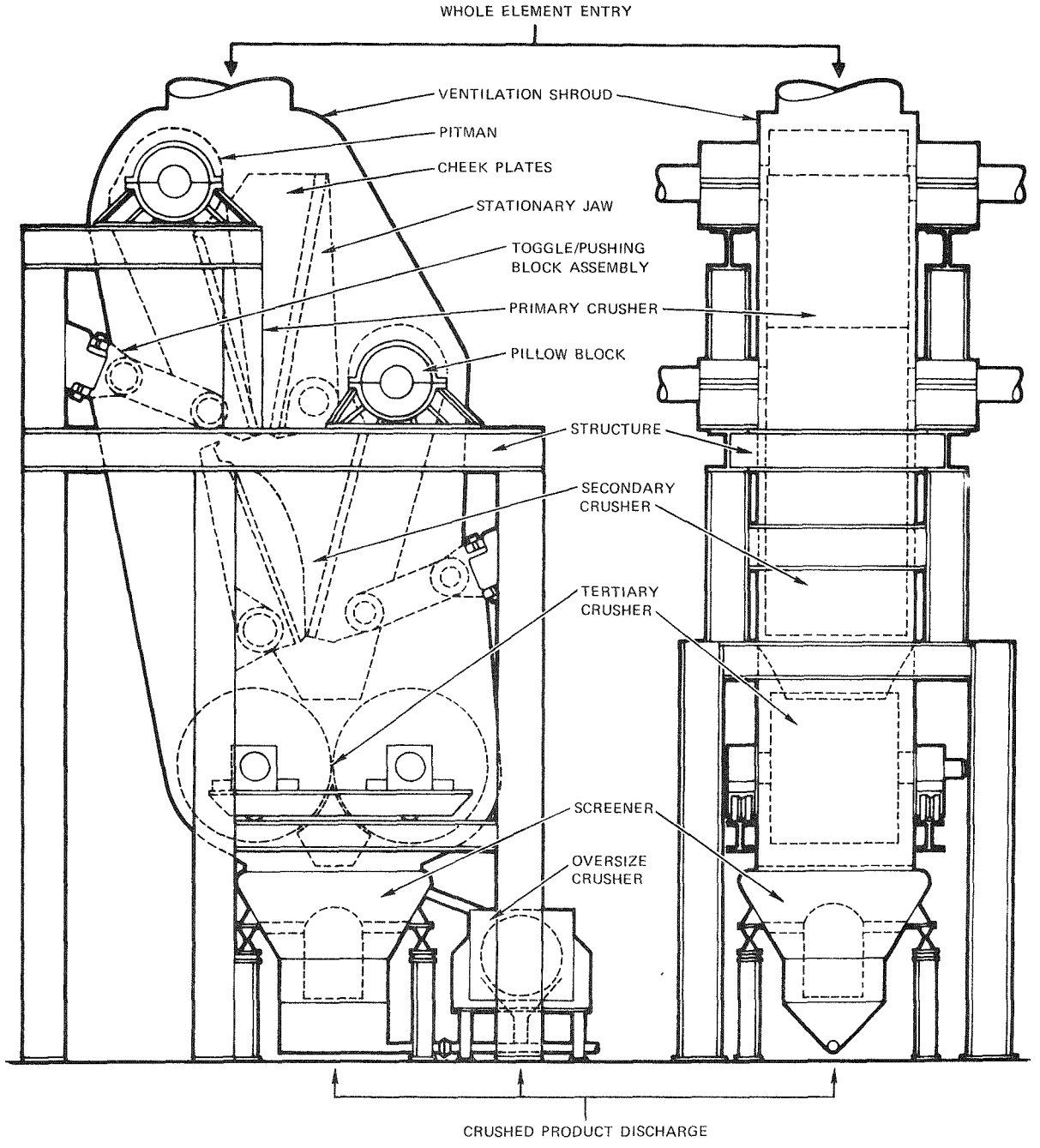

Fig. 2-1. UNIFRAME size reduction system

5. Oversize crusher: an eccentrically mounted single-roll crusher for reduction of oversize fragments to acceptable product size.

The components of the UNIFRAME system have been categorized into five subsystems to provide a logical plan for the design efforts. These subsystems are:

1. Structural: the special framework replacing standard machine frames to enable an efficient array of the equipment.

2. Ventilation: the enclosure that provides containment and collection of radioactive materials and dusts while minimizing the surfaces exposed.

3. Lubrication: the standard and special lubrication and bearings for equipment that make it more reliable and compatible with the radioactive environment and the remote operation requirements.

4. Drive: the standard and special drive components required to make the UNIFRAME system compatible with remote operation requirements and the radioactive environment.

5. Mechanical: the standard and special components required to make the major equipment items compatible with the structural, ventilation, and remote operation requirements.

2.1.2. Documentation

As the design of the UNIFRAME progresses, continuing formal documentation will be provided as an information exchange for Title I and Title II design phases of the proposed reprocessing demonstration facility at Allied Chemical Company, Idaho Facilities.

To date, the "Process Design Criteria - Fuel Element Size Reduction System" (document DC-521001, Issue A) has been issued, and the "Equipment

Design Criteria - Fuel Element Size Reduction System" (document DC-521002, Issue A) has been written and is being reviewed.

2.1.3. Current Status

Standard parts for the primary and secondary jaw crusher pitman assemblies (pitman castings, eccentric shafts, flywheels, and internal components) have been ordered. The pitman casting design was modified to accomodate a specially designed toggle (see Fig. 2-1).

The toggle/pushing block assembly design is 50% completed. The requirements and improvements incorporated in the design include: (1) compatibility with the ventilation requirements, (2) minimization of the number of parts in the assembly, (3) elimination of the tension rod and spring assembly, and (4) improved reliability.

Designs for the primary crusher pitman wear and cheek plates are complete and the drawings are being checked prior to release for approval.

The pillow blocks for the primary and secondary crushers are interchangeable to reduce spare part requirements and to provide ease in maintenance. The design is complete (Fig. 2-2), and a purchase requisition has been issued.

The stationary jaw and cheek plates for the primary crusher (Fig. 2-1) have been designed and the drawings have been released for approval. The design of remotely removable anchor blocks for the stationary jaw assembly is 60% complete.

Construction of the foundation has begun. The hole has been dug to accommodate the 12.5-ft-long by 10.5-ft-wide by 5-ft-deep pad required to anchor the UNIFRAME system.

Computer analysis of the UNIFRAME structure is complete. Four analyses were considered: (1) static, (2) mode shapes and frequencies, (3) response

NOTES:

1. REMOVE BURRS & SHARP EDGES.
2. DIMENSIONS & TOLERANCES PER ANSI Y14.5
3. FILLET WELD TO BE ¼ TYP EXCEPT AS NOTED.
4. WELDS TO BE INSPECTED PER DIST COMM. PRACTICE.
5. WELD SURFACES, CONTOURS AND JOINTS TO BE SMOOTH AND FREE FROM UNDERCUTS, OVERLAPS, ABRUPT RIDGES OR VALLEYS.
6. STRESS RELIEVE WELDED ASSY BEFORE MACHINING.
7. - CARR-LANE COCHRAN & CO. 7951 NORTH AVE., LEMON GROVE, CA.
8. - HEAT TREAT ROCKWELL 'C' 50/55.

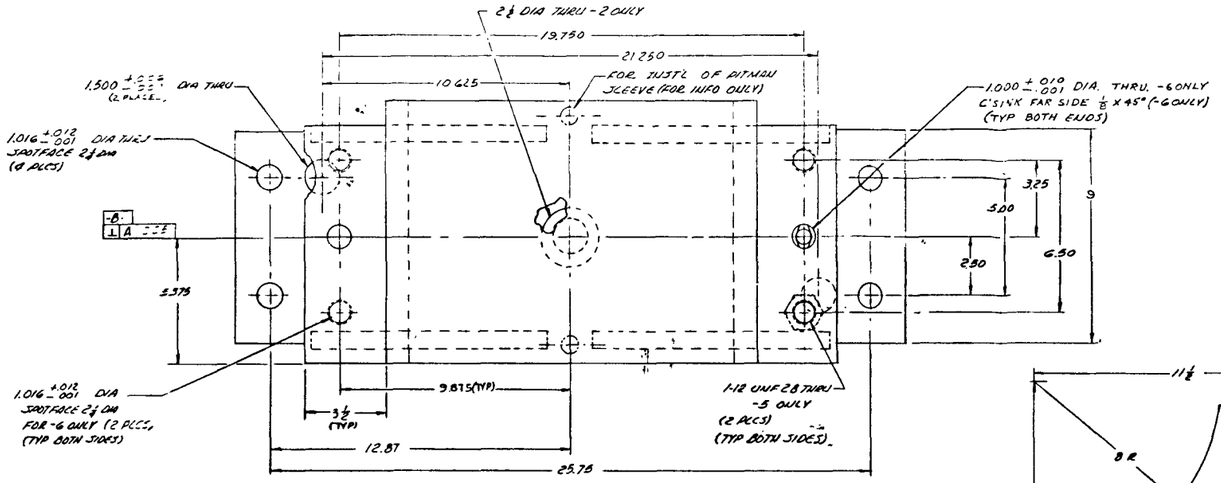

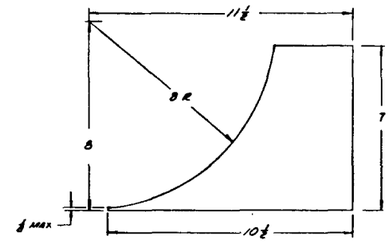

④

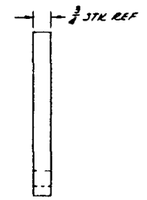

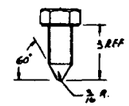

⑨

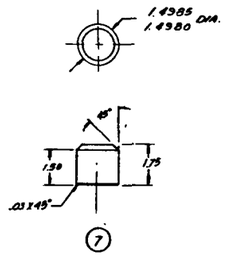

⑦

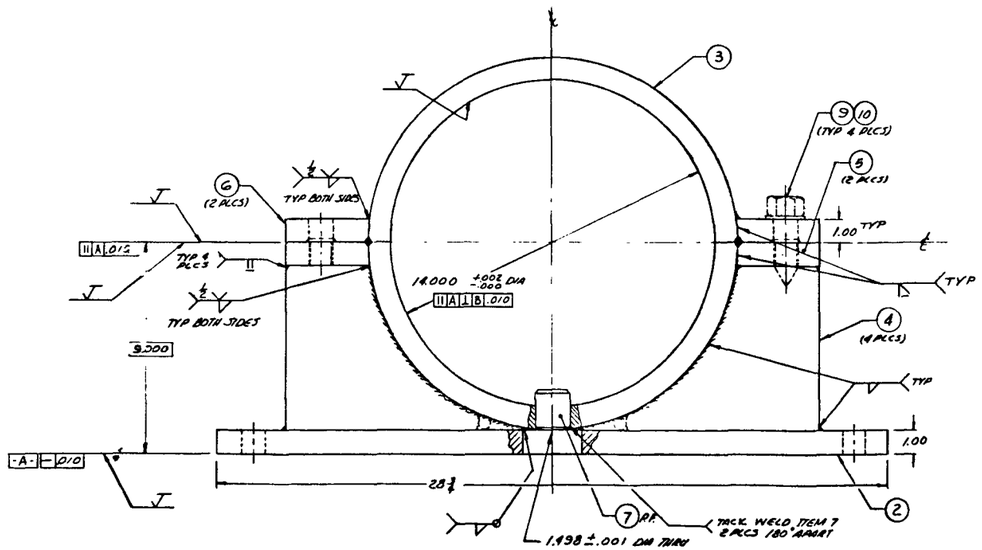

(-1) PILLOW BLOCK ASSY.

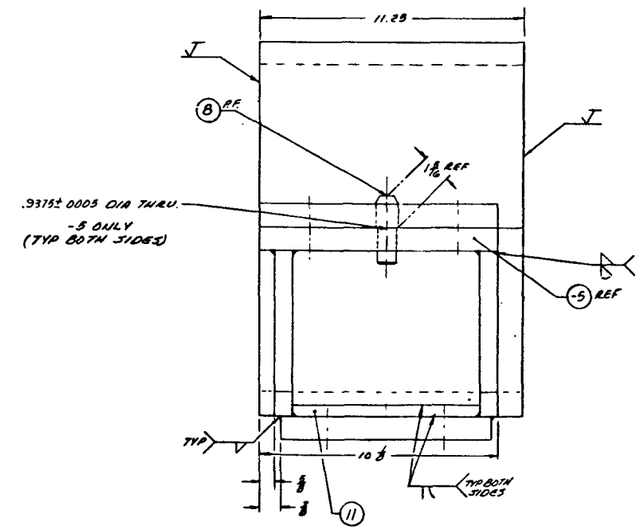

Fig. 2-2. Pillow block assembly for primary and secondary crushers

history, and (4) seismic. These analyses will be repeated when the equipment designs have been sufficiently detailed to ensure the exact dimensions of the structural components.

The rolls, pillow blocks, and drive gears for the tertiary double-roll crusher have been ordered.

Discussions with screener manufacturers on the axisymmetric screener are completed, the bids have been reviewed, and the purchase order for design and fabrication has been issued.

The purchase order for an 8-in.-wide by 8-in.-diameter Centerol crusher, manufactured by the Joy Manufacturing Company, has been issued. This standard crusher with special inlet and discharge chutes will comprise the UNIFRAME oversize crusher system.

3. SOLIDS HANDLING

3.1. PNEUMATIC TRANSPORT

Transfer of material between unit operations in the head-end reprocessing system will be by pneumatic transport. Investigation of vacuum pneumatic transport systems began in 1973 for the purpose of evaluating the conveyance of product streams. Vacuum transport was determined to be the best conveyance method for radioactive materials. Any leakage in the piping loop will be toward the negative pressure side and thus internal. This eliminates the potential hazard posed by pressure pneumatic systems in the event of a leak.

Three separate pilot plant systems were operated to demonstrate the utility of vacuum pneumatic transport and to obtain design information:

1. System A: crusher to primary burner.
2. System B: primary burner to air classifier.
3. System C: secondary burner to leachers.

Each of the above systems includes a positive displacement pump, stainless steel transfer lines, a suitable material pickup device, and a product hopper as supplied by VAC-U-MAX.

Although installation of the piping systems provided experience with actual process material, the length of time for material transfer was not sufficient to obtain parametric data for use in subsequent designs. Information needed for design of the prototype system is therefore being obtained with a separate experimental pneumatic transport unit. Solids to be

studied in the experimental schedule include (1) crushed graphite (-3/16-in. ring size), (2) primary burner fines, (3) secondary burner product, (4) fuel particles, and (5) fresh feed.

3.1.1. Pilot Plant Systems

3.1.1.1. System A: Crusher to Primary Burner

Crusher product (-3/16-in. ring size) is transported to the 30-ft^3 primary burner feed hopper via approximately 40 ft of 1-1/2-in. stainless steel tubing. A schematic drawing of this system is shown in Fig. 3-1. This system is intended as a loading aid for filling the 20-cm primary burner feed hopper. The material pickup connection is 36 in. of flexible tubing, which can be inserted into drums of the feed material.

3.1.1.2. System B: Primary Burner to Air Classifier

The purpose of this system is to transport the SiC coated particles and residual graphite from the 20-cm primary burner to the air classifier feed hopper. The initial configuration of this system included approximately 65 ft of transport piping connected to a collection hopper. The material entrance to the hopper consisted of an elbow welded to the vessel and directed perpendicularly to the opposite wall, as shown in Fig. 3-2a.

A test of this system revealed significant fuel particle breakage. A feed rate of 5 lb/min (total sample size = 1.1 lb) with a superficial air velocity in the transport line of 200 ft/sec yielded 65% breakage. In order to obtain a substantial reduction in particle breakage, changes were made in the orientation of the bunker entry from perpendicular to tangential (Fig. 3-2b).

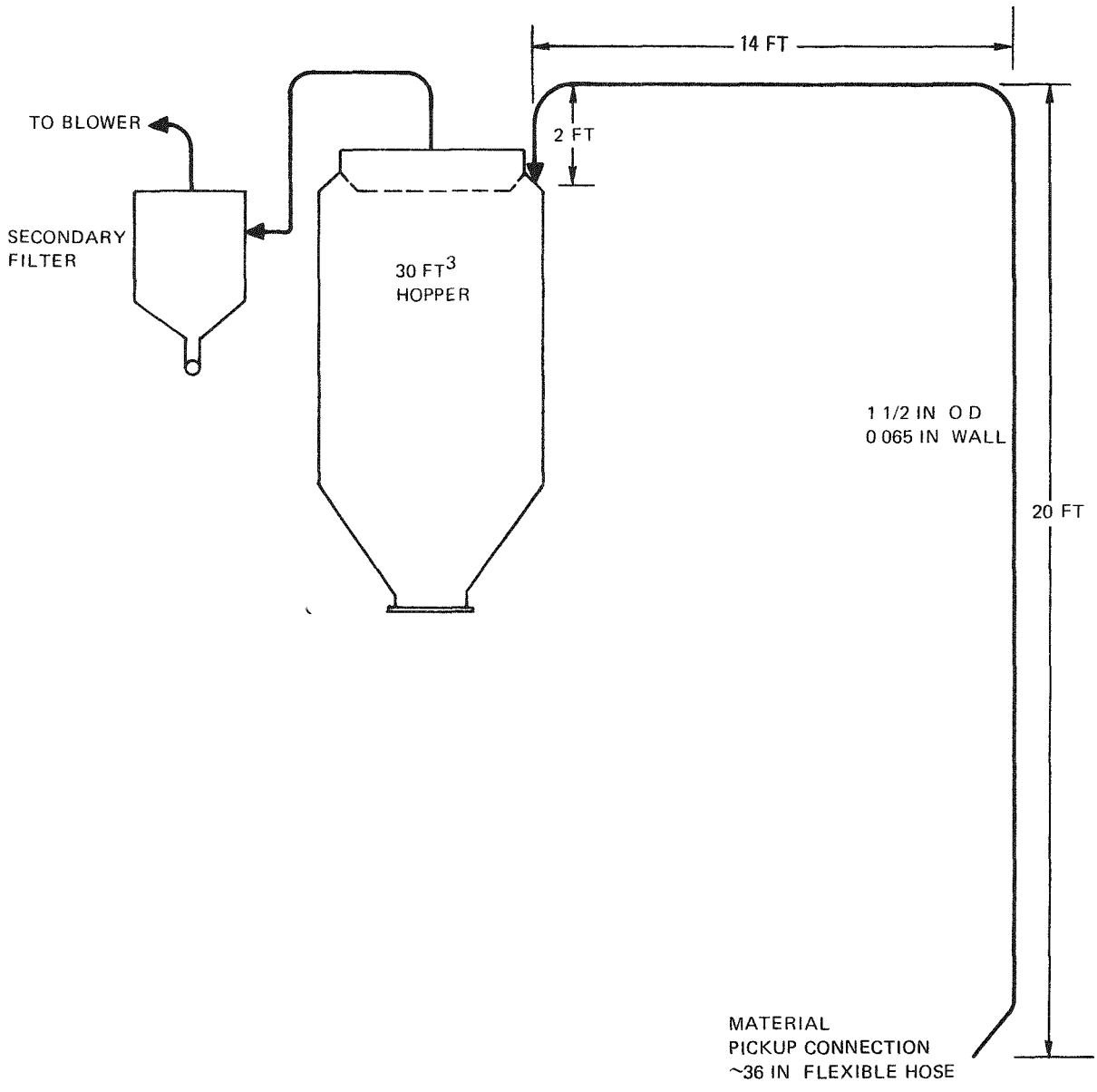

Fig. 3-1. System A, primary burner feed

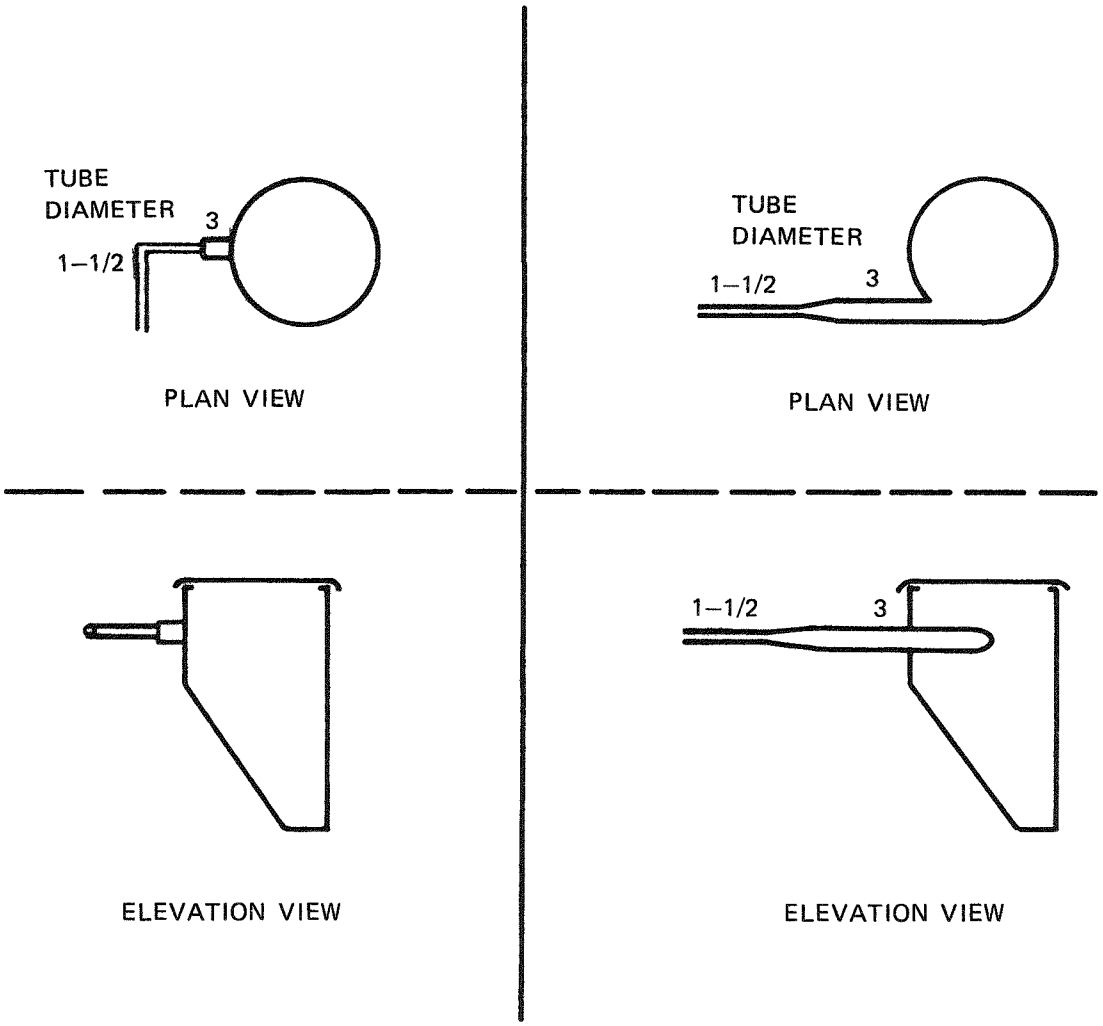

Fig. 3-2. System B, 20-cm primary burner product bunker

The revised system configuration is illustrated in Fig. 3-3. Particle breakage tests at various loading rates and feeding configurations have been performed with the new configuration providing the data shown in Figs. 3-4 and 3-5. These figures relate the data describing particle breakage as a function of loading for two inlet configurations. The following observations can be made from these graphs:

1. The percentage breakage was less for the obtuse feeding configuration (Fig. 3-4) since the normal entry (Fig. 3-5) of both particles and gas causes the particles to bounce off the bottom of the tee before being transported.

2. Different sample amounts at similar feed rates show less breakage for the larger samples. This arises from the dispersion of the leading and trailing edges, which allows more interaction between the gas and particle flows and contributes to particle attrition. Hence, the attrition is a larger weight percent of the smaller samples.

3. Breakage increases for samples transported more than once due to the SiC coating of the particles being fractured but not broken in the preceding run. Since an all-particle system is transported only once before classification, this phenomenon has no impact on crossover.

Future experimental plans for this system include the testing of a carrier gas removal system (Fig. 3-6). The inertial filter is a sintered metal filter encased in a housing. The material and the carrying fluid flow through the inside of the filter tube and a portion of the carrying fluid is withdrawn through the tube. It is believed that much of the particle breakage occurs through energy dissipation with the wall of the collection hopper. The concept of the inertial filter is to reduce the particle velocity, hence energy, by removing part of the carrying gas but not to the extent of causing saltation inside the filter tube.

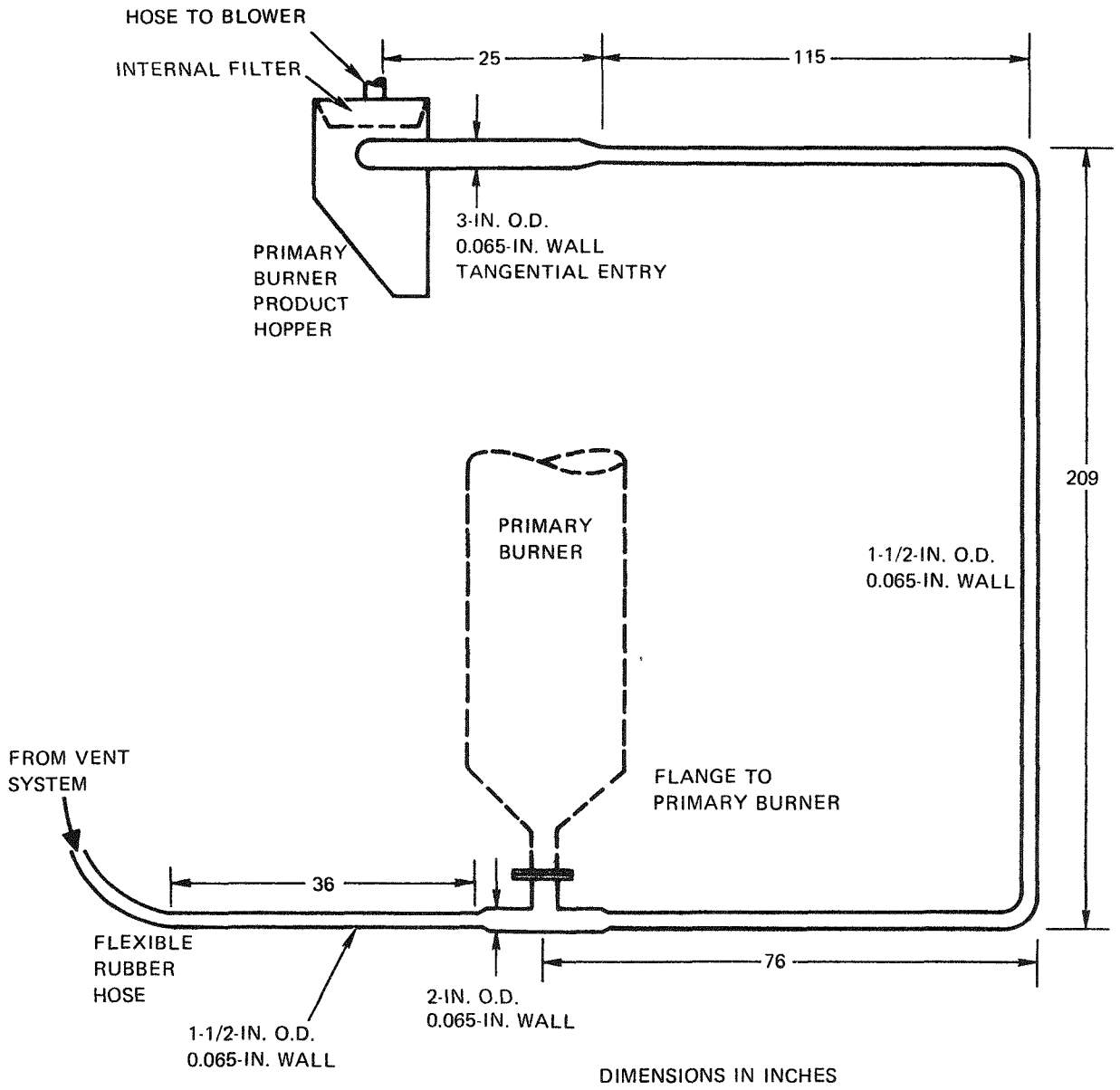

Fig. 3-3. System B, 20-cm primary burner product transport

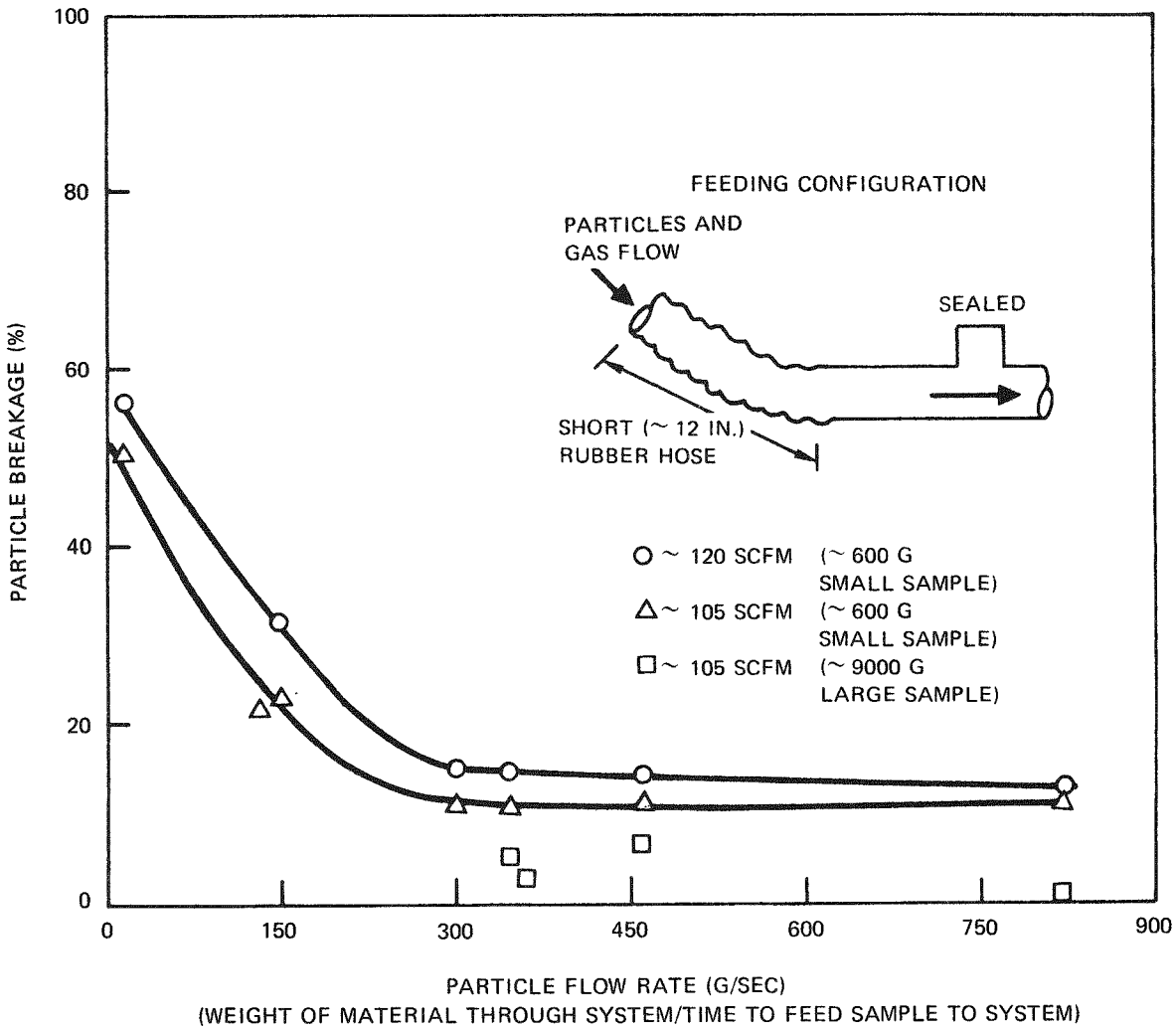

Fig. 3-4. System B, particle breakage versus solids flow rate for obtuse particle entry

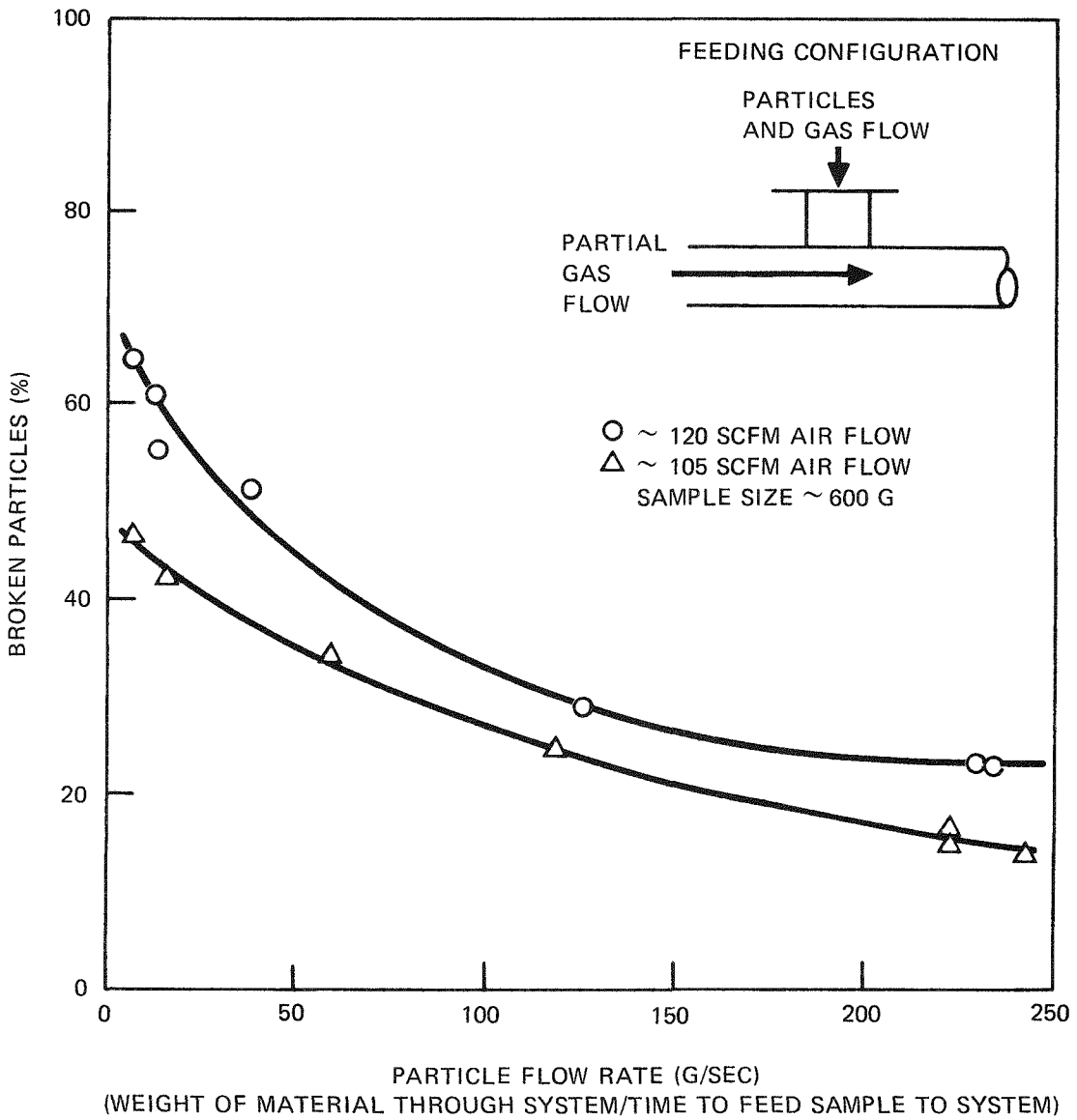

Fig. 3-5. System B, particle breakage versus solids flow rate for normal particle entry

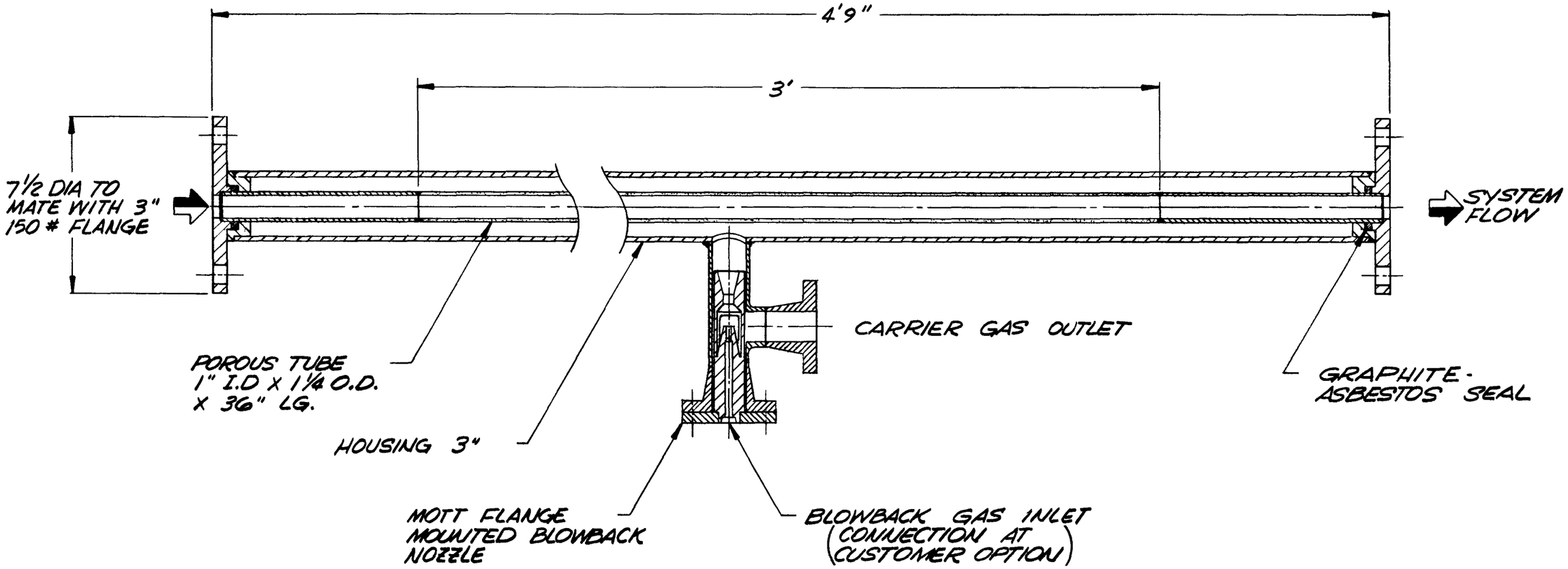

Fig. 3-6. Carrier gas removal system

3.1.1.3. System C: Secondary Burner to Leachers

The purpose of this system is to transport the broken SiC shells and ThO_2 powder product from the secondary burner to a receiver hopper. Material is transferred through approximately 35 ft of 1-1/2-in.-diameter tubing to a 1.5-ft^3 capacity hopper, as shown in Fig. 3-7.

A pneumatically operated valve flush-mounted with the secondary burner inside wall empties the bed during transport. Successful operation of this valve, without plugging of the transport line, requires an initial opening stop on the actuator to reduce the flow rate of solids through the valve to 11 lb/min.

This system has successfully demonstrated the use of pneumatic transport for secondary burner product. Further testing of secondary burner product will be done on the pneumatic transport test apparatus to complete the work in this area.

3.1.2. Pneumatic Transport Test System

An experimental pneumatic transport system, separate from the equipment associated with the pilot plant facility, has been assembled to obtain information on equipment operation and the effects of process variables. The system as shown in Fig. 3-8 is capable of testing a variety of equipment and modes of operation. The experimental system consists of six basic subsystems:

1. Material feed vessel
2. Material feeder
3. Transport piping
4. Filter vessel
5. Material receiver
6. Positive displacement blower

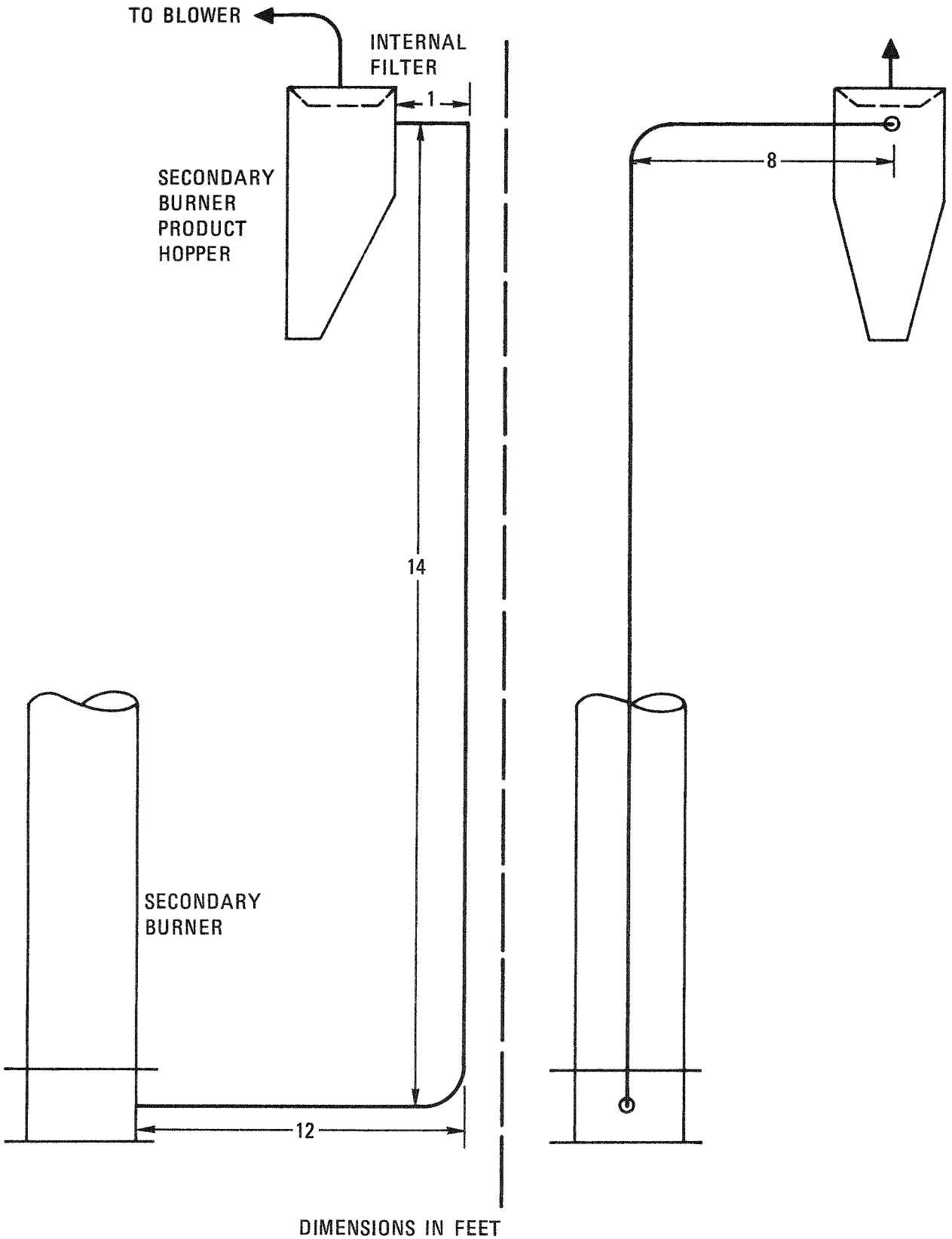

Fig. 3-7. System C, secondary burner product transport system

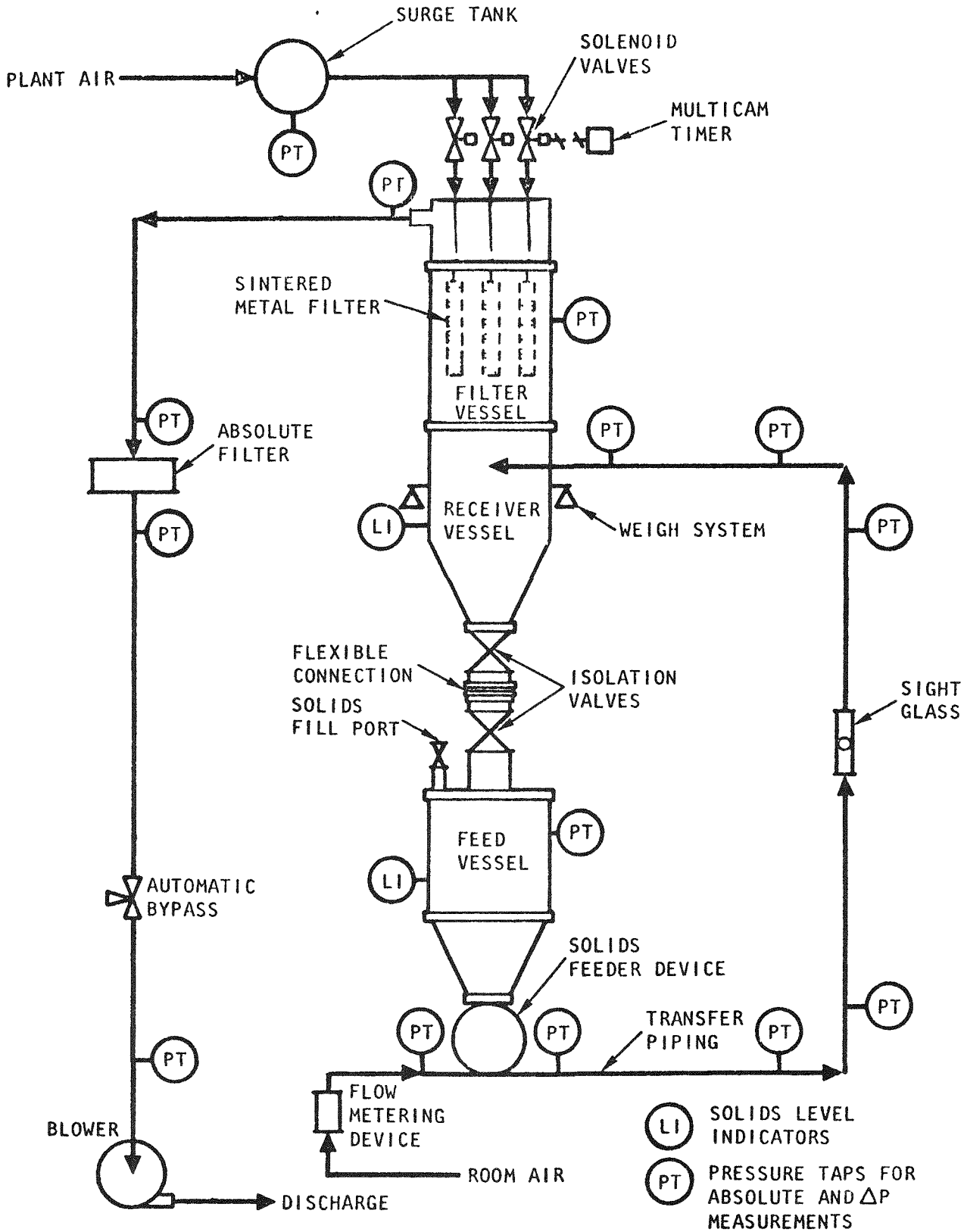

Fig. 3-8. Pneumatic transport system

Shakedown testing of the pneumatic transport test unit is complete. The feeder used for these tests was a 2-in. rotary valve powered by a variable speed 1/2-hp motor, close coupled through a 30 to 1 gear reducer. Calibration on crushed graphite yielded a linear range up to a maximum of 8 lb/min. Observations during the shakedown runs showed all system components to be operating satisfactorily except for the in-vessel filter blow-back system. Only one or two tubes in each of the nine bundles were being cleaned with each air pulse, thus indicating nonuniform distribution of the blow-back air. A check after the initial run revealed the air supply tubes were off-center. Guide sleeves (Fig. 3-9), which fit inside the filter tube bundles to maintain the air supply tubes in a center position, were made. The filters are now blowing back adequately at an air pressure setting of 80 psig and a sequential actuation every 7 sec with a duration of 1.5 sec.

The shakedown tests were conducted with two separate charges of crushed graphite (-3/16-in. ring size), each weighing 18,000 g. The first batch was sent through two complete cycles of the test system piping loop before being discharged for weighing and sieve analysis, while the second batch was cycled six times. Figures 3-10a and 3-10b show a comparison of the uncycled versus cycled material. Particle attrition is evident and was observed to be due to action in the rotary valve. Material loss percentages for the two samples were 0.47 and 1.09%, respectively. The increased percentage for the second series of runs is probably due to a more permanent buildup of material in the sintered metal filters and material deposition on the top of the tube bundles (Fig. 3-11). In future designs this source of holdup will be eliminated.

Experimental testing will continue on the pneumatic transport test system. The information to be obtained from the test unit is as follows:

1. Saltation and choking gas flows at the design transfer rate.

2. Material balance and material attrition.

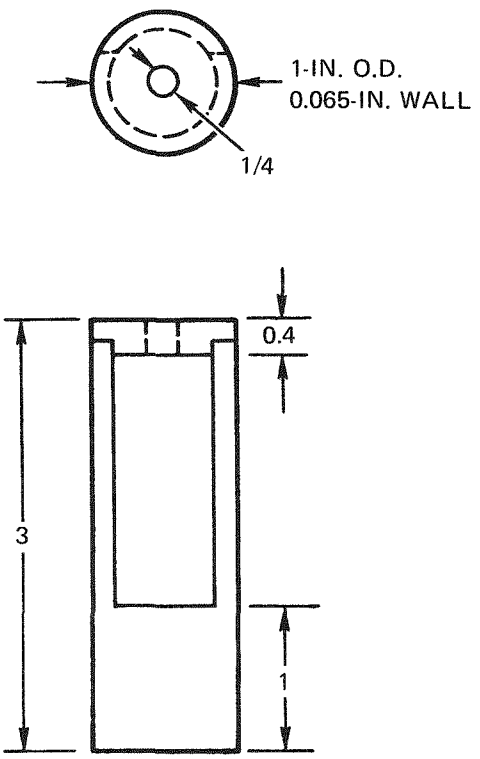

Fig. 3-9. Guide sleeve for filter tube bundle

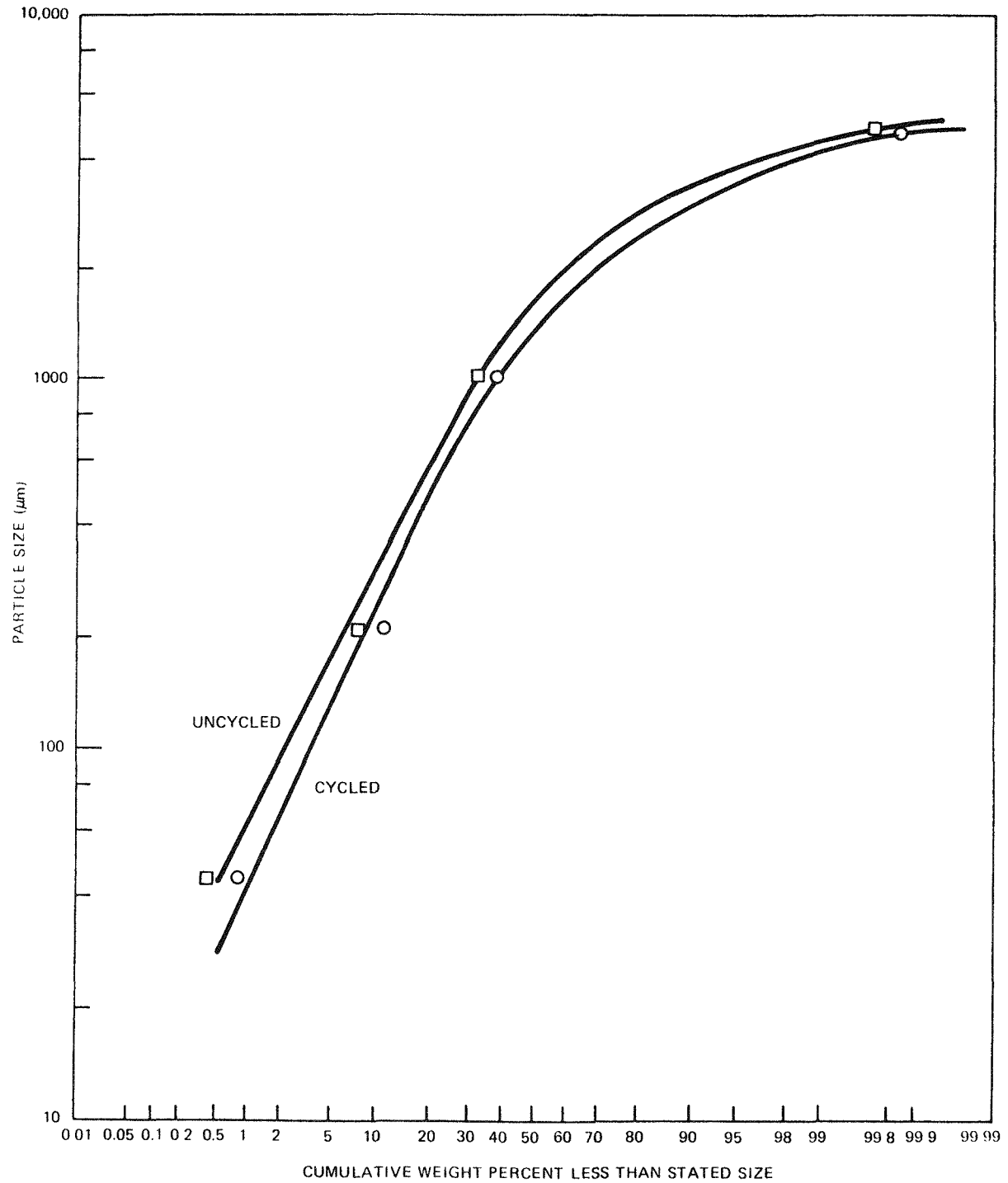

Fig. 3-10. Size-weight distribution for pneumatically transported crushed H-327 graphite: (a) two cycles

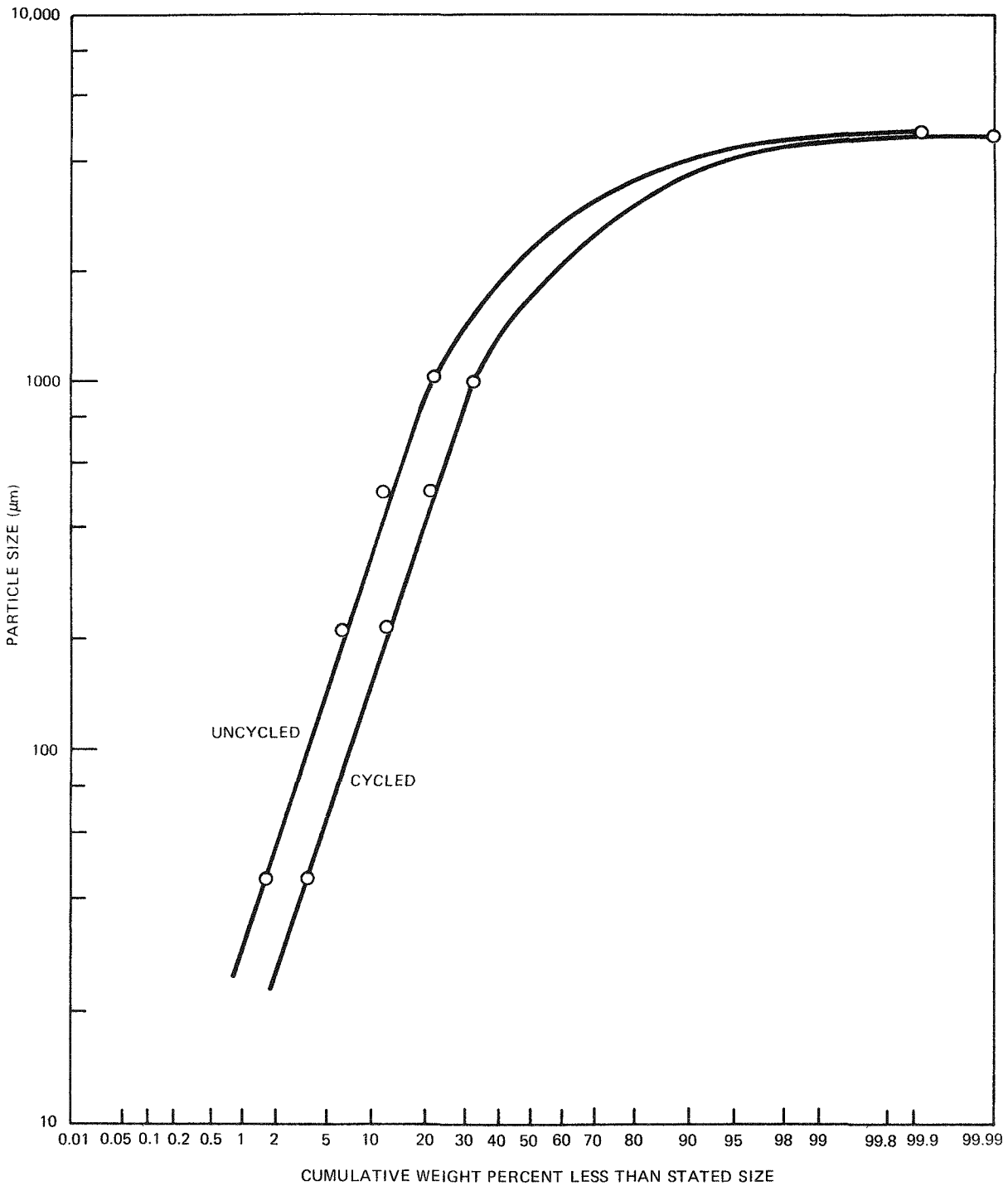

Fig. 3-10. Size-weight distribution for pneumatically transported crushed H-327 graphite: (b) six cycles

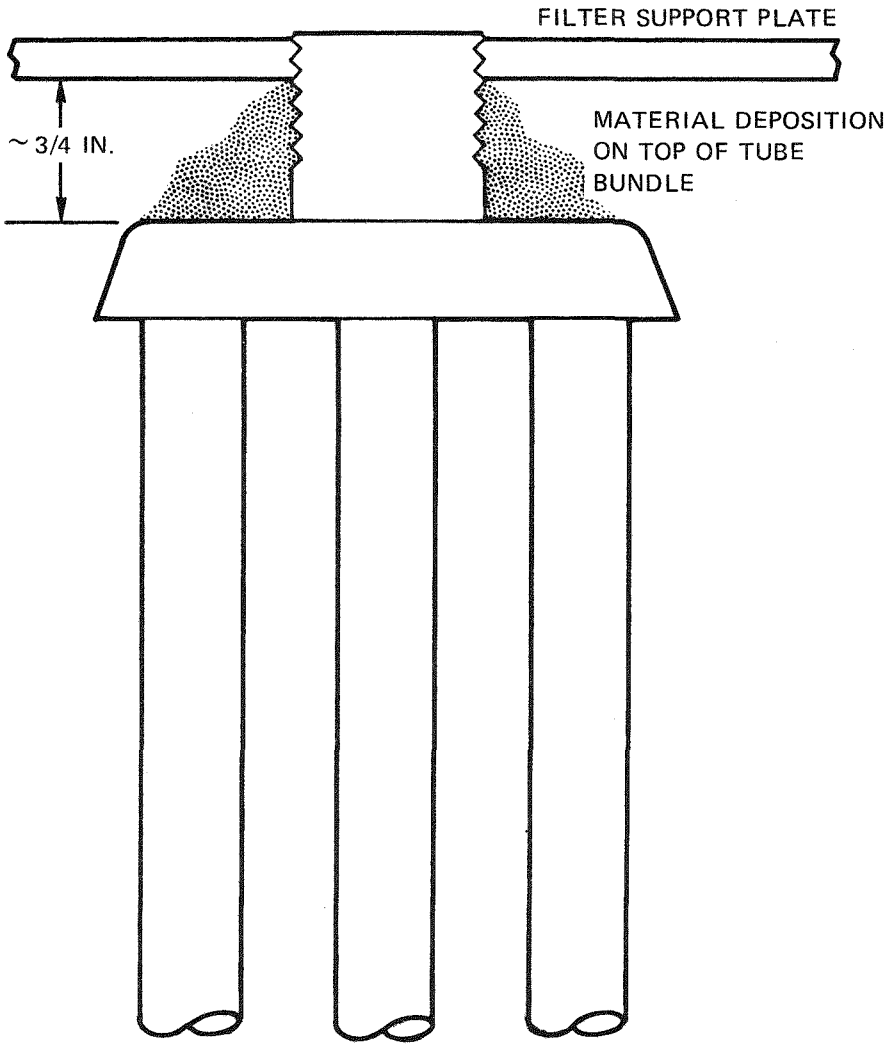

Fig. 3-11. Filter tube and support plate

3. Comparison of pressure drop data with existing correlations.

4. Wear data at the pickup and discharge points and at the elbows.

5. Determination of the optimum feeding method for each particular system.

6. System limitations such as piping configuration, discharge velocity (particle breakage versus inertial filter), material feeders, and receivers.

These tests will be conducted on the various particulate systems in the head-end flowsheet in the following order:

1. Crusher product without fuel particles
2. Primary burner fines
3. Secondary burner product
4. Fuel particles
5. Fresh feed

3.1.3. Prototype Pneumatic Transport System

The prototype head-end reprocessing line presently being designed and constructed will encompass the following unit operations: crushing, primary burning, classification, and secondary burning. These individual operations will be linked by a solids transporting system that will provide recycle capability and surge capacity, as well as material accountability. Several options were considered (gravity, interchangeable containers, and pneumatic) before selecting vacuum pneumatic transport. Once the method was selected, based on the constraints imposed by the various unit operations, design of the pneumatic transport system was initiated.

The first part of the design involved satisfying the feed, withdrawal rates, and storage capacities of the particulate streams in the four unit

operations (Table 3-1). Next, the requirement of material accountability resulted in the inclusion of a weighing system to measure the amount of material into and out of each unit operation. Finally, based on standard engineering correlations, the transport lines and positive displacement pumps were sized. The resulting design is shown in Fig. 3-12.

For accountability, the particulate stream will be weighed before and after each unit operation. The weighing system will consist of three electronic load cells supporting each feed and product bunker. The signals from these load cells will be converted into a digital readout and a 4 to 20 mA signal with a minimum accuracy of ±1 part in 10,000 of full scale or 1 part in 1000 of the reading, whichever is greater. To attain this accuracy the bunkers must have flexible connections for all incoming and outgoing lines.

The solids/gas separation is made with sintered metal, multitube filter assemblies (Fig. 3-13) similar to those described earlier (Ref. 3-1) with the following two exceptions: (1) they are mounted with a flange, and (2) they are fitted with internal venturis to assist the blow-back. The flanged design will allow removal of a filter without exposing the entire filter bundle and will reduce the exposed surface area in the vessel since the underside of the filter tube manifold will be flush with the tubesheet. The filters will be blown back sequentially as determined by the experiments on the test system in groups of either 1, 2, or 3 depending upon the total number of filters per vessel. The total filter surface area required was determined so that the linear velocity through the filters was 7 ft/sec for filter tubes less than 20 in. and 6 ft/sec for filter tubes greater than 20 in. in length.

The final design has six forward and two recycle lines with two surge bunkers, one between the crusher and the primary burner and the other between the primary burner and the pneumatic classifier. Each receiving vessel is designed with a tangential entry and has pneumatic-actuated isolation valves on all inlets and outlets.

TABLE 3-1
SPECIFICATIONS FOR THE FOUR PROTOTYPE UNIT OPERATIONS

	Solids Rates (lb/min)		Bunker Capacity (lb)	
	Feed	Withdrawal	Feed	Product
Crushing	26.5	26.5 minimum	--	1150 (19.4 ft^3)
Primary burning	1.0	27.6 minimum	230 (3.9 ft^3)	600 (4.8 ft^3)
Classification	1.5	18.5	414 (2.9 ft^3)	414 (2.9 ft^3)
Secondary burning	30.0	11.5	176 (1.2 ft^3)	176 (1.66 ft^3)

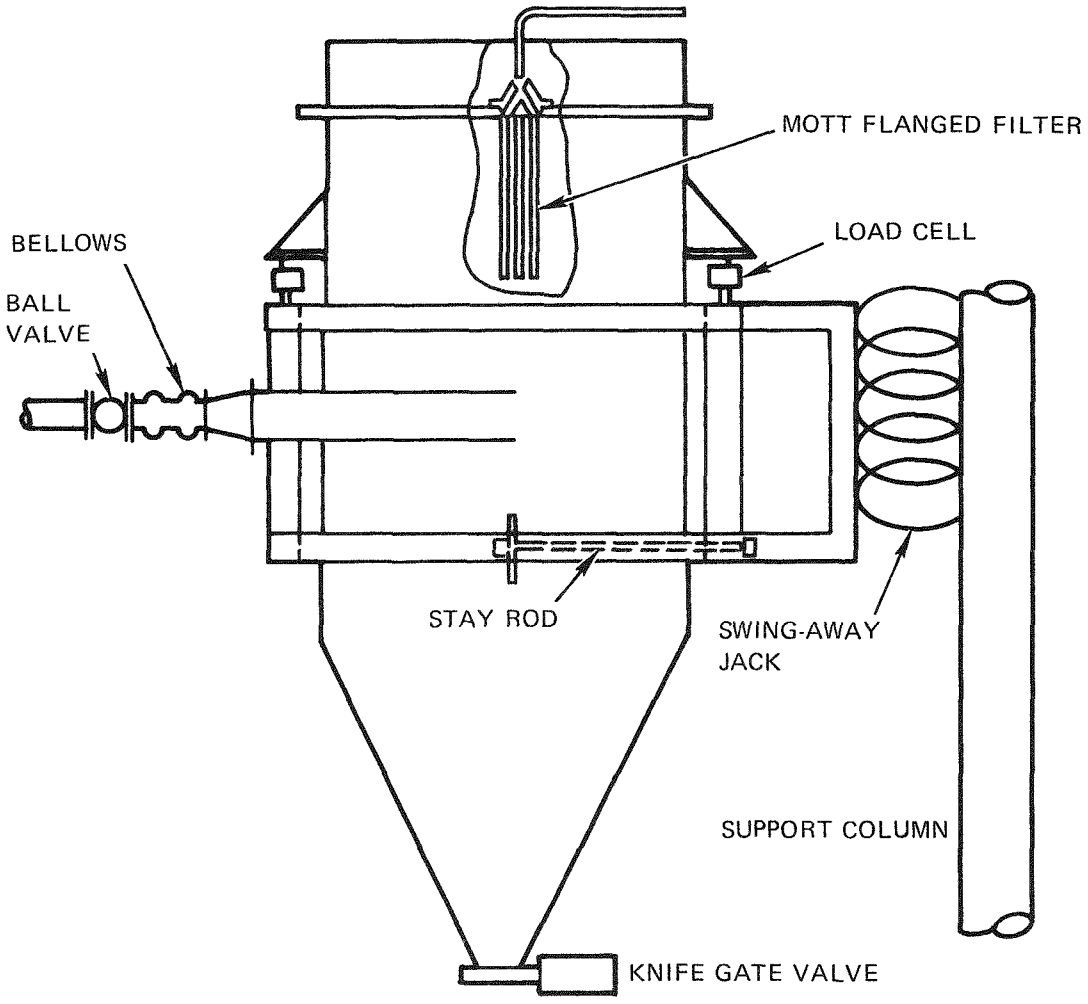

Fig. 3-12. Material weighing arrangement for prototype pneumatic transport system(s)

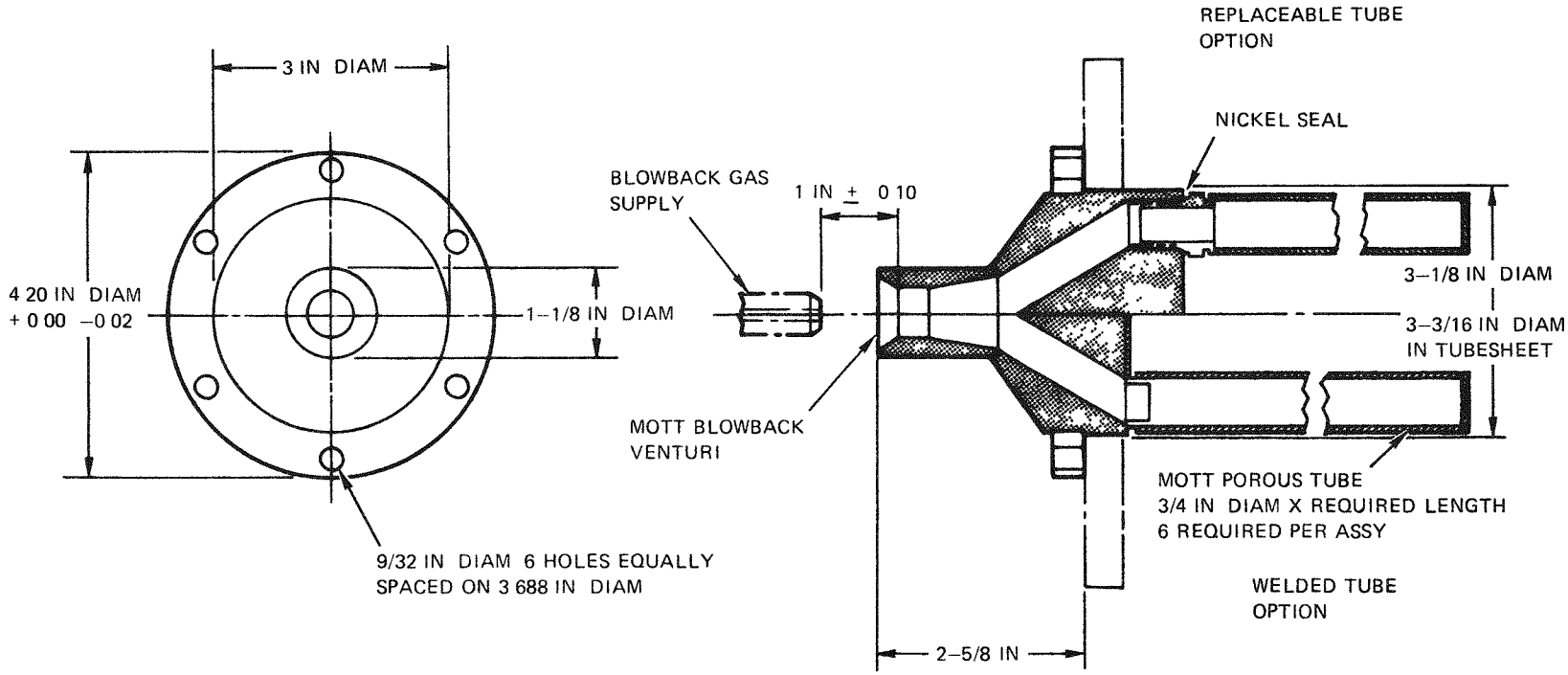

NOTES
1 MATERIAL POROUS 316C ST STL
HARDWARE 304 ST STL

Fig. 3-13. Multitube filter assembly

A typical startup sequence will position all valves for the desired transport and start the cam timer of the filter blow-back system. After the valves are positioned, the blower starts. The feeder will then start after the transporting gas has accelerated and, finally, the valve above the feeder opens. This startup sequence will be activated by one button to eliminate any possible operator errors either in the activation of the correct equipment or in the timing of this activation. In addition, the possibility exists of activating a transport subsystem that shares some equipment with an operating subsystem. For this reason, the subsystems will be interlocked to prevent this occurrence.

3.2. PNEUMATIC CLASSIFICATION

The economics of reprocessing HTGR and LHTGR fuel are affected by the ability to separate the fissile and the fertile fuel. This separation allows isolation of the bred U-233 in the fertile stream from the neutron poison U-236, which is contained in the fissile particles. Presently, the flowsheets for the TRISO/TRISO and the TRISO/BISO fuels are identical through the crushing, primary burning, and initial classification stages. By taking advantage of the differences in diameter and density of fissile and fertile particles, separation can be achieved through pneumatic classification.

In addition to separating the fissile and fertile particles, pneumatic classification has an additional location in the flowsheet. This place is in separating the whole unbroken TRISO particles from the SiC carbide hulls that remain as a solid stream after leaching. This separation will recover any whole particles that were not broken prior to burning in the secondary burner and will improve the recovery of fuel material in the flowsheet.

3.2.1. TRISO/TRISO Fuel Blend

The TRISO/TRISO fuel blend is that presently being used in the Fort St. Vrain reactor and consists of fissile and fertile components. Both

components are spherical particles with the following characteristics:

1. A spherical, heavy metal carbide kernel (ThC_2/UC_2 for the fissile and ThC_2 for the fertile).

2. A pyrolytic low-density carbon buffer coating on the kernel.

3. A low-temperature isotropic (LTI) graphite coating on the buffer coating.

4. A SiC coating on the inner LTI graphite coating.

5. Another LTI graphite coating on the SiC coating.

These particles are mixed in the proper ratios for the zone of the reactor where they are to be used, formed into cylindrical rods 1/2 in. O.D. by 2 in. long, and inserted into the graphite fuel elements. Following removal from the reactor, these fuel elements are reprocessed. In the first steps of this process the element is crushed and the graphite is then burned off to expose the fuel particles that have the SiC coating as the outer coating. At this point, the particles are ready for separation.

While both types of fuel particles have the same construction, the kernel size of the fissile particles is smaller than that of the fertile particles. Since the coating thickness is the same for both types, a separation based on size can be made. To determine how well these fuel particles can be separated, a parametric study of pneumatic classification and mechanical sieving was undertaken. The outcome of this study is reported in a GA topical report (Ref. 3-2), which is expected to be published in June and was summarized in the previous quarterly report (Ref. 3-3).

3.2.2. TRISO/BISO Fuel Blend

The TRISO/BISO fuel blend is currently the reference fuel for the large HTGR (LHTGR). The major difference between the TRISO/BISO and the TRISO/TRISO fuels is in the fertile fuel particle. In the TRISO/TRISO fuel blend the fertile and fissile particles have a similar construction, whereas in the TRISO/BISO fuel blend the fertile particle has the following design:

1. A thorium oxide spherical kernel.
2. A low-density carbon buffer coating on the kernel.
3. A low-temperature isotropic carbon coating on the buffer coating.

The fissile particle is similar to the fissile particle of the TRISO/TRISO system except that the kernel is a 100% uranium compound with no thorium present. The TRISO/BISO fuel system is handled the same as the TRISO/TRISO system from the loading into fuel elements to separation in reprocessing. At this point, the fertile particle has the kernel exposed after initial burning while the fissile particle has the SiC coating exposed. This results in the diameters of the particles being close while the densities are much different. Since the density of the fertile kernel is approximately three times that of the fissile particle and since the diameters are nearly the same, the separation must relay on the difference in density or on the fact that the ThO_2 kernel can be dissolved and the SiC cannot be dissolved. From these two considerations, pneumatic classification was chosen for the initial separation with leaching for the final separation.

A parametric set of tests was performed to determine the degree of separation that could be achieved through pneumatic classification. These tests showed that a crossover of less than 2 wt % can be achieved for a feed rate of 2000 g/min, providing the gas flow is varied as a function of the fissile-to-fertile ratio (Fig. 3-14). Specifically, the gas flow rate must vary from 4.98 to 3.42 m/sec to accommodate a range of fissile weight fraction from 0.06 to 0.63 with an average of 0.22. This range

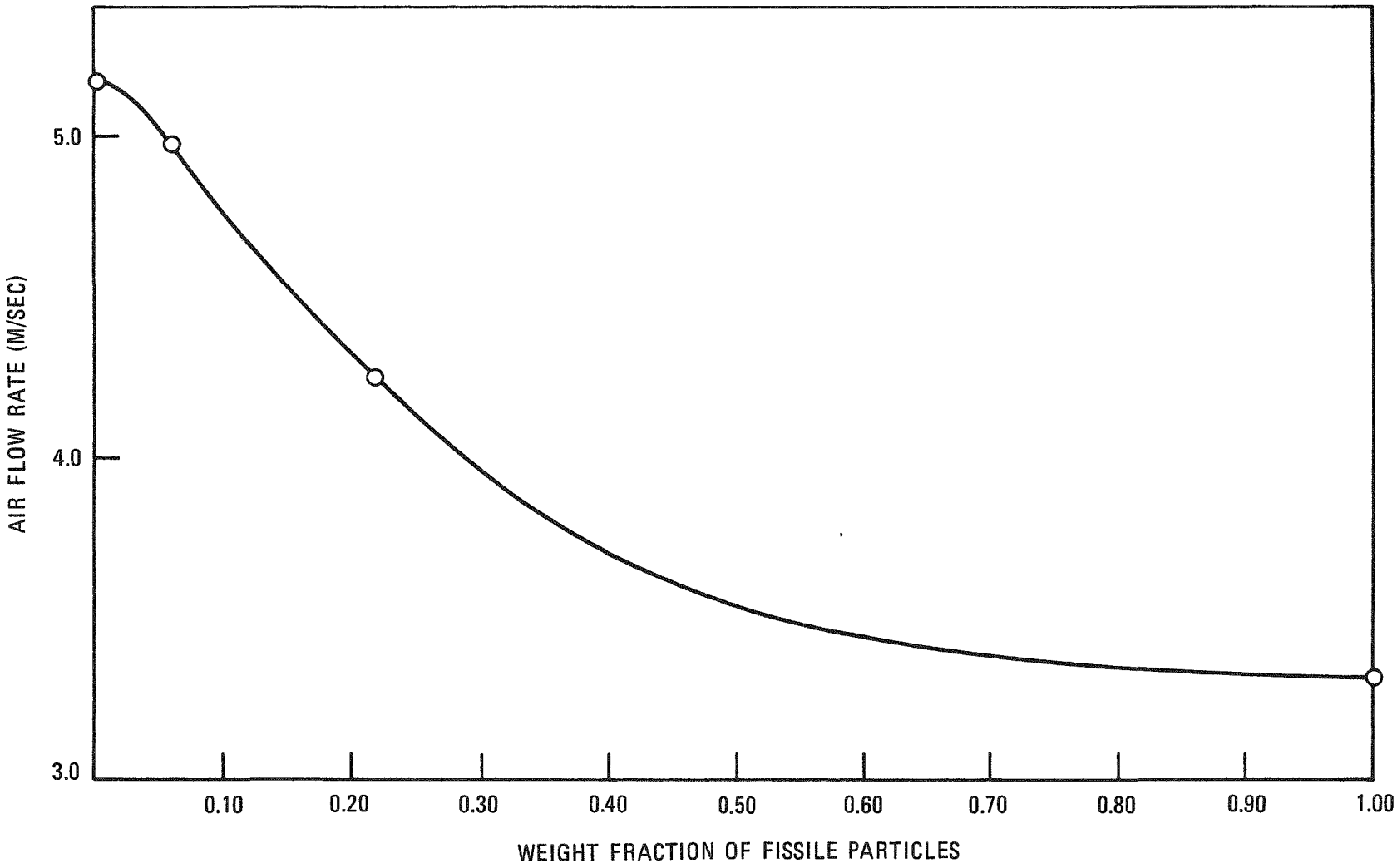

Fig. 3-14. Air flow rate versus weight fraction of fissile particles for minimum crossover at 2000 g/min

of weight fraction is found in the LHTGR where it is required in order to achieve the proper ratio of uranium to thorium in the different regions. The tests were performed on the modular classifier in the configuration given in Fig. 3-15.

3.2.3. SiC Hulls/TRISO Particle System

One additional location on the flowsheet requires the separation of a particulate system. The system is SiC hulls and whole TRISO fuel particles, which make up the product of the leaching insols dryer. At this point the unbroken TRISO fuel particles must be separated from the leaching insols and returned to the particle crusher to recover the heavy metals and to reduce the solid waste. Because of the difference in size and density, and for compatibility with the pneumatic insols dryer, pneumatic classification was selected as the method for separation.

From these tests, a separation that gives a >99% SiC stream and a 100% fertile TRISO fuel particle stream can be achieved using the modular classifier (Fig. 3-15) with a feed rate of approximately 100 g/min and a gas flow rate of 1.1 m/sec. The feed contained up to 26 wt % fertile particles.

3.3. SOLIDS PROPERTIES TESTING

Due to the nature of the head-end processes of the Thorium Utilization Program, many areas exist that require handling of particulate systems. For this reason, the literature is constantly surveyed for better methods of handling particulate systems and for better methods of predicting the behavior of these systems. From this survey, several points have become evident.

1. The quality or performance of a process involving particulate systems hinges on the performance of the feeders and the bunkers above these feeders.

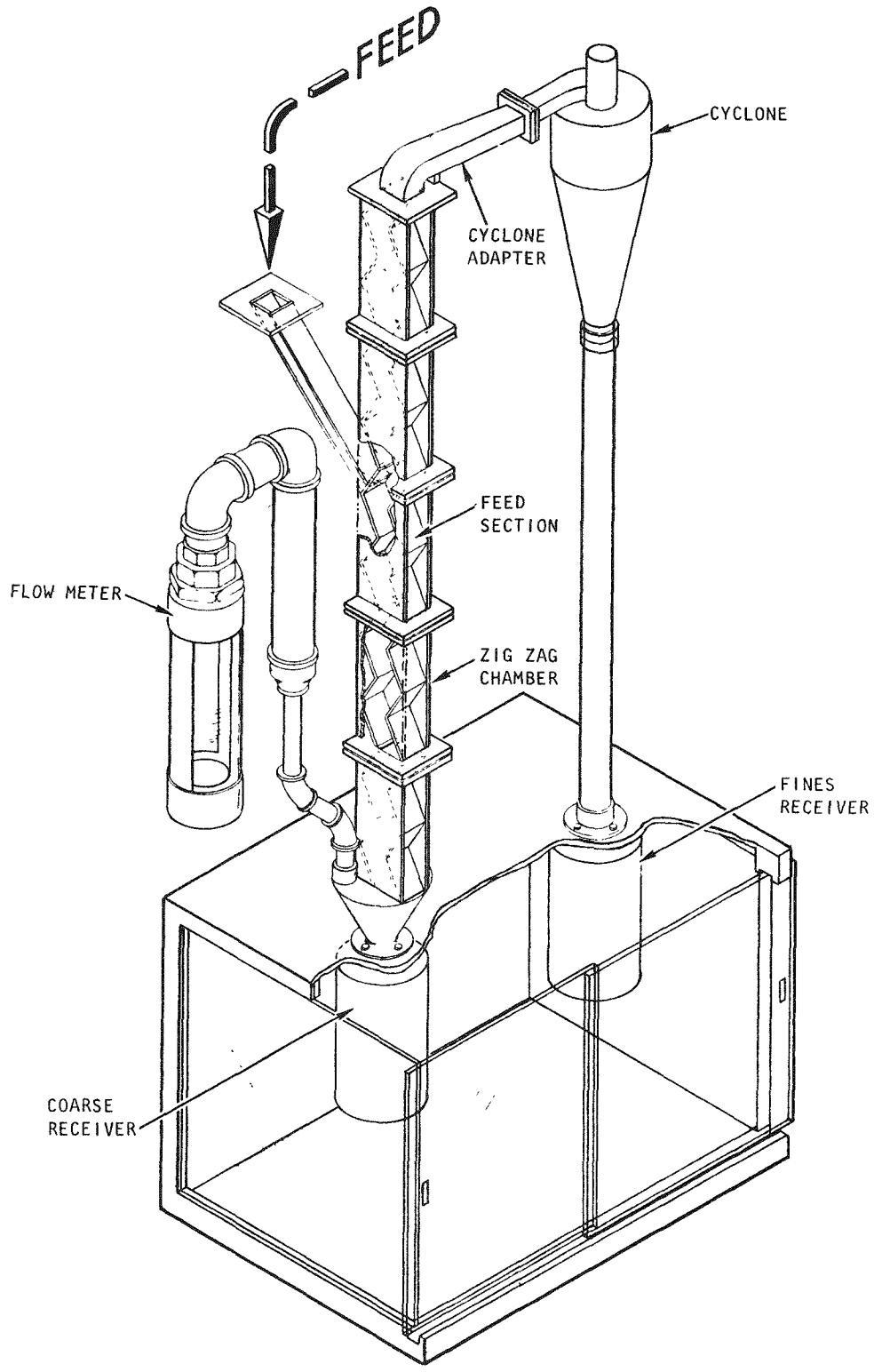

Fig. 3-15. Schematic of modular pneumatic classifier

2. The feeder and its associated bunker cannot be treated separately.

3. Specific information on the behavior of materials similar to those encountered in the head-end flowsheet is almost nonexistent.

Because of the above points, a method was sought that would aid in the prediction of particulate behavior and in the design of the bunkers and the feeders associated with the flowsheet. A method that has enjoyed considerable success over the past few years is one developed by Jenike (Ref. 3-4). This method combines a theoretical approach developed from soil mechanics with empirical data gathered to support the theory. Through the use of this method combining theory with testing, the behavior of powders in bunkers and feeders can be predicted and used for designing the bunkers and the feeders.

In order to perform these tests on the particulate systems of the head-end flowsheet, equipment that had been perfected by Jenike was purchased. With this equipment the behavior of the unirradiated particulate system can be studied. Unfortunately, the effect of irradiation on these powders and their properties is not fully understood. For this reason a proposal has been submitted for conducting parallel tests on irradiated material at the ORNL hot cells. These additional tests would allow the accurate prediction of the flowing properties for the irradiated particulates of the head-end process.

3.3.1. "Cold" Testing

Upon receipt of the solids flow testing equipment, it was installed in a glove box fitted with humidity control equipment. This served two purposes. First, it contained the radioactive material and allowed efficient handling of the equipment. Second, the controlled atmosphere was required since the flow characteristics of powders is dependent on their moisture content and thus the humidity of their environment.

The humidity control equipment consisted of a closed loop including a pump that pulls air from the glove box through a saturated salt solution and then back to the glove box. In this closed circuit, the volume of air is finite, thereby maintaining a constant humidity dependent only on the salt used and, to a lesser degree, the temperature. The operation of the humidity control has been erratic, but the problem has been traced to the pneumatic load cell in the testing equipment, which allowed dry air to enter the glove box. This caused the glass gas dispersion frit to plug with precipated salt crystals as the dry air extracted water from the salt solution. An electronic load cell is on order to replace the pneumatic load cell.

Testing to date has involved the effect of time on the flow properties of primary burner elutriated fines at 50% relative humidity and the instantaneous flow properties of secondary burner fines at 20 and 60% relative humidity. The data from these runs are still being reduced and interpreted.

Because the data for primary burner fines were obtained at the low end of the capabilities of the equipment, an electronic load cell is being purchased that will give better accuracy in the low end. A tensile tester (Fig. 3-16) is now being fabricated to provide additional data.

REFERENCES

3-1. "Thorium Utilization Program Quarterly Progress Report for the Period Ending August 31, 1974," USAEC Report GA-A13178, General Atomic Company, October 31, 1974.

3-2. De Lesdernier, D., and B. Baxter, "Pneumatic Classification of FSV Fuel Particles," ERDA Report GA-A13135, General Atomic Company, to be published.

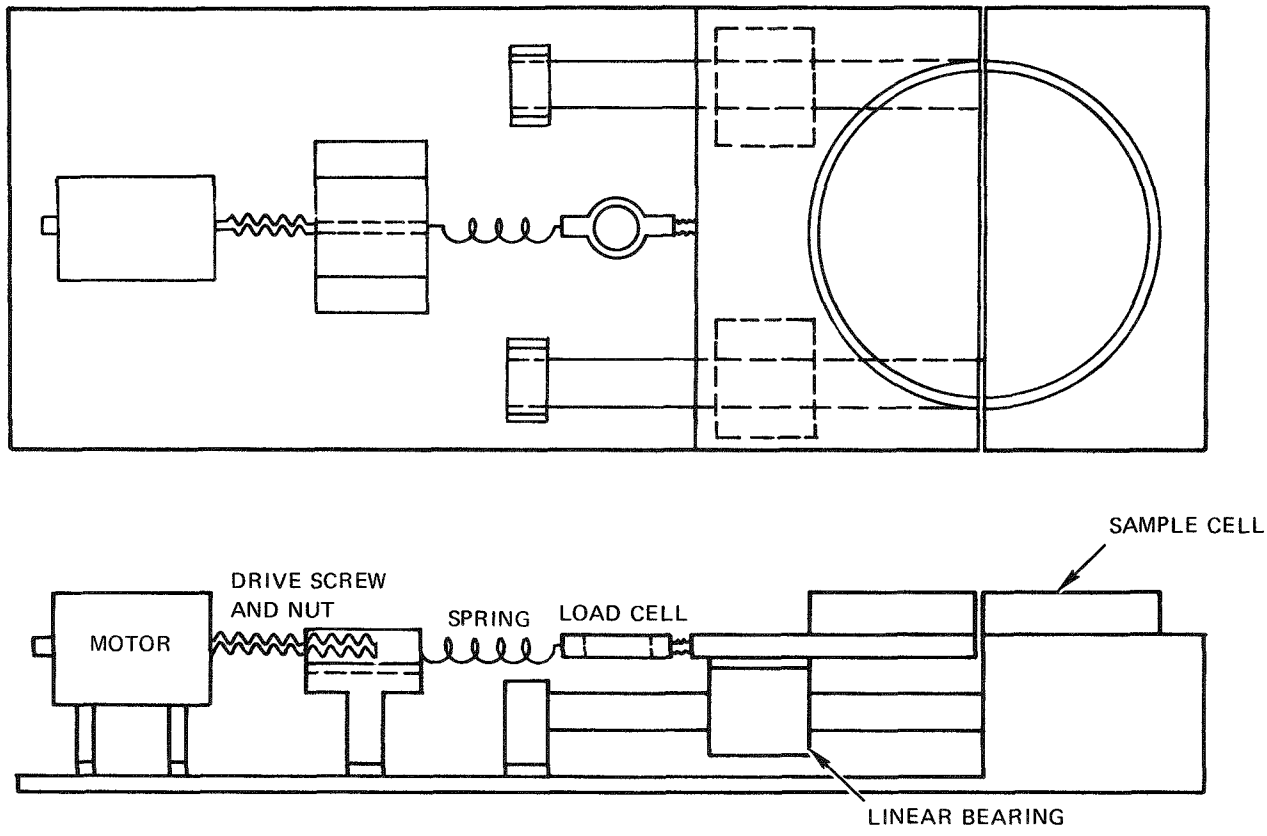

Fig. 3-16. Tensile tester

3-3. "Thorium Utilization Program Quarterly Progress Report for the Period Ending February 28, 1975," ERDA Report GA-A13366, General Atomic Company, May 30, 1975.

3-4. Jenike, A. W., "Storage and Flow of Solids," University of Utah Engineering Experiment Station Bulletin 123, March 1970.

4. FLUIDIZED-BED COMBUSTION

The development program continues to be heavily oriented toward the design and construction of the prototype line. The 20-cm primary burner has been operated to verify the perforated conical distributor design. The dense-phase pneumatic transport system is being installed for testing during the next quarter. The 10-cm secondary burner has been utilized for further design verification and to obtain heat transfer data on both primary and secondary burner bed materials. The designs of the prototype primary burner (vessel and heating-cooling package) and the instrumentation for the prototype line are being reviewed and completed.

4.1. PROTOTYPE INSTRUMENTATION

4.1.1. Process Flow Diagrams

Preliminary process flow diagrams have been prepared for the following head-end reprocessing steps in the prototype plant: fuel element size reduction (Fig. 4-1), solids transport (Figs. 4-1 through 4-3), primary fluidized-bed combustion (Fig. 4-2), air classification and particle crushing (Fig. 4-3), and secondary fluidized-bed combustion (Fig. 4-3).

These diagrams schematically show the orientation of major equipment, control loops, and flow streams. In addition they give material and heat balance information at various key locations in the process. Completion of these diagrams will be coordinated with the development of required information from current and future planned experimental runs on the 20-cm primary burner and the 10-cm secondary burner.

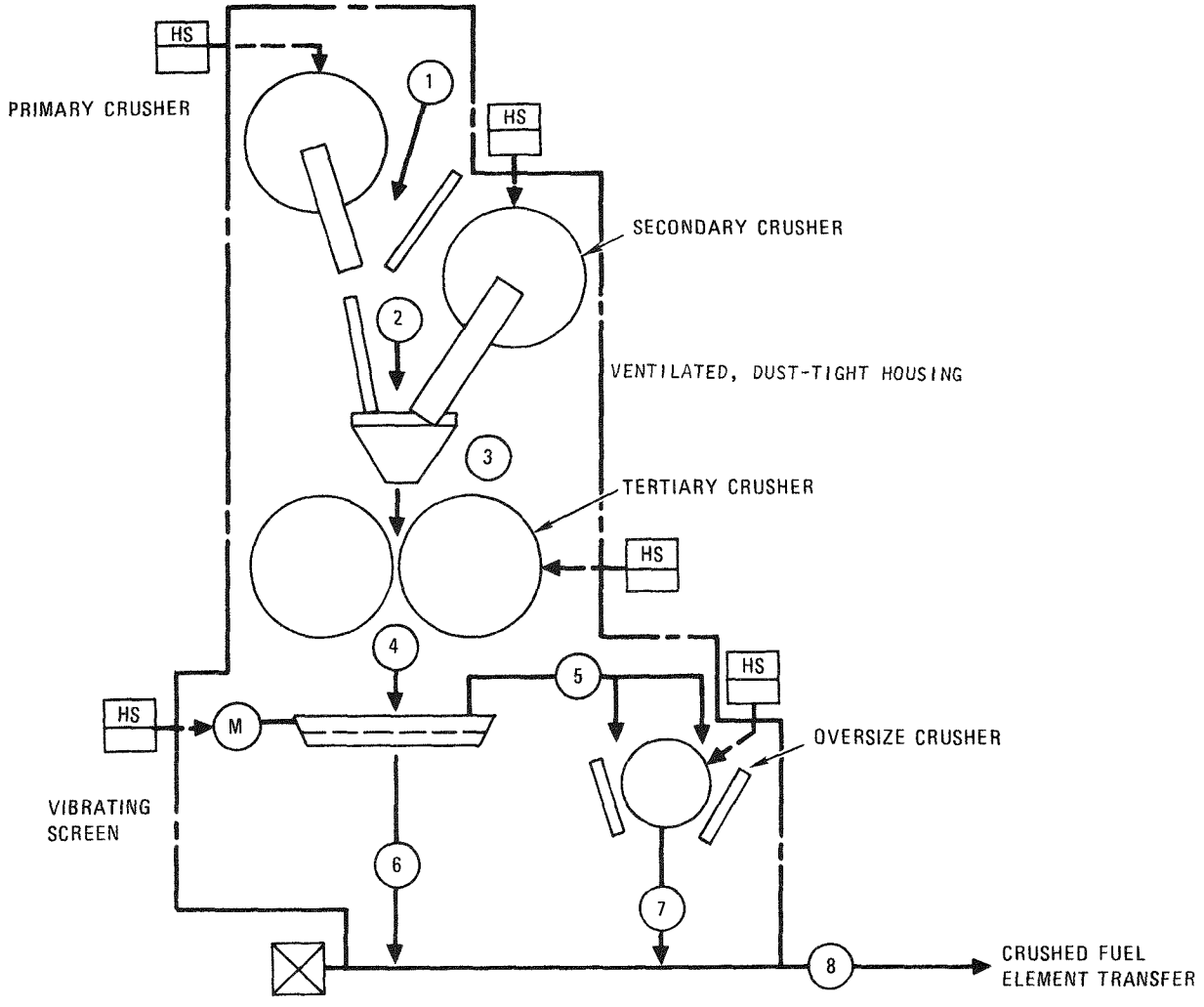

STREAM NO.	1	2	3	4	5	6	7	8
FLOW (MAX), KG/HR	720	720	720	720	72	720	72	720
TEMPERATURE	AMB	AMB	AMB	AMB	AMB	AMB	AMB	AMB
PRESSURE, PSIG	-0.1	-0.1	-0.1	-0.1	-0.1	-3.0	-3.0	-6.0
FLUID	SOLID	SOLID	SOLID	SOLID	SOLID	SOLID	SOLID	AIR/ SOLID
CARBON CONTENT, WT %	82.6	82.6	82.6	82.6	82.6	82.6	82.6	82.6
NOMINAL PARTICLE SIZE, IN.		6	3/4	3/16	>3/16	≤3/16	≤3/16	≤3/16

BURNABLE CARBON ONLY
FUEL ELEMENT

Fig. 4-1. Process flow diagram for fuel element size reduction

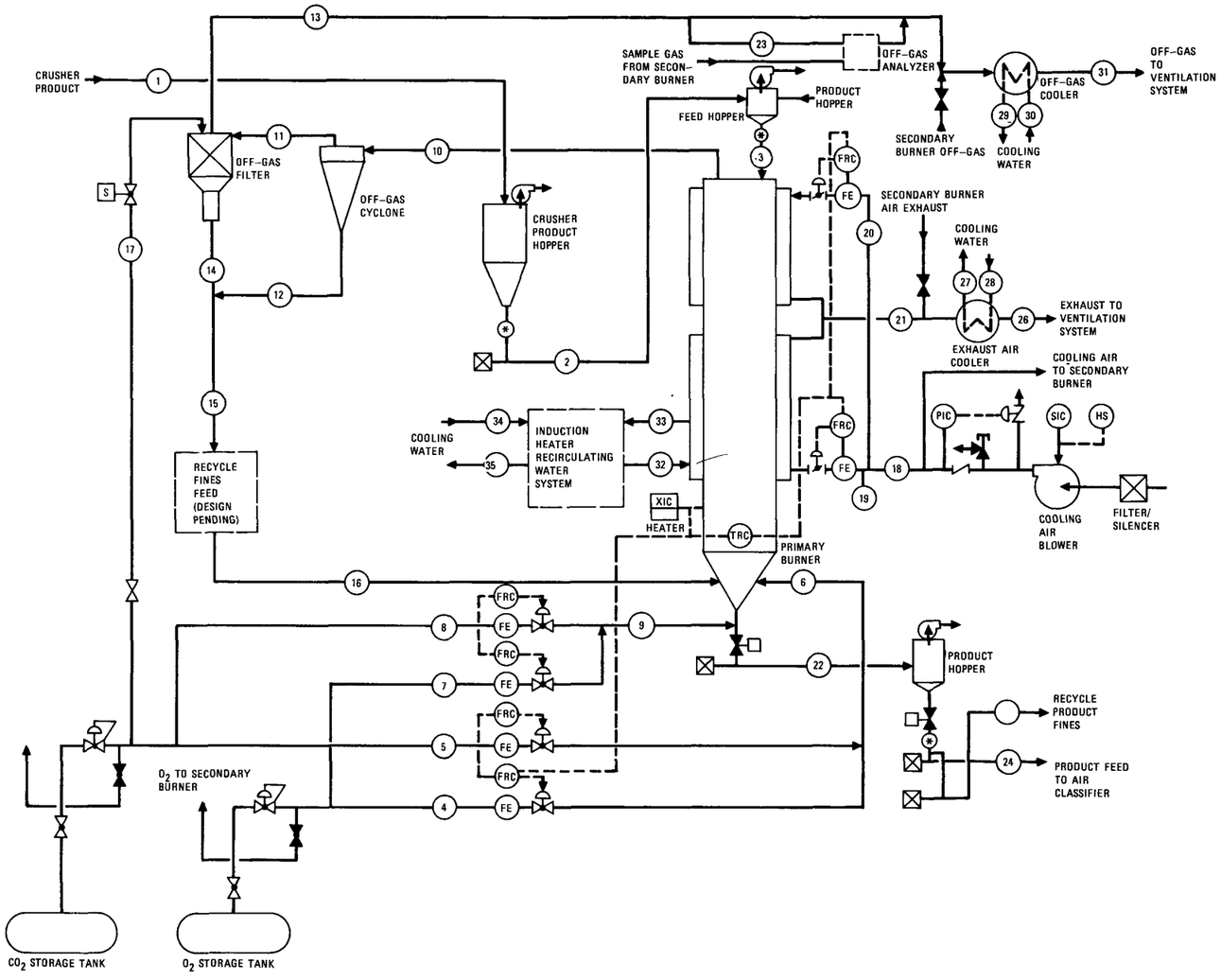

STEADY-STATE COMBUSTION PHASE

STREAM NO.	1	2	3	4	5	6	7	8	9	10	11	12	13	14	15	16	17	18	19	20	21	22	23	24	25	26	27	28	29	30	31	32	33	34	35
FLOW																																			
KG/HR	720	680	58.11		0												*					0		503	503										
SLPM	5660	5660		788		788	386	386	772	1618	1618		1618				809	56,600	42,500	14,100	56,600	0	14	4250	5660	56,600	303	303	**	**	1618	114	114	114	114
TEMPERATURE,°C	AMB	AMB	AMB	20	20	20	20	20	20	700	650		400				20	50	50	50	423		AMB	AMB	AMB	66	43	24	**	24	66	32	41	21	29
PRESSURE, PSIG	-6.0			60		7.5	60	60	7.5	0.7	0.6		0.3				60	12	12	12	1		~0	-6.0	-6.0	0	94	100	**	100	~0	55		100	
FLUID	AIR/ SOLID	AIR/ SOLID	SOLID + AIR	O_2	CO_2	O_2	O_2	CO_2	O_2/CO_2	CO_2/CO C	CO_2/C CO		CO_2/CO				CO_2	AIR	AIR	AIR	AIR		CO_2/CO	AIR/ SOLID	AIR/ SOLID	AIR	C.W.	C.W.	C.W.	C.W.	CO_2/CO	C.W.	C.W.	C.W.	C.W.
CARBON CONTENT, WT %***			82.6	-	-	-	-	-									-	-	-	-	-					-	-	-	-	-	-	-	-	-	-

*INTERMITTENT FLOW ONLY (~1-SEC DURATION/MIN)
**PERFORMANCE CHARACTERISTICS OF HEAT EXCHANGER NOT AVAILABLE
***BURNABLE CARBON ONLY

Fig. 4-2. Process flow diagram for 40-cm prototype primary burner

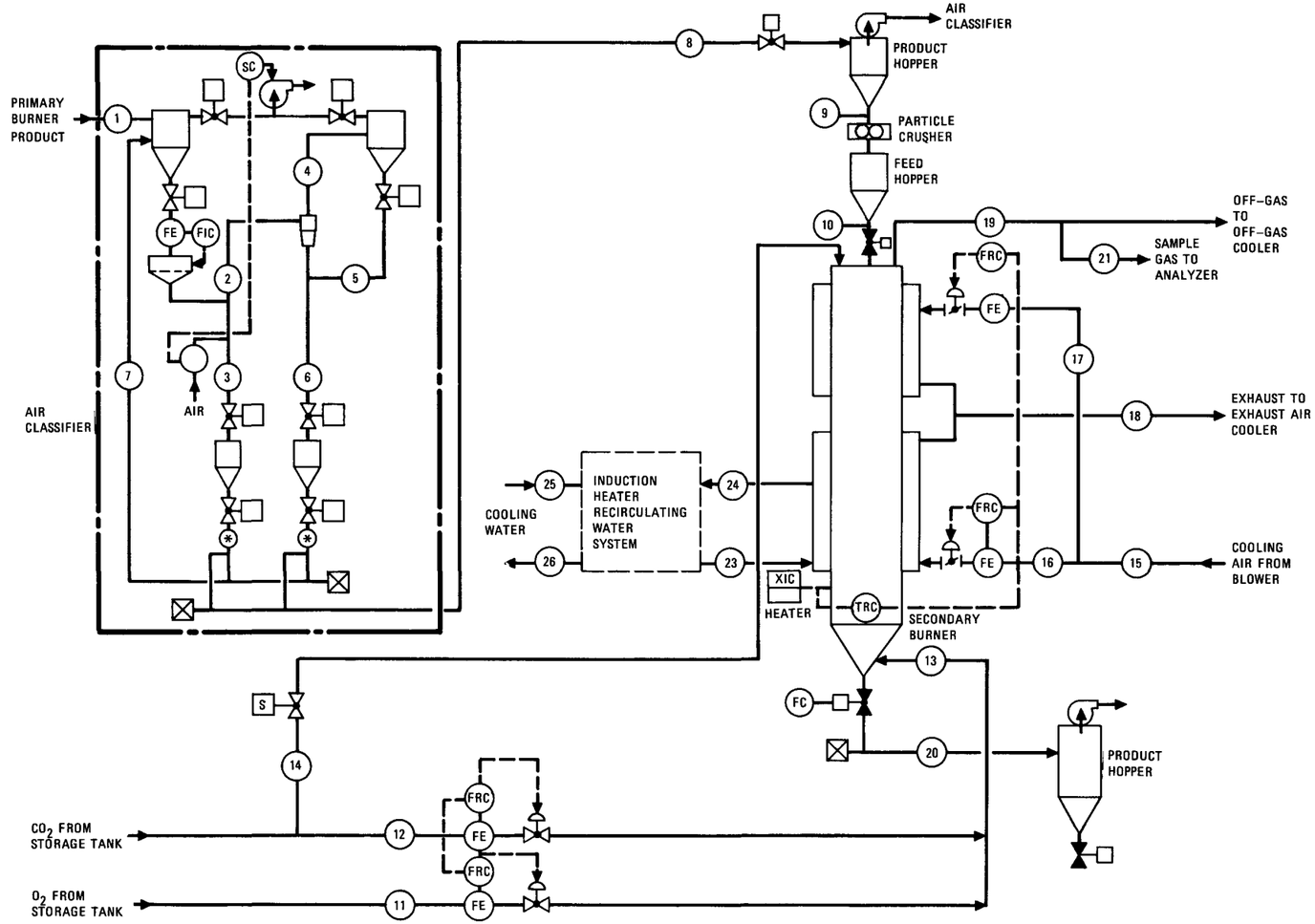

STEADY-STATE COMBUSTION PHASE*

STREAM NO.	1	2	3	4	5	6	7	8	9	10	11	12	13	14	15	16	17	18	19	20	21	22	23	24	25	26	27	28	29	30
FLOW		**	**																											
KG/HR	503	90	90	NEG	NEG	90	503	503	30	0				***						0										
SLPM	4250	1130	(1130)	1130	-	-	4250	4250	-		478	0	478	239	36,800	22,600	14,200	36,800	478	0	14		114	114	114	114				
TEMPERATURE,°C	AMB	AMB	AMB	AMB	AMB	AMB	AMB	AMB	AMB		20	20	20	20	50	50	50	180	400	AMB			32	41	21	29				
PRESSURE, PSIG	-6.0	-6.0	-6.0	-6.0	-6.0	-6.0	-6.0	-6.0			60	60	6.0	60	9.0	9.0	9.0	~0	~0	~0			55		100					
FLUID	AIR/ SOLID	AIR/ SOLID	AIR/ SOLID	AIR/ SOLID	AIR/ SOLID	AIR/ SOLID	AIR/ SOLID	AIR/ SOLID	SOLID	SOLIDS	O_2	CO_2	O_2/CO_2	CO_2	AIR	AIR	AIR	AIR		CO_2/CO			C.W.	C.W.	C.W.	C.W.				

*BATCH PROCESS
**MAXIMUM FLOW IN EITHER DIRECTION
***INTERMITTENT FLOW ONLY (~1-SEC DURATION/MIN)

Fig. 4-3. Process flow diagram for 20-cm prototype secondary burner

4.1.2. Piping and Instrumentation (P&I) Diagrams

Preliminary P&I for the same head-end reprocessing steps are in progress. These diagrams give detailed design information such as piping, valve, and control and instrumentation hardware requirements.

Major control loops have been defined for the primary and secondary burners as follows:

Primary Burner

1. Heating: a two-zone induction heating system to automatically establish and limit susceptor, vessel wall, and bed temperatures to acceptable values.

2. Oxygen flow: plenum flow adjusted to control bed temperature and ramped down near end of run to limit oxygen concentration in off-gas; cone vertex flow initiated by time delay after plenum oxygen flow reaches design steady-state value and ramped down near end of run (before plenum oxygen ramp is initiated) to limit oxygen concentration in off-gas.

3. Fluidizing gas (CO_2) flow: plenum flow adjusted to maintain constant total gas (O_2 + CO_2) flow to plenum; cone flow adjusted to maintain constant total gas (O_2 + CO_2) flow to cone vertex.

4. Cooling: flow of cooling air to burner jackets initiated and terminated by burner vessel temperature; flows ramped to establish nearly constant heat rejection rate.

Secondary Burner

1. Heating: a single zone induction heating system to establish and limit susceptor, vessel wall, and bed temperatures to acceptable values.

2. Oxygen flow: controlled on automatic ramp upon startup; adjusted near end of run to limit oxygen concentration in off-gas.

3. Fluidizing gas (CO_2) flow: adjusted to maintain constant total gas (O_2 + CO_2) flow below "threshhold" (minimum fluidization velocity) oxygen flow rate; CO_2 flow stopped above this "threshhold" O_2 rate.

4. Cooling: flow of cooling air to lower vessel jacket adjusted to control bed temperature; flow of air to upper jacket initiated and terminated by in-vessel filter temperature.

4.2. PRIMARY FLUIDIZED-BED COMBUSTION

The development program continued its focus on the 20-cm primary fluidized-bed burner during this reporting period. Test runs were made that emphasized performance during the initial period of the operating cycle, during which time the high bed graphite concentration and large mean particle size impose the most severe operating conditions. The operational response of the perforated conical distributor to increases in fresh feed size was studied. Figure 4-4 shows the feed size specification established with the 20-cm perforated distributor. Final bed carbon burnout, product removal, and pneumatic product transport were also analyzed. All components of the dense-phase fines recycle system for the 20-cm primary burner have arrived and installation is proceeding. Testing will begin in late May.

Preliminary results from studies of heat transfer and fluidization of primary burner material in the induction-heated 10-cm secondary burner vessel indicate a possibility that the minimum fluidization velocity of

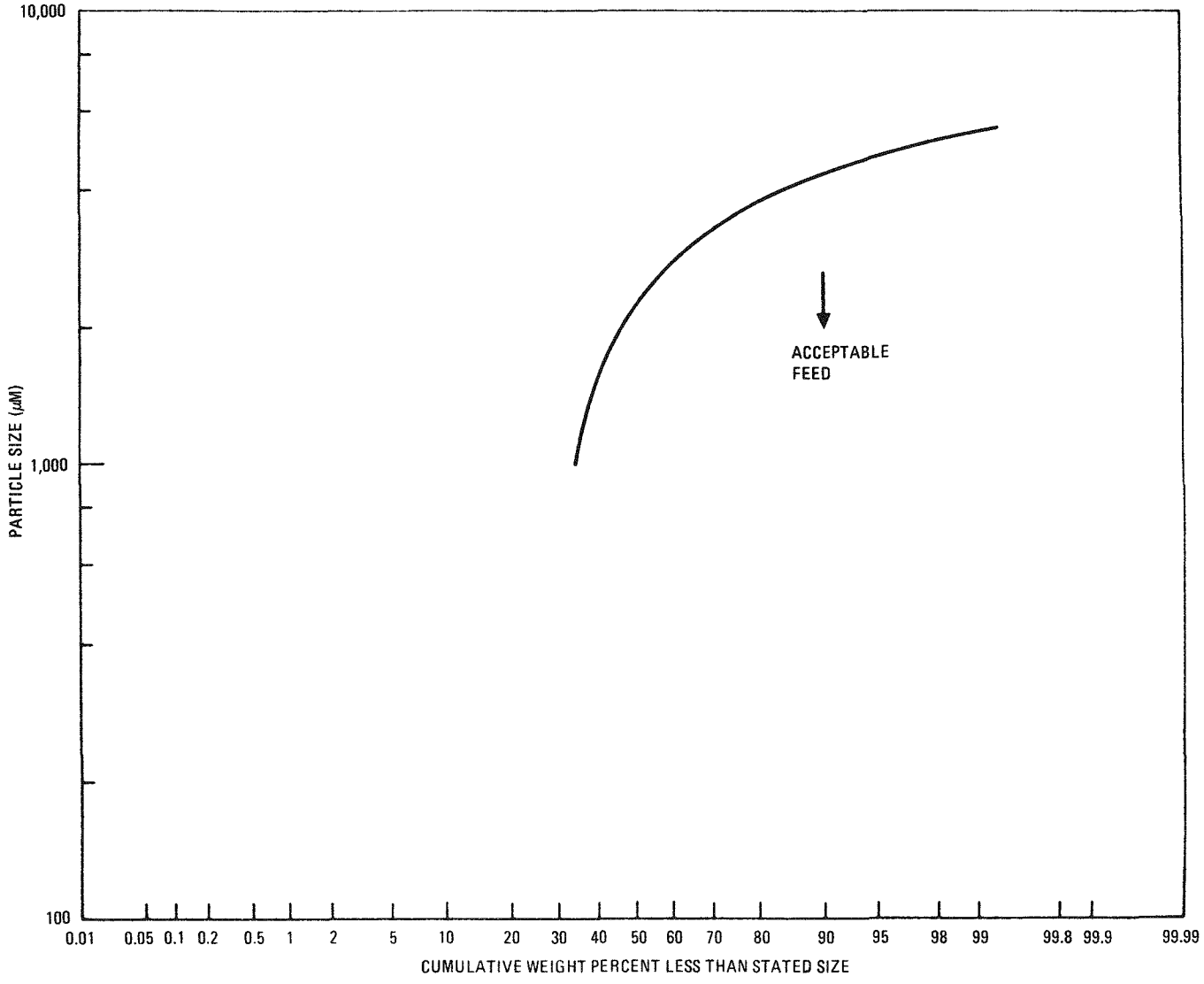

Fig. 4-4. Feed size specification, maximum feed size distribution

the large (>500 μm) material does not decrease with increasing temperature as predicted by standard correlations. The fluidization characteristics and heat transfer properties of the various types of bed material (the fresh feed bed during the initial operation period, the "steady-state" bed, and the final bed of SiC coated particles) will be investigated further.

4.2.1. 20-cm Primary Fluidized-Bed Combustor

Five runs and three startup tests were performed on the 20-cm primary burner during the last quarter. These runs are summarized in Table 4-1.

Burnout of the final bed carbon was significantly improved using a revised operating procedure allowed by the new high-capacity CO_2 diluent system. These runs were made without fines recycle. The carbon concentrations of the final bed in Runs 17, 18, and 19 were less than 0.1%. Carbon concentrations of 0.2% in the bulk bed and 0.93% in the top bed were found in Run 20 in which off-gas O_2 was minimized (18% O_2) using 66% CO_2 feed gas. Bed burnout temperature excursions in past runs had been dampened predominately with cooling air increases as the maximum N_2 diluent flow was insufficient to control elevating temperature. The revised procedure involves reducing the cooling air to zero as the bed burns out, while maintaining sufficient CO_2 diluent to control the bed temperature. Apparently improved heat retention and solids mixing within the bed, when using diluent rather than external cooling to control bed temperature during burnout, induces more efficient burning of the remaining carbon in the final bed which contains a high percentage of SiC coated fuel particles.

The burner operated acceptably with a bed of "oversize" (up to 5% >3/16 in.) fresh feed, the only significant observation being in-core temperature fluctuations of 10° to 30°C above the bulk bed temperature. This cycling temperature occurred every 90 to 120 sec but disappeared completely after about 3.5 hr operation as the SiC coated particle concentration within the cone increased. The cycling local temperature was attributed to burning of the largest size fractions (the least heat convective portion) of the fresh feed.

TABLE 4-1
SUMMARY OF 20-CM PRIMARY BURNER RUNS[a]

Run	Objectives	Observations/Conclusions
16	Testing of the 50° included angle perforated conical distributor with a larger bed weight of "oversize" feed (the feed was "oversize" based on fluidization criteria established in the 10-cm burner using a ball/cone distributor).	34-kg final bed was high in carbon especially in the upper region. Lower 33.6 kg (17.8% carbon) dumped through 1/2-in. vertex at 15 kg/min. Top 1.4 kg (62.7% carbon) contained some fresh feed size graphite and bridged at the 1/2-in. opening. The 40-cm prototype distributor design was subsequently revised to allow enlarging the diameter of the cone vertex opening.
	Introduction of pure O_2 to vertex of perforated cone early in run.	Vertex O_2 injection was too abrupt as it was accompanied by a bed temperature excursion. Revised system for incremental O_2/CO_2 ratio adjustments later in the run.
16.1, 16.2, 16.3	Torch startup tests with varied amounts of fresh feed size graphite and particle beds using new high-capacity CO_2 diluent system.	The large bed material volume and the high CO_2 gas rates required to fluidize the bed create heat losses greater than the heat input available with the present torch system. Standard small bed/coke startup to be used until induction system is installed.
17	Further study of burner response to oversize feed with revised thermocouple locations including an in-cone thermocouple.	In-cone temperature cycling 10° to 30°C above bulk bed temperature. Cycling analogous to cyclic spouting seen with the single inlet ball/cone distributor and thought to be a result of the larger fraction of the fresh feed graphite periodically gravitating into the cone. The larger graphite chunks are possibly less mobile than the smaller bulk of the graphite

TABLE 4-1 (continued)

Run	Objectives	Observations/Conclusions
17 (contd)		and hence the decreased convective particle heat transfer caused temporal increases in local cone temperature. These oscillations dampened as the run progressed. This was attributed to an increase in in-cone fuel particle concentration and resultant dampening of locally intense combustion of larger graphite.
	Gas distributor vertex/cone perforation gas balance study with revised capability to ramp CO_2/O_2 flows in small increments.	Burner operated in pure O_2 with no problem when O_2 level was increased in small increments as the run progressed and the bed particle concentration increased.
	Tests of bed burnout using the new high-capacity CO_2 diluent system. Increased diluent flow during bed burnout phase to allow cooling air reductions (instead of increases in cooling air as necessary in past runs with low-capacity N_2 diluent system).	Bed burnout very successful with revised operating procedure. About 0.07% carbon in the final bed.
18	Characterization of operation with a higher particle concentration bed using "oversize" feed similar to Run 17.	No in-core temperature oscillations noted. Apparently verifies fuel particle dampening effects on local temperature problems and indicates that equilibrium operation should be smooth compared with the difficult initial period of operation with high bed carbon content.
	Duplicate bed burnout of Run 17 to recheck diluent increase/cooling air decrease procedure.	Bed burnout to less than 0.1% carbon.

TABLE 4-1 (continued)

Run	Objectives	Observations/Conclusions
19	Operation with an oversize feed specially sieved to fall on 10-cm ball/cone poor fluidization line (∿3% > 3/16 in.).	Operation acceptable. In-cone temperature cycling of 10° to 30°C every 90 to 120 sec disappeared as run progressed (after about 2 hr of operation).
	Bed burnout with ∿20% CO_2 diluent to study limiting off-gas O_2 concentration (prior successful burnouts used 100% O_2 in feed gas).	Final bed carbon again less than 0.1%.
20	Operation with an oversized feed (5% > 3/16 in.)	Same as Run 19.
	Increased CO_2 diluent/O_2 ratio (66% CO_2 feed gas) to test effects of limiting off-gas O_2 at burnout (18% O_2 in off-gas).	Top bed carbon 0.93% and bulk bed carbon 0.2%, indicating some decrease in burnout and graphite "floating" on top of particle bed when using low O_2/CO_2 feed gas ratio.

(a) No fines recycle.

Investigations of the O_2/CO_2 gas flows best suited for the cone perforation and the cone vertex openings indicated a requirement of high CO_2 flows to the cone vertex in the initial period of the run. However, it was possible to decrease CO_2 and increase O_2 by increments to operation with nearly pure O_2 as the run progressed and the SiC coated particle concentration increased. This, together with the dampening of local cone temperature cycling after about 3.5 hr operation, indicates that the "worst case" situation, which must be dealt with in the period immediately after startup with a fresh feed bed, occurs with beds having high graphite concentrations. It also indicates that the "equilibrium" period of the run (higher SiC coated fuel particle concentrations) is much more manageable in terms of operation and presents few problems relative to the startup period.

Torch ignition attempts with varied amounts of fresh feed size graphite and particle beds were not successful. It is felt that the present CO torch system is limited to heating small beds to the ignition temperature. Both the large bed material volume and the high CO_2 gas rates required to fluidize the bed create heat losses greater than the heat input available with the present torch system. Major torch system revisions and testing would be required to demonstrate fresh feed full-bed startup; therefore, the standard torch startup with coke will be used until the induction heating system is installed.

Preliminary testing was performed on the 20-cm primary burner product pneumatic transport system. These initial experiments have demonstrated that for identical burner operating conditions, particle breakage is minimized by:

1. Increasing the rate of product mass loading.
2. Decreasing the transport gas flow rate.
3. Increasing the batch size of material transported.

The minimum breakage obtained was 1.1% with product mass flows of 50 kg/min in a 1.37-in.-I.D. tube using 105 ft^3/min of transport gas.

Product removal through the 0.5-in.-diameter cone vertex outlet was very rapid for high particle concentration final beds. Approximately 15 kg/min of final bed material were removed by gravity when the bed was fluidized. However, graphite material in the fresh feed upper size range bridged and plugged the 0.5-in. outlet. The 40-cm prototype distributor design was subsequently revised to allow enlarging the diameter of the cone vertex opening. Cold tests are planned to analyze bed removal with outlet diameters of up to 1.0 in.

The reference product take-off valve has been changed to a knife (self-cleaning) edge slide valve for on-off control, rather than a rotary valve (Ref. 4-1, Section 4.1.2.5). This decision is based on several factors:

1. The necessity for high solids loading, when using pneumatic transport, to eliminate excessive particle breakage.

2. Past problems with rotary valves, including bridging and binding of the rotor when using the tight tolerances necessary to prevent excessive gas leakage.

3. The current batch cycle (Ref. 4-1, Section 4.1.2.1) does not require product removal except at the end of the run with on-off control.

For longer operating cycles (over 24 hr) continuous or semicontinuous operation will be necessary. An intermediate hopper may be necessary to allow this type of operation and to maintain the high loadings necessary to prevent excessive particle breakage.

Bench testing of the pressurized, dense-phase pneumatic fines recycle system indicated that the rotary valve/single fines hopper combination would not hold sufficient pressure to transport fines against the burner bed back-pressure. Good pressurized fines transport was achieved when the rotary valve was removed and the hopper sealed. The dual pot system presently being installed will be included in burner runs in the next reporting period.

Installation of a 20-cm plexiglas column is complete and cold testing of varied distributors and bed internals is to be initiated. Observation of bed removal rates with different sized product lines and fluidization characteristics with several conical distributors will be emphasized. The relation of gas/solid contact, solids mixing, and fines carryover to differing in-bed and above-bed internals will also be observed. In addition, qualitative performance of an above-bed gravity fines recycle system will be briefly evaluated as part of the glass work.

4.2.2. Prototype Primary Burner

4.2.2.1. Heating System Design

A two-zone induction heater is being evaluated as a means for providing the startup capability for startup of a normal 0.7 fuel element bed and for reignition of a whole bed after a process upset. This two-zone heating system will also provide additional flexibility in burnout of the bed, when the bed height shrinks substantially thus reducing the effective heat transfer surfaces. Normally only the lower induction zone will be utilized for startup and bed burnout; for a whole bed startup situation, both the lower and upper zones will be used for heating.

4.2.2.2. Temperature Transient Analysis

A computerized mathematical burner model, utilizing the TAC2D computer code (Ref. 4-2), is employed to analyze the startup capability for the shorter startup bed based on the revised operating cycle (Ref. 4-1). This model also includes the following.

1. 140-kW M-G set power input at 88% efficiency (∿150 kW of developed power at the susceptor).

2. The fully remote clamp, which behaves as a substantial heat sink during bed startup.

3. Conduction and radiation losses to the top and bottom of the burner.

4. A 40-in. susceptor heated zone (the lower zone) for heat transfer.

Figure 4-5 shows the temperature transients for the susceptor, the vessel wall, and the bed. The bed reaches 800°C in approximately 45 min and is ready for ignition at the introduction of oxygen. Figure 4-6 shows the transient response curves for the Grayloc fully remote hub and clamp assembly for the same period. A maximum temperature gradient of 650°F between the hub and clamp occurs after 2600 sec of startup. The large temperature gradient produces undesirable high thermal stress in the remote clamp assembly that substantially reduces the life of the clamp especially in a batch cycle operation. Auxiliary heating is required to reduce the clamp-to-hub gradient to around 200° to 300°F. A 30-kW electric heater system is being designed to supply heat to the clamp.

4.2.2.3. Experimental Heat Transfer Coefficient Measurement

For the fresh feed condition, the bed-to-wall heat transfer coefficient, h_i, was measured from the steady-state combustion portion of a 20-cm primary burner run (Run 15) with the perforated cone distributor. The overall h_i measured was on the order of 95 Btu/hr-ft^2-°F, with the local h_i values running as high as 100 to 110 Btu/hr-ft^2-°F near the bottom and middle portion of the fluid bed and tapering off to ∿60 Btu/hr-ft^2-°F near the top of the bed. Also, with the present mode of burner operation, the overall h_i drops to ∿60 Btu/hr-ft^2-°F toward the end of burnout when the reduction in the oxygen supply lowers the superficial velocity in the bed, possibly decreasing the convective motion of the fuel particles in the bed.

For the burnout phase condition the preliminary h_i for a "particle" bed with 2% carbon was measured utilizing the unique temperature control capability in the present 10-cm secondary burner. At a bed temperature of 800°C and 2.5 ft/sec superficial velocity, the particle bed has an overall

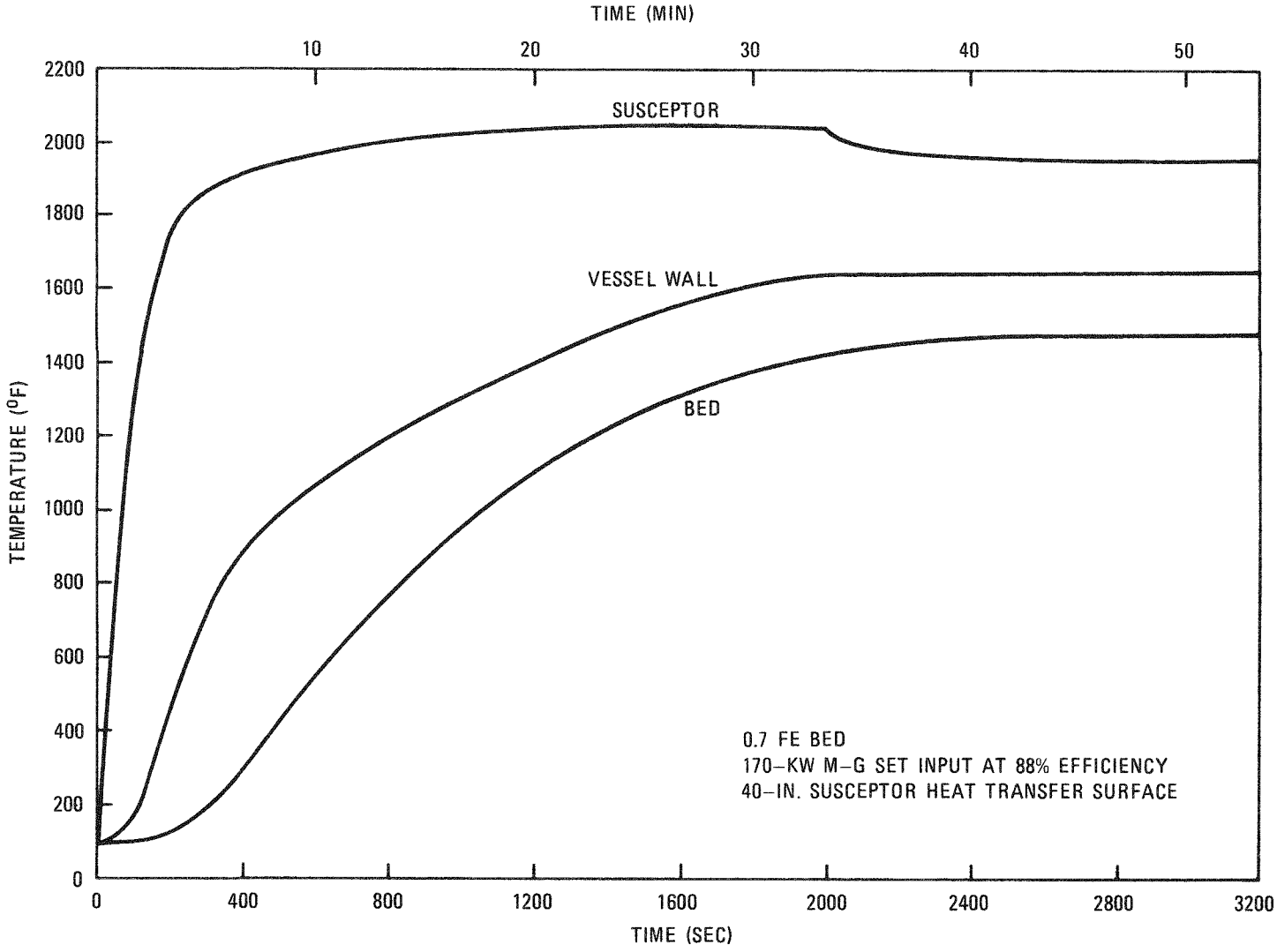

Fig. 4-5. Startup temperature transients

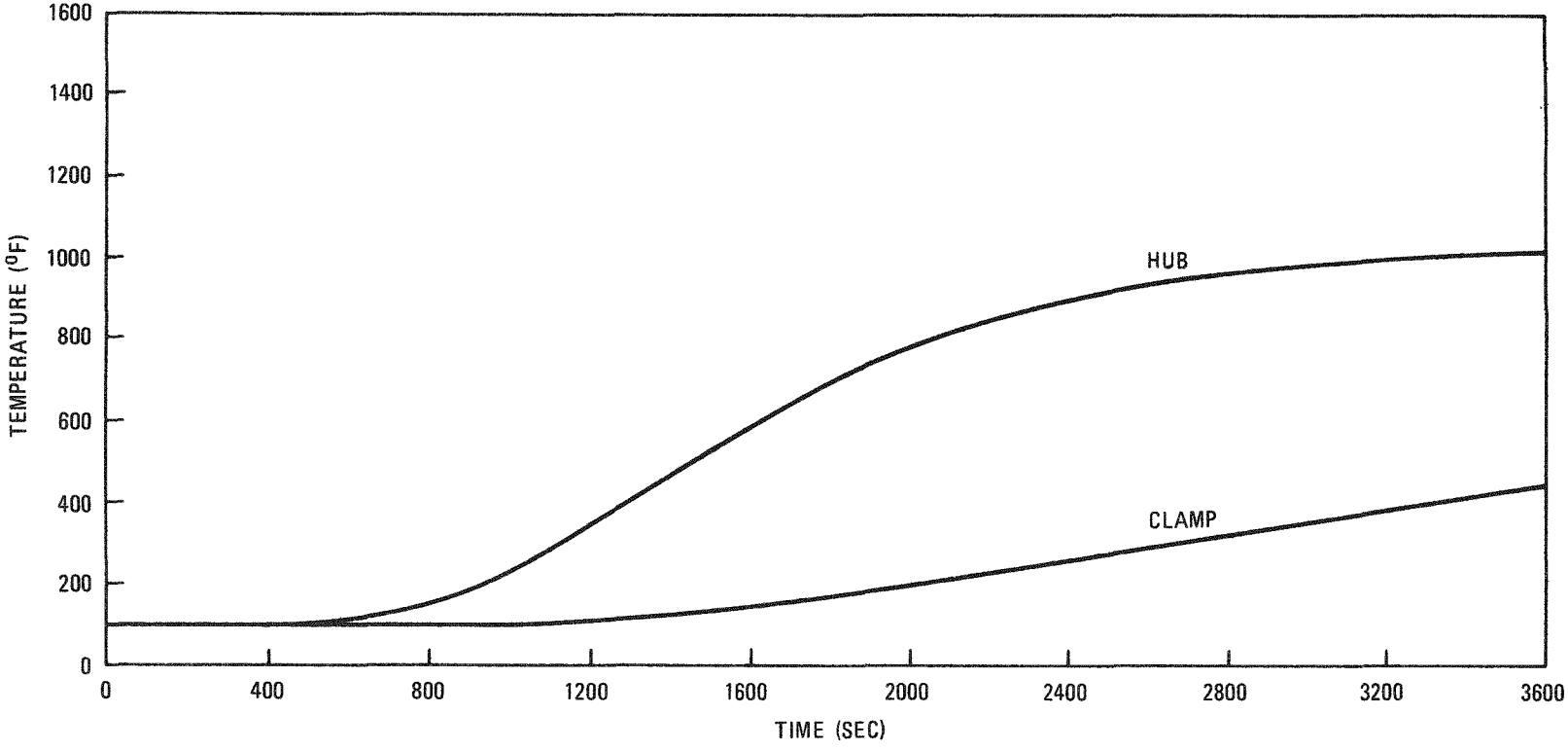

Fig. 4-6. Grayloc remote clamp and hub assembly temperature transients

h_i of 40 to 50 Btu/hr-ft^2-°F. This h_i value will be used in the burnout phase bed temperature control design.

4.2.2.4. Vessel Configuration

Figure 4-7 shows the configuration of the prototype primary burner after incorporating design review comments. The two areas that were modified were the vessel support and the bottom inlet of the cooling jacket. The ring-stiffened gusset design (Ref. 4-1, Fig. 4-2) was susceptible to thermal fatigue and has been replaced by a slotted circumferential skirt designed to accommodate a temperature gradient of 1530°F between the vessel and ambient while maintaining acceptable stress levels. Preliminary structural and thermal stress analysis confirms that the support will perform satisfactorily. The lower cooling shroud inlet was raised above the remote clamp. This simplifies the design, thus minimizing sealing surfaces and potential leakage. Transient and steady-state thermal analysis of the distributor plenum (Ref. 4-1, Fig. 4-14)) indicated that the stresses due to gas pressure and thermal stresses will be acceptable. Weld locations were positioned to minimize thermal fatigue.

4.3. SECONDARY FLUIDIZED-BED COMBUSTION

Work on the secondary burner development program has continued to support the prototype secondary design effort by testing out design concepts.

4.3.1. 10-cm Secondary Fluidized-Bed Combustor

The bed removal system and the off-gas filtration system were evaluated in depth and recommendations were made for future use of these systems. A burner run was made to test these recommendations and to provide data for the prototype design effort.

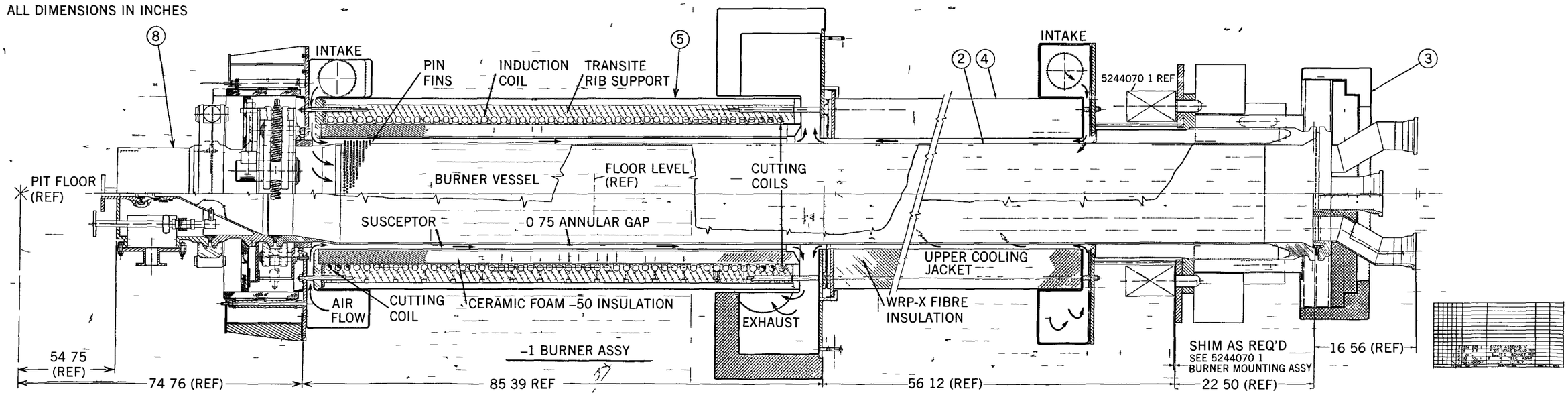

Fig. 4-7. Primary burner assembly

4.3.1.1. Evaluation of the High-Temperature Bed Removal System Integrated with the Pneumatic Transport System

The product removal device for the secondary burner consists basically of a circular valve that seats flush with the burner wall just above the inlet gas distributor. Product flows through the valve into a pneumatic solids conveyor, in which it is transported to the next step in the flowsheet, the leachers. This system has been utilized in making 25 secondary burner runs, during which time several improvements have been incorporated in the design.

4.3.1.1.1. Design. The product removal system was designed with the following features in mind:

1. Use of a distributor plate.
2. Ability to empty the burner quickly.
3. Ease of interface with a pneumatic transport system.
4. Minimum internal burner ledges, etc., which could cause holdup.
5. Remote operability.
6. Simplicity.

The system (illustrated in Figs. 4-8 and 4-9) consists of a 1-in. exhaust valve and a mating valve seat (welded into the burner wall) from an air-cooled, spark ignition engine. The valve is opened and closed by a double acting pneumatic cylinder. The valve stem is supported by a standard valve guide equipped with a nitrogen purged seal.

All materials exposed to high temperatures are Hastelloy-X with the exception of the product valve and seat, which are forged stellite.

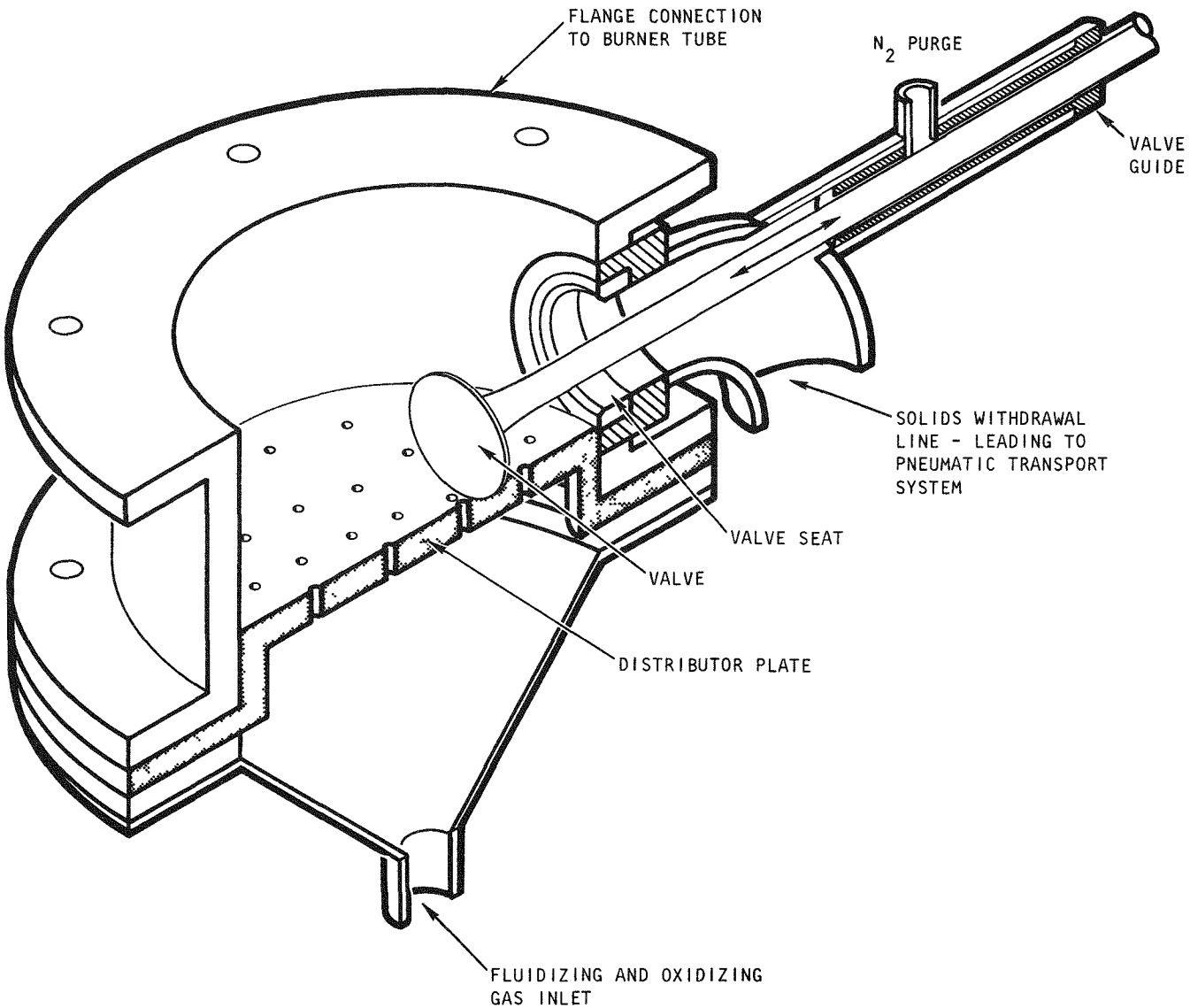

Fig. 4-8. High-temperature bed removal system for 10-cm secondary fluid-bed burner

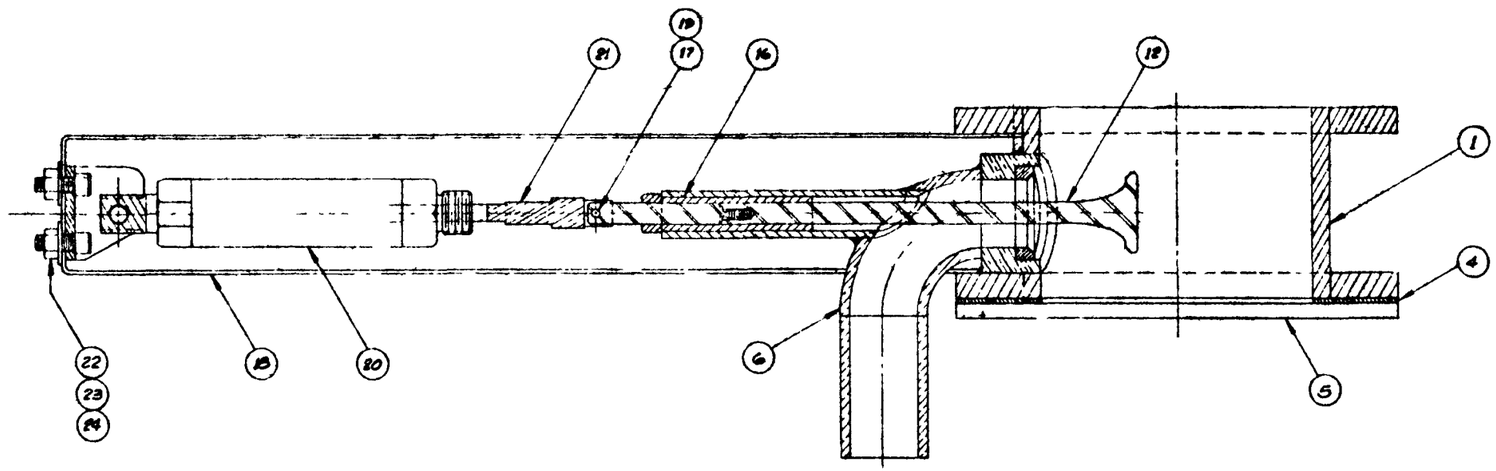

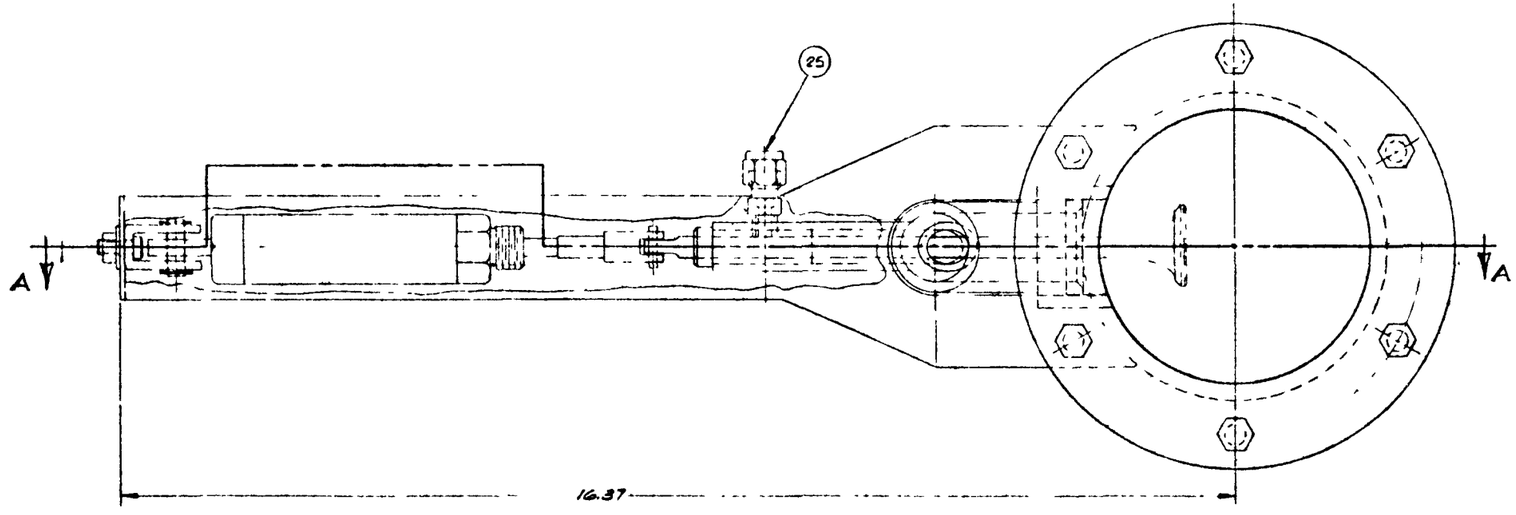

	1	-25	220002-25	SWAGELOK FITTING 1/4 TUBE TO 1/8 NPT		316 SST
	2	-24	-	-24	HEX NUT 1/4 20	
	2	-23	-	-23	WASHER, 1/4" PLAIN	
	2	22	-	22	BOLT 1/4 20×1/2 LG	
	1	-21	-	21	VALVE ACTUATOR EXTENSION 1/2 DIA × 1 3/16 LG	DRILL ROD
	1	20	-	-20	VALVE ACTUATOR (DIGIT AIR CYL FTM 3/4-2)	
	2	-19	-	-19	RETAINER RING	
	1	-18	-	-18	SUPPORT BRACKET 1/16 PLATE	304L SST
	1	-17	-	-17	PIN 5/16 DIA × 5/8 LG	DRILL ROD
	1	-16	-	-16	VALVE GUIDE (MODIFY), REPCO	113-109-401C
1		-15	-	15	VALVE EXTENSION, 5/16 DIA × 2 1/2 LG	DRILL ROD
1		-14	-	-14	VALVE EXTENSION, 5/16 DIA × 2 3/8 LG	DRILL ROD
		-13	-	-13	VALVE, REPCO (MODIFY)	113-109 G12
X	1	12	-	-12	VALVE ASSY	
1		-11	-	-11	GUIDE LOCATOR, 3/4 DIA × 2 7/8 LG	304L SST
1		10	-	-10	PIPE, 1 NPS × 2 1/4 LG SCH 40S	
1		-9	-	-9	ELBOW, 1 NPS 90° SCH 40S	
1		-8	-	-8	VALVE SEAT, 1.380 DIA × 11/32 LG	WELLITE W130
1		-7	-	-7	PIPE BOSS, 1 1/2 DIA × 1 1/4 LG	304L SST
X	1	-6	220002-6		DUMP VALVE WELDMENT	
	1	-5	220003-1		DISTRIBUTOR PLATE	
	1	-4	220002-4		GASKET	
2		-3	-	-3	FLANGE, 6.50 DIA × .98 THK, HASTELLOY X	AMS-5536
1		-2	-	-2	TUBE, 4 NPS SCH 40S × 2 3/4 LG	
X	1	-1	220002-1		BODY WELDMENT	
			220002		BURNER DUMP VALVE ASSY	
	-1	ITEM	PART NO.		DESCRIPTION	MATL / MATL SPEC

Fig. 4-9. Burner dump valve assembly

The design of the distributor plate (Fig. 4-10) is based on the methods presented in Ref. 4-3. The general criterion is that the pressure drop across the plate must be the maximum of the following two values:

1. 10% of the bed pressure drop (35 cm H_2O).

2. 100 times the pressure drop encountered in gas expansion into the distributor plenum.

The maximum is calculated to be 35 cm H_2O. Evolution of the distributor plate design is included in the discussion of operating experience. A plot of flow versus pressure drop for the distributor plate is shown in Fig. 4-11.

The transporter is of the vacuum type for the following reasons:

1. Vacuum transport is inherently cleaner than pressure transport due to the fact that leaks will not spray material about, as is the case with pressure transport.

2. Burner cleanout through the product removal valve is aided by the slightly negative pressure at the valve outlet.

In operation, the product flows essentially by gravity through the partially opened product valve into a moving air stream, as shown in Fig. 4-12. When ∿90% of the product has been removed, the product valve is opened fully (2 in.), followed by actuation of the distributor plate sweep and closing of the air supply valve. This causes the transport air to be drawn through the burner product valve, effecting a positive air sweep through the burner tube and valve.

The transport line is horizontal for 13 ft, vertical for the next 17 ft, and then horizontal for the 10-ft run into the filter receiver. The tube turns have a short radius (6 in.) in all cases. The transport pump is

a 150 ACFM positive displacement type with a maximum suction vacuum of 15 in. Hg (limited due to pump cooling requirements). The line size is 1-1/2 in., giving a superficial line velocity of 150 ft/sec when the pump suction is at 8 in. Hg and 100 ft/sec when the pump suction is at 14 in. Hg.

4.3.1.1.2. Burner Run Operating Experience. The first 13 burner runs using the high-temperature bed removal valve were made before the pneumatic transport system was installed. The runs were made from December 1973 to June 1974. Data from these runs are therefore related only to distributor plate performance, as the bed removal valve is designed for use with a pneumatic transporter.

In the first two runs, a distributor plate with 21 holes (1/16-in. diameter) was used. This plate, which was borrowed from the primary burner, gave good burning characteristics, and no hot spots were noted. When the bed was removed by gravity through the product valve, a heel of ∿2500 g remained. This heel was pierced by jetting holes from the distributor plate and defluidized. A wire mesh laminate was then tried as a distributor, but thermal stresses buckled it during the burner run. Returning to a drilled distributor plate, the jetting behavior was reduced by increasing the number of holes to 71 and decreasing the diameter to 0.025 in. to reduce the jet strength of each hole. The heel with this plate averaged 830 g in six runs (maximum 1589 g and minimum 403 g).

A distributor plate burn-through occurred during one startup. The burner at that time had a resistance heater, which necessitated low burner gas flow (0.6 ft/sec) at startup to achieve the minimum ignition temperature. This low flow led to stagnation and a hot spot burned through the plate. The induction heater was then installed, which allowed reasonable startup flows (2 ft/sec). No further startup problems have occurred due to poor heat removal capabilities.

It is interesting to note that the distributor plate failure did not cause any damage to the product removal valve section. Replacement of the plate served to repair the burner. Also, while making a batch primary burner

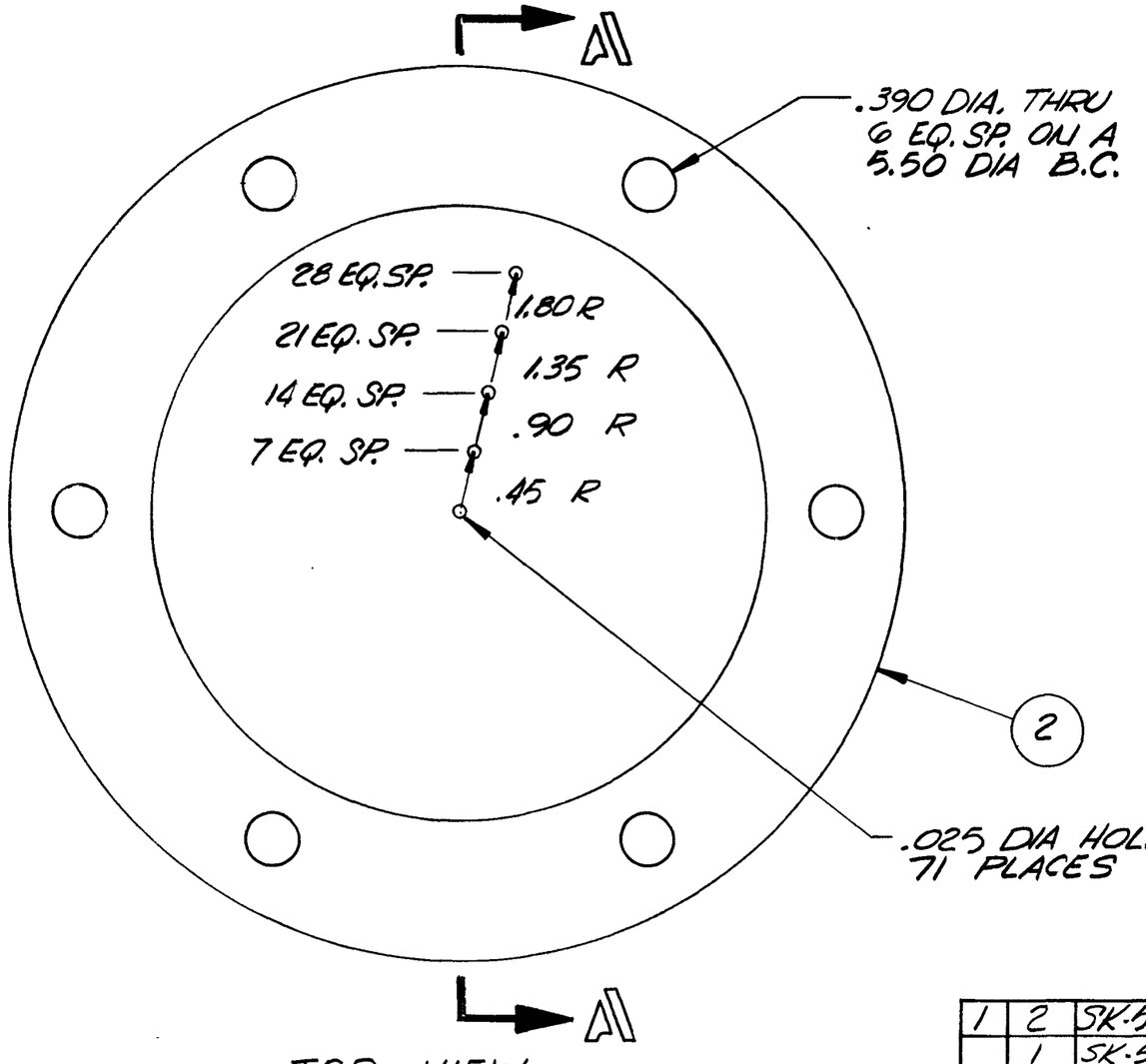

TOP VIEW

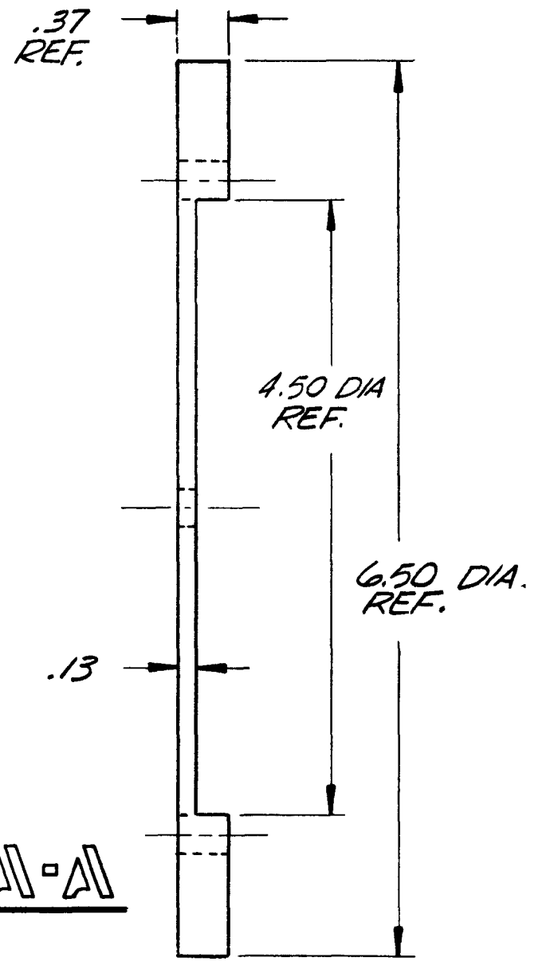

SECTION A-A

ITEM	PART NO.	DESCRIPTION	MATL	
.1				
1	SK-5246015	DISTRIBUTOR PLATE		
2	SK-5246015-2	PLATE, 6.50 O.D. x 4.50 I.D. x .37	HASTELLOY "X"	AMS 5536

Fig. 4-10. Distributor plate, secondary burner

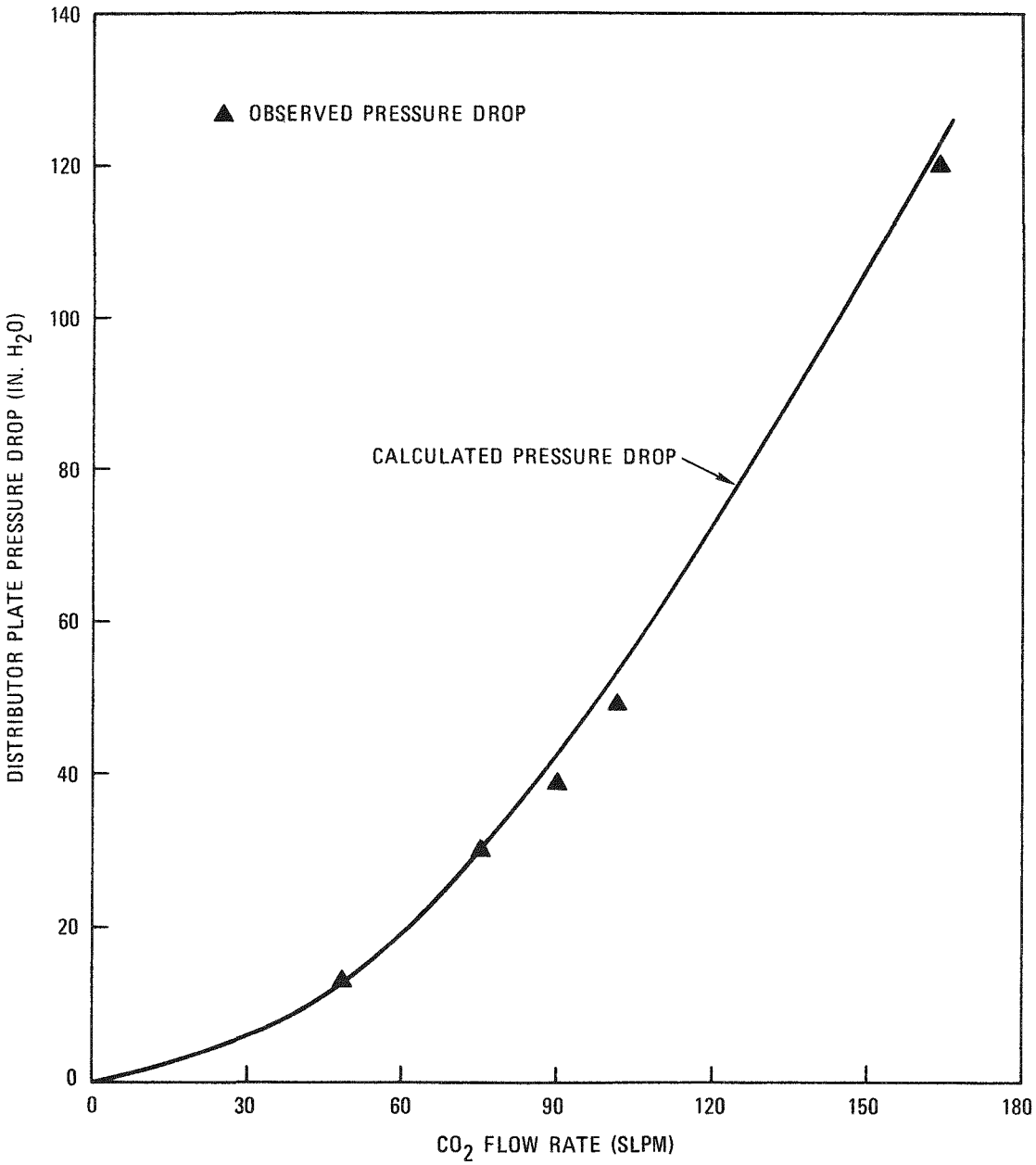

Fig. 4-11. 10-cm secondary burner distributor plate flow - pressure drop characteristics (plate is 1/8 in. thick with 71 holes 0.025 in. in diameter)

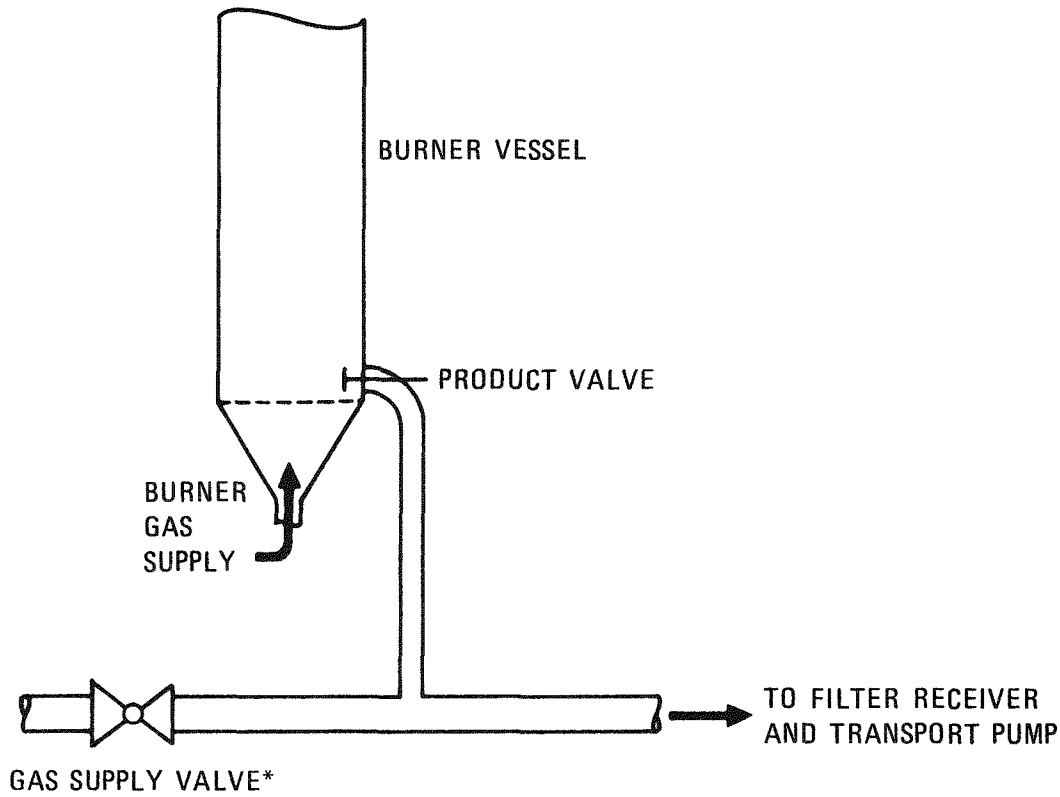

*OPEN DURING REMOVAL OF INITIAL ~ 90% OF PRODUCT TO GIVE SUFFICIENT AIR FLOW; CLOSED DURING CLEANOUT OPERATION TO GIVE A POSITIVE AIR SWEEP THROUGH THE BURNER TUBE AND PRODUCT VALVE

Fig. 4-12. Product removal operational modes

run, a burn-through of the product removal spool piece occurred due to bed stagnation. In spite of extensive damage to the burner wall adjacent to the product valve, the valve was still operable and seated smoothly. This shows that the burner valve assembly could withstand temperature extremes encountered during burner upset conditions.

The pneumatic transporter was installed in June 1974 and has been used in all subsequent runs. It was found that opening the product valve fully resulted in an excessive solids-to-air ratio, such that choking occurred in the vertical section of the transport tube.

The valve was then tried at a variety of initial openings (1/8 to 3/8 in.) for the bulk of product removal, followed by opening the valve fully in each case for burner heel cleanout. Openings of 3/16 in. and smaller were found to be subject to bridging of the product as it tried to exit through the valve. Openings of 3/8 in. and larger were found to cause too high a solids-to-air ratio, resulting in choking flow in the vertical transport tube. Initial openings of 1/4 in. were found to be satisfactory throughout seven separate runs. The bulk of the bed is removed in the first several minutes through the 1/4-in. opening.

Burner heel cleanout is accomplished using a gas sweep nozzle arrangement that penetrates the burner tube above the plate. A 1/4-in.-O.D. by 1/8-in.-I.D. tube is welded closed on one end and swaged into place perpendicular to and at the same elevation as the valve stem, parallel to the distributor plate and crossing the burner tube center line. High-pressure (80 psig) gas is routed through 15 holes (1/32-in. diameter) in the sweep tube, yielding a total flow of 400 SLPM. The holes are arranged such that five holes point straight down and the other ten point 45° either way from straight down. The holes are equally spaced across the burner diameter.

This distributor plate sweep is actuated in discrete 2-sec pulses when the product valve is opened fully (2 in.). The heel (averaging 800 g, as noted earlier) is blown up into the burner and flows through the product

valve to the transporter in dilute phase transport. In the eight runs utilizing the sweep, the distributor plate was completely cleaned off. The only heel remaining in the burner was a dust precoat on the filters and the dust clinging to the vessel walls.

In four of the last runs, the product was transported through the 1/4-in. valve opening for varying time durations prior to full opening for cleanout. In all cases, 5 min of heel cleanout time was utilized (with the valve fully opened and the sweep utilized).

In the first run, 93% of the product (∿11 kg total) was removed in 5 min, whereas 84% was removed in the second run in 5 min. During the third run, 90% was removed in 2 min, and during the fourth run 74% was removed in 1 min. It appears that 2 min gives sufficient time for the bulk of the product to be removed, and 5 min is adequate for heel removal. This 7 min is small compared with the 2 to 3 hour batch cycle times. These numbers indicate that the product is removed at about 5 to 6 kg/min during the initial product removal stages with a 1/4-in. valve opening.

The vacuum-pneumatic transport system operates with a total pressure drop of ∿14 in. Hg during the initial dump operations (with loadings of ∿2 lb solid/lb air). The pressure drop during the initial stage is broken down as follows:

Air flow in transport tube	2 in. Hg
Solids transport in transport tube	5 in. Hg
Main filters	4 in. Hg
Pump prefilter	3 in. Hg
	14 in. Hg

When the system is transporting the final heel, with a negligible loading, the total pressure drop is ∿8 in. Hg as follows:

Air flow in transport tube	2 in. Hg
Main filters	3 in. Hg
Pump prefilter	3 in. Hg
	8 in. Hg

It is planned to test secondary burner product pneumatic transport on the solids handling test rig to determine saltation velocities, choking loadings, pressure drops, wear rates, etc. Product removal with larger transport lines will be tried in an attempt to lower the solids-to-air ratio, thus enabling larger initial product valve openings. Product receivers representative of prototype design will be utilized on this system.

4.3.1.1.3. Conclusions and Recommendations. It is concluded that the high-temperature bed removal system incorporating a valve and seat arrangement in the burner tube, a flat multiorifice distributor plate with a sweep provision, and a vacuum-pneumatic transport system is capable of rapid and complete batch bed removal at high temperature. The system causes no interference with normal burner operation and does not permit any ledges or pockets of static material since it is flush with the internal diameter of the tube. The system is also well suited to remote operation and has only one moving part, which results in high mechanical reliability. It is therefore recommended for future use on larger scale burners by direct scaleup.

4.3.1.2. Evaluation of In-Vessel Off-Gas Filter System

The 10-cm secondary burner incorporates in-vessel filters to separate the off-gas flow from the particulate fines elutriated from the fluid bed. Sixty-four batches of crushed particles have been processed through the 10-cm secondary burner, providing a significant amount of performance data to aid in larger burner design. This section analyzes the data covering such areas as the filter pressure drop dependence on process variables, the high-temperature metallurgy of the filters, and controls required to avoid excessive filter temperatures.

4.3.1.2.1. Filter System Components. Figure 4-13 shows a cross section of the 10-cm secondary burner filter chamber. The filters are 2-3/4 in. O.D. by 36 in. long with 1/8-in.-thick walls. They are made of 316L stainless steel, porosity grade H (largest pore size is 12 μm and the mean pore size is 5 μm). For gas filtration, they remove 100% of the 1-μm particles and 98% of the 4-μm particles. There are two filters in the chamber, with a total surface area of 4.6 ft^2.

The basis for selection of grade H filters is presented in Ref. 4-4. Grade H is the finest pore size available and is attractive for use with fine powders of the type encountered in the secondary burner (up to 5% of the product is less than 44 μm by screen analysis).

Filter blow-back is effected through two 1/8-in. orifices located 1 in. above the venturi plate. These venturis (see Fig. 4-14) are based on a design recommended in Ref. 4-5. The blow-back gas pulse causes a reverse pumping action as it passes through the venturi, drawing filtered off-gas back through the filters. This increases the effectiveness of the blow-back while keeping the volume of gas added to the system at a minimum. In this way, the quantity of burner off-gas is reduced, yielding a decreased load on the off-gas cleanup system. Reducing blow-back gas is also desirable to minimize dilution of the off-gas, which is sampled throughout each run to provide an indication of combustion efficiencies.

During approximately one-third of the 10-cm secondary burner runs, the main blow-back gas supply consisted of recycled burner off-gas. A diaphragm pump was coupled with a surge tank to yield an ∿45-psig blow-back gas supply with essentially the same composition as the gas exiting the burner. This eliminated gas sampling errors associated with the previous practice of using N_2 for the blow-back gas, and thus allowed a more accurate study of burning characteristics. A compressed CO_2 blow-back supply is now available and will probably be used in later applications since it will not obscure the data as markedly as the N_2 supply (burner off-gas is very nearly 100% CO_2 in many cases).

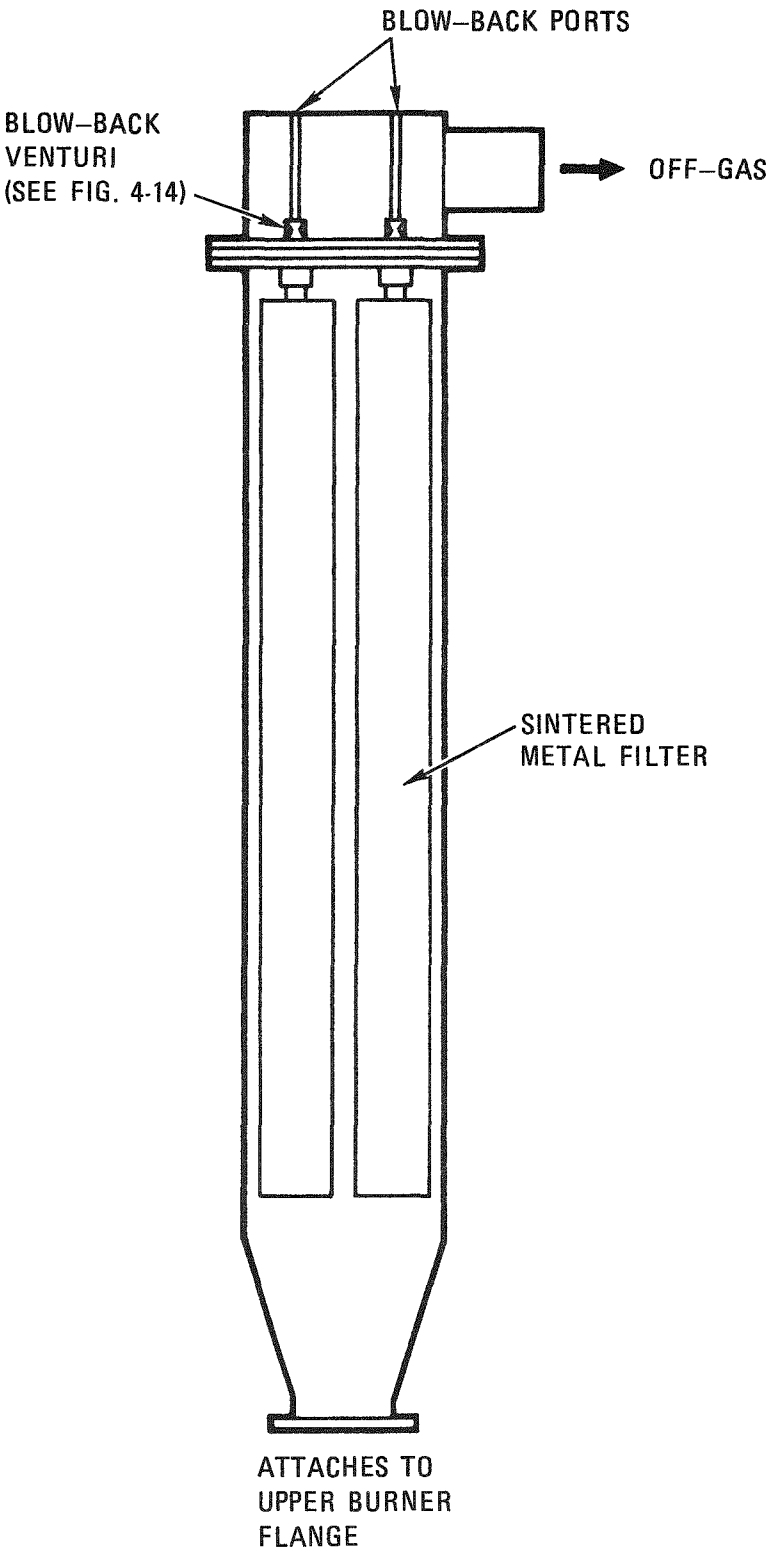

Fig. 4-13. 10-cm secondary burner filter chamber (cross-sectional side view)

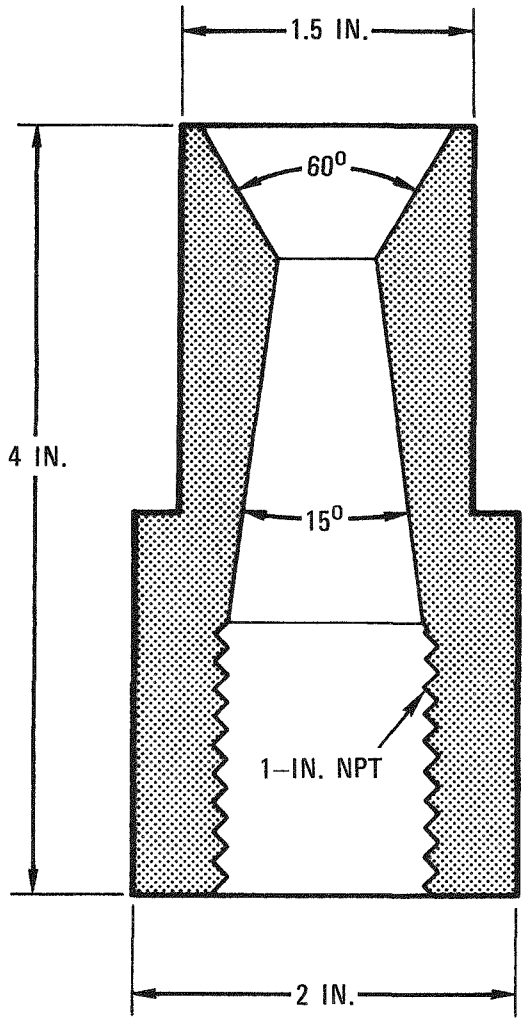

Fig. 4-14. Filter venturi

Blow-back at ∿50 psi through the 1/8-in. orifices yields about 5 liters of gas per each 1-sec pulse. This yielded 15 liters/min in the most recent runs, which is about 10% of the process flow. Keeping the blow-back rate this low precludes pressurization of the burner vessel during blow-back; the filter chamber pressure rise at present is ∿10 in. H_2O during each pulse.

4.3.1.2.2. Operating Experience. The first 40 secondary burner runs were made without filter pressure drop instrumentation. In the next 24 runs the pressure drop was continuously recorded, as were temperatures between the two filters. Table 4-2 contains parameters from 18 runs.

Filter blow-back was used throughout each run, at the frequency noted in Table 4-2. The filter pressure drop increased in the early portion of the run to a maximum, where it remained during the main burning portion of the run. In this constant ΔP period, fines were removed via blow-back at the same rate that they were being re-elutriated into the filter chamber. When the off-gas analysis indicated that the bed was about to burn out (carbon content becoming low), the process gas flow was lowered both to conserve heat in the bed and to allow carbonaceous fines to re-enter the bed more easily.

The filter pressure drop was slowly reduced throughout this burnout period as fines re-entered the bed. An air-actuated vibrator mounted on the filter chamber upper flange was actuated at intervals during this final burning portion to help disoldge fines from the filter chamber. It is definitely effective in this function as seen by increases in O_2 utilization following vibrator actuation.

During Run 42, one of the blow-back pumps stopped functioning about halfway through the run, resulting in essentially no blow-back. The result of this was a quick buildup of fines in the filter chamber, as evidenced by high filter pressure drops.

TABLE 4-2
BURNER OPERATING PARAMETERS

Run	Bed Weight (kg)	Max. ΔP (in. H_2O)	Max. Filter Temp (°C)	Max. Process Flow (SLPM)	Blow-back Frequency (min^{-1})	$\bar{D}p$ Feed (D_{sv})
27	12	4	700	100	1	227
29	13	9	800	100	1	222
30	14	6	700	100	1	258
31	15	6	725	120	1	258
32	15	11	900	140	1	291
33	17	23	900	140	1	291
34	18.5	>50	900	120	1	111
35	20	31	900	140	1	160
36	20	45	800	140	2	145
37	20	25	800	140	2	150
38	18	21	800	160	2	155
39	18	35	800	160	2	167
41	18	45	800	160	2	167
42	18	--	--	160	2	156
43	18	--	--	160	2	120
44	14	15	750	140	3	167
45	14	20	800	140	3	165
46	14	16	800	140	3	165
47	14	18	820	140	3	160
48	14	17	820	140	3	160

The run was terminated when high temperatures (925°C) were noted in the filter chamber, although the bed temperature was only at 700°C. The high temperatures are believed to be caused by carbon depletion of the fluidized bed allowing O_2 to enter the filter chamber and to cause burning of the large amount of fines contained therein. Local temperatures may have been much higher than 925°C because the carbon fines formed a cake surrounding the filters, resulting in poor heat transfer to the filter thermocouple.

At the same time that the high temperatures were noted, the filter pressure drop decreased to about 10 in. H_2O, which is somewhat less than normal when fines are in the filter chamber. The burner was shut down, emptied, and later dismantled.

One of the filters was deformed in its upper portion as if flattened by a hammer. The longitudinal weld seam formed one of the flattened edges and was cracked open as shown in Fig. 4-15. This opening explains the sudden reduction in filter pressure drop.

The most probable cause of the filter failure is as follows:

1. The blow-back system became inoperative, allowing large amounts of fines to build up around the filter, which caused high (∿4 to 5 psig) filter pressure drops.

2. When the fluid bed burned down to a low carbon content, oxygen was allowed to pass through unreacted and to enter the filter chamber.

3. The fines packed around the filters began reacting with the oxygen and generating significant amounts of heat, thus causing localized hot spots due to the static nature of the fines.

4. One of the filters developed a local hot spot that reduced the filter strength sufficiently to allow it to collapse due to the

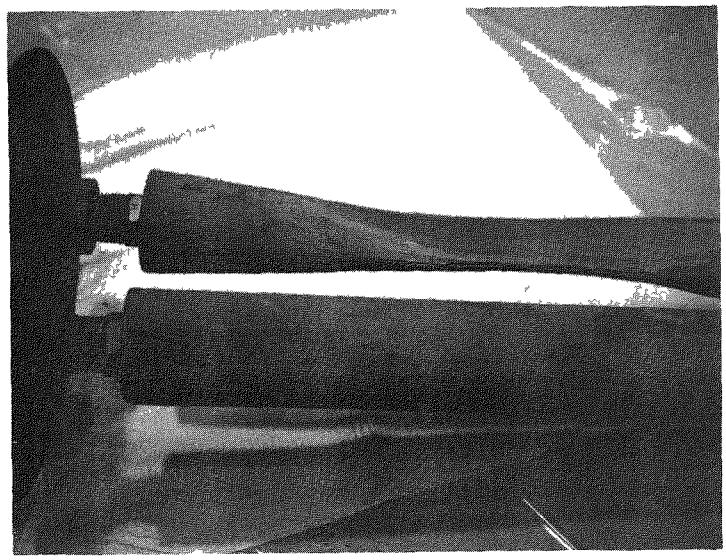

Fig. 4-15. 10-cm secondary burner off-gas filter following Run 42

pressure drop across the filter. When the filter collapsed, the weld seam was put in severe stress and cracked, producing an opening in the filter that quickly reduced the pressure drop to a low value.

In the subsequent run (Run 43), the feed was 18 kg of finely crushed TRISO fertile particles. The <100 μm fraction was 25 wt % and the <50 μm fraction was 10 wt % as compared to values of 11 wt % and 4 wt %, respectively, in previous feeds.

The run proceeded uneventfully with a filter ΔP of 20 in. H_2O (using 60 psi N_2 for blow-back). During the bed burnout phase, when O_2 appears in the off-gas, the filter ΔP suddenly dropped to a very low value, indicating an opening in one of the filters. At this point, the run was terminated.

Subsequent disassembly of the burner revealed that the lower end of one filter had been burned off. Use of the finely crushed feed had left a higher portion of unburned material on the hot filter surfaces throughout the run. When the O_2 front reached the filters, in situ combustion occurred and melted the filter.

To prevent further filter failures, the large fines buildup and the presence of O_2 in the filter chamber when filter temperatures are high must be prevented. The first problem is handled by reducing the bed size to 14 kg and reducing the total flow 15%. This will reduce the fines loading in the filter area. The second problem is handled by reducing flow to bring fines down from the filter chamber when the off-gas CO gets below 5% (indicating the O_2 front is nearing the filter chamber). This lowers the filter temperature caused by the expanded hot bed before the O_2 enters the chamber. Another control is to not use finely crushed feed.

Five runs have been made since these two filter failures with no further filter problems encountered.

The long-term buildup of fines in the filters is of concern as it tends to raise the pressure drop. Figure 4-16 illustrates the filter pressure drop measured between runs (no fluid bed, only gas flow) as a function of the number of runs made. It appears that the first run added a precoat that approximately doubled the ΔP observed with a new filter. Modest increases followed after sixteen runs, which can be attributed either to a larger precoat or migration of material into the filter voids.

The precoat is composed of colonies of fine particles that congregate at the filter pore opening, yielding much finer filtration than the porous material. This minimizes filter clogging by keeping small particles out of the filter internal pores.

It is important to note that the filter and cake pressure drop during the run is approximately ten times the drop across the filter alone. Thus a large amount of interstitial pore clogging is allowed before the pressure drop during the run is significantly affected.

4.3.1.2.3. Metallurgical Evaluation of Run Data. To determine the expected useful life of the filters, a set of SS316L filters was subjected to 30 typical burner cycles. A sample was cut from each end of the filters, representing the extremes in temperature to which the filters were subjected. During each cycle (1-1/2-hr duration), one sample was at 800°C and the other sample was at 300°C. The gas atmosphere was 20% CO, 70% CO_2, and 10% N_2 at 15 psia. The normal gas flow through the filters was 0.85 $ft^3/min/ft^2$.

The filters were used to remove fine carbon and ThO_2 (-40 μm) from the gas stream. To prevent carbon buildup on the filter surfaces, a backflow of gas was effected every 2 min for a short duration (1 to 2 sec).

Both samples were submitted to Metallography. The hardness of the sample exposed at 800°C was measured at DPH 250, and the 300°C sample was measured at DPH 140.

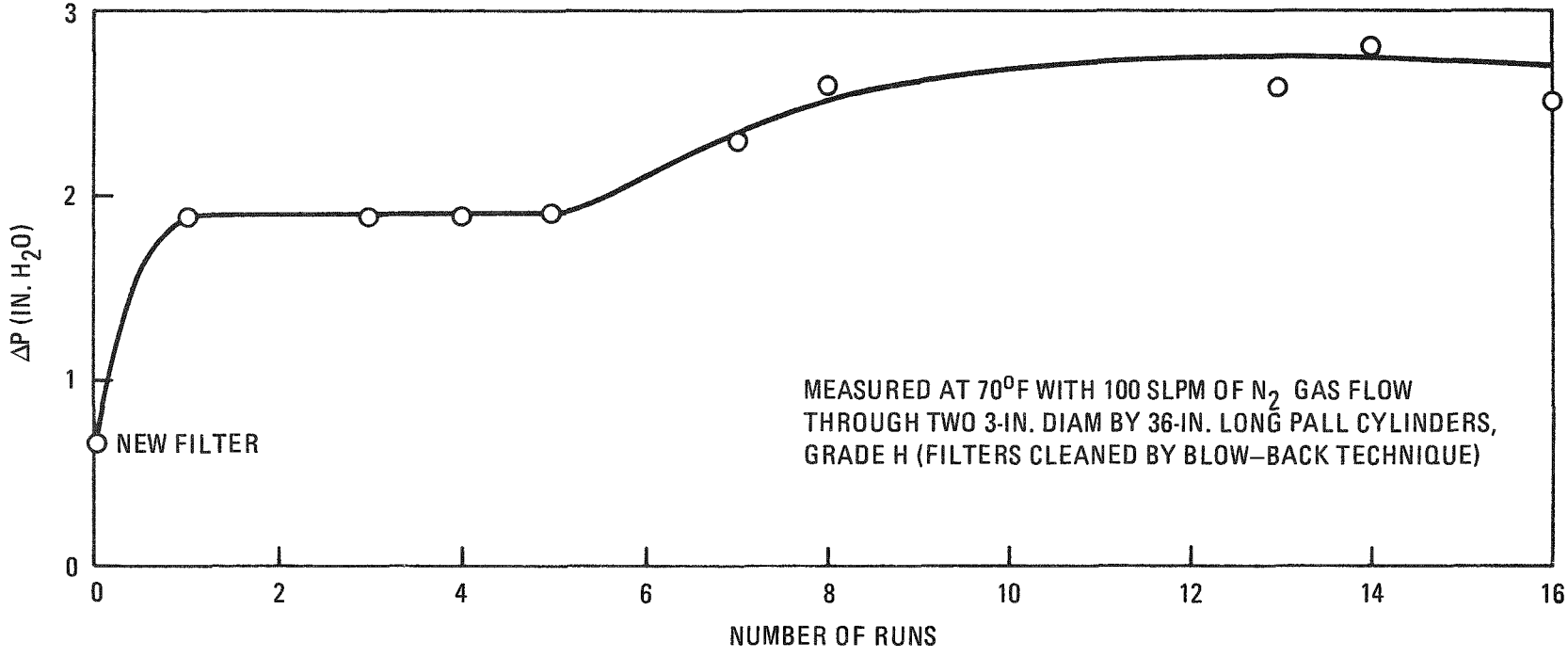

Fig. 4-16. Filter pressure drop prior to 10-cm secondary burner runs

The following observations were made from photomicrographs (Figs. 4-17 through 4-20):

1. The section exposed at 300°C revealed no signs of oxidation or carburization and no signs of significant microstructural changes.

2. The section exposed at 800°C revealed significant oxidation attack (∿0.5 mil on each side). Considering that the porous structure is held together by a metal network on the order of 1 to 2 mils thick, approximately half of the "useful" life of the filter is used up. The only significant microstructural change observed in the photomicrographs was precipitation of $M_{23}C_6$ carbides, predominantly at grain boundaries (sensitization).

The above observations are considered normal for type 316L stainless steel. It is not believed that the sensitization phenomenon played any role in the high rate of oxidation at 800°C.

In view of these results, the use of materials such as Hastelloy-X, which is more resistant to oxidation and carburization (in that order), is recommended. Hastelloy-X filters have been ordered and will be tested in the 10-cm secondary burner to determine oxidation rates. Filter manufacturers have indicated that experimental data are the only guide to the actual operating life of these Hastelloy-X filters.

4.3.1.2.4. Statistical Evaluation of Run Data. The data from 18 recent runs were examined to determine which process variables affect the filter pressure drop most significantly. Minimizing this pressure drop accomplishes two tasks:

1. Reduction of the absolute pressure of the burner (which is 30 psia maximum).

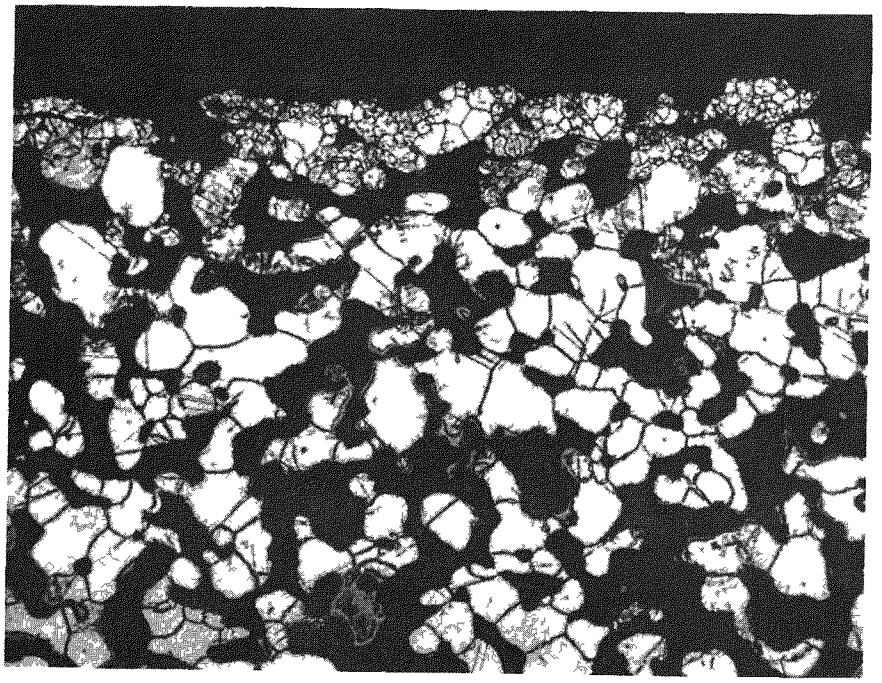

M40627-3

Fig. 4-17. Filter cross section, 800°C sample (250X)

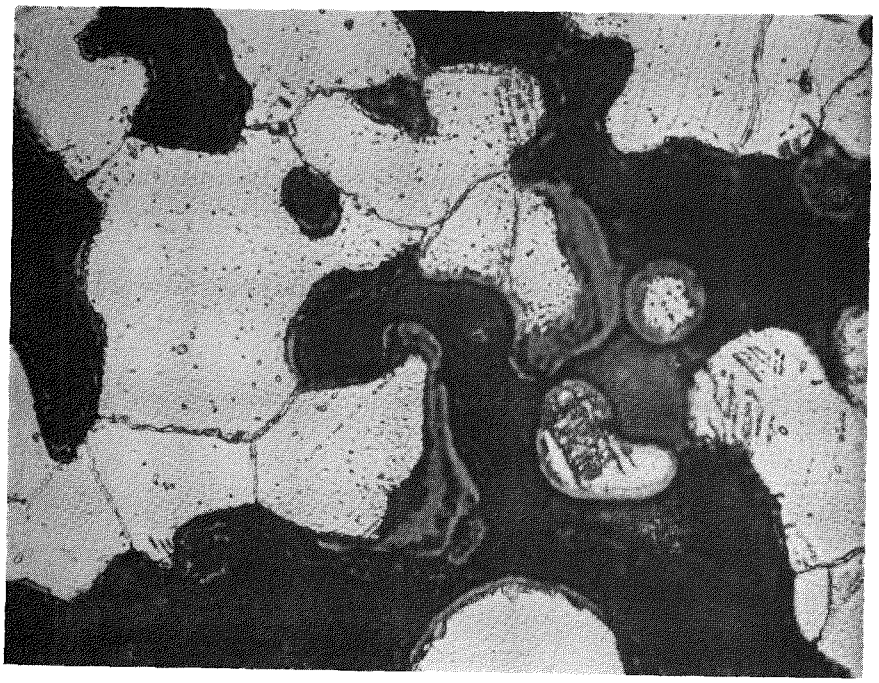

M40627-4

Fig. 4-18. Filter cross section, 800°C sample (1000X)

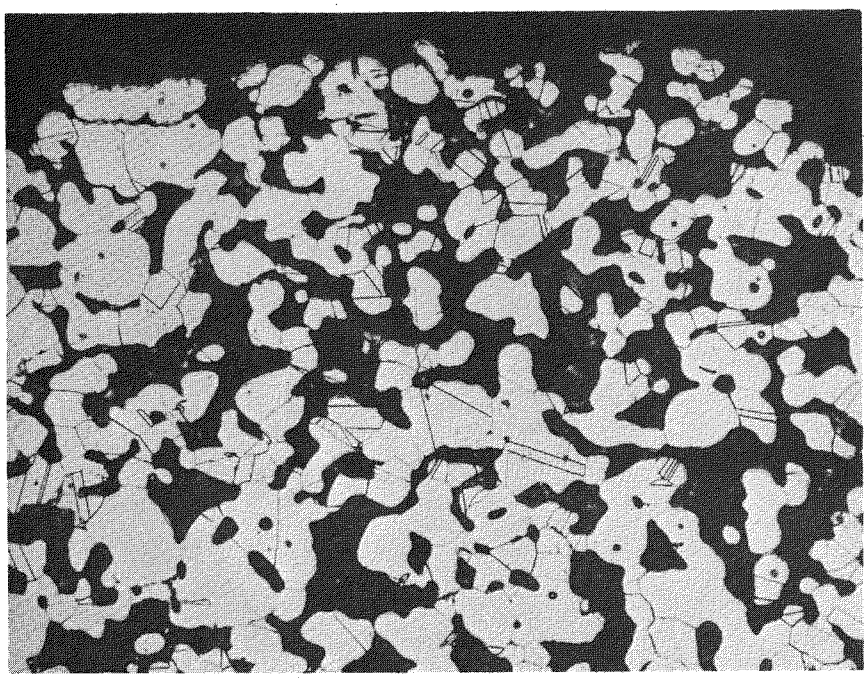

M40628-1

Fig. 4-19. Filter cross section, 300°C sample (250X)

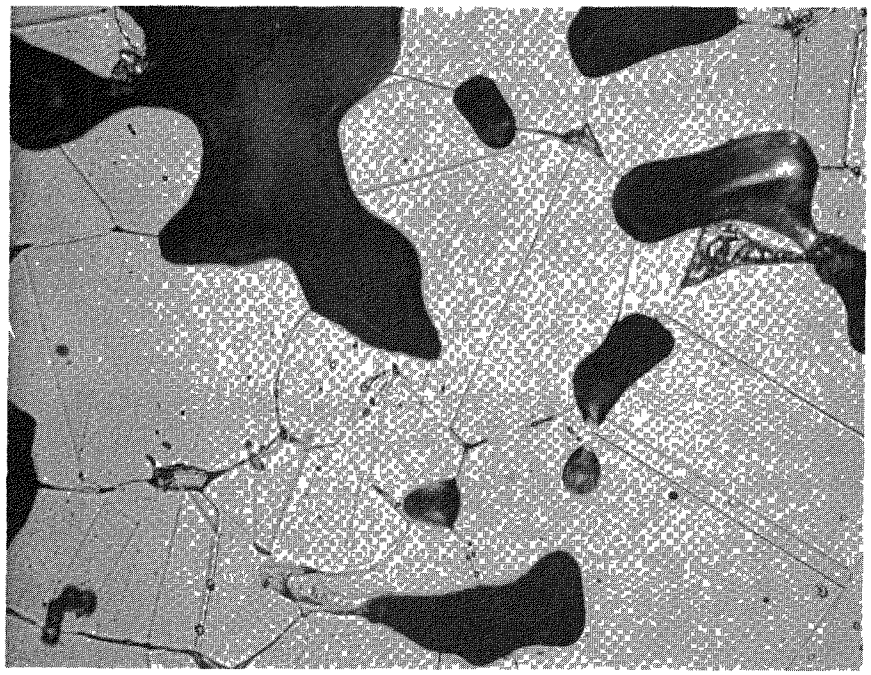

M40628-2

Fig. 4-20. Filter cross section, 300°C sample (1000X)

2. Reduction of the pressure-induced stress on the filter to help prevent collapse during high-temperature operation, as in Run 43.

The data were analyzed using a multiple linear regression analysis routine on the Tymshare computer. It was found that the filter pressure drop in these 18 runs was approximated by the following equation:

$$\Delta P = -5.9 + 0.16V + 2.4W - 0.13\,\bar{d}_{sv} - 3.8\nu$$

where ΔP = filter pressure drop, in. H_2O,
V = fluidizing gas flow rate, SLPM,
W = fluid bed weight, kg,
$\bar{d}_{sv}$ = fluid bed average particle size, μm,
ν = filter blow-back frequency, min^{-1}.

It was also determined that there is less than a 0.1% chance that the variables examined are not significant with respect to the dependent variable, filter pressure drop. A further calculation provided the information shown below. For each independent variable, a percent change is listed for the hypothesis that the given variable is responsible for deviation of actual data from the multiple linear regression equation.

Flow	50%
Weight	85%
Size	92%
Frequency	50%

A larger number percentage indicates a more positive correlation with the dependent variable; thus, weight and size are more certain to affect the pressure drop than flow and frequency.

Extrapolation of this curve outside the defined range is not strictly allowed, but may be done in a modest step without undue risk. Thus, reducing the pressure drop further from the last few runs (where it was

$\sim$17 in. H_2O) can be accomplished by increasing the particle size or blow-back frequency or by decreasing the bed weight or fluidizing velocity. Particle size cannot be increased without yielding >1% unbroken particles; thus, this variable cannot be modified to lower the ΔP. It should be noted that this gives a definite impetus for maximizing the particle size in the crushing operation. The blow-back frequency can be increased; doubling the frequency should give a reduction of 11 in. H_2O. This is probably too far outside the range of the previous work to be valid, but it does indicate significant reductions. The burner is presently operated with 100 SLPM O_2 and 40 SLPM N_2 (or CO_2) in the main burning portion. There is no reason why this cannot be changed to 100 SLPM of O_2 (without sacrificing burn rate) to lower superficial velocities with a predicted filter ΔP decrease of 6 in. H_2O. It is desirable to maximize bed weight with respect to increasing burner throughput; thus, bed weight should not be changed. From these arguments, further burner experimental runs will include reduced flow rate in the main burning portion and increased blow-back frequency to reduce the maximum filter pressure drop during the run.

The filter maximum operating temperature in the burner runs has been in the 700° to 900°C range. This is excessive and should be reduced both to minimize the metal oxidation rate and to increase the margin of safety from filter collapse due to reduced strength at higher temperatures.

The prototype secondary burner filter chamber was designed with an 18-in.-long expanded space between the main burner tube and the bottom of the filters. This should help reduce filter operating temperature and will thus be incorporated in the 10-cm secondary configuration to give an indication of what reduction is actually attained. Baffles are located in the prototype between each set of two filters (six filters total) to prevent the dislodged fines from simply traveling from one set of filters to another, without reaching the fluid bed.

4.3.1.2.5. Future Work. As noted earlier, further studies to be accomplished on the filter system include: (1) the effect of increasing

the filter chamber length (on both operating temperature and ΔP), (2) the metallurgical behavior of Hastelloy-X filters, and (3) the effect of lower process flow and increased filter blow-back frequency on the filter pressure drop. Items (1) and (3) were investigated in burner Run 49, which is summarized in the following section.

4.3.1.3. Run 49

A batch secondary burner run was successfully made to test several improvements as follows: (1) CO_2 inert gas was used instead of N_2, (2) a prototype-sized feeder was used, (3) an 18-in. filter chamber extension was installed and more frequent blow-back pulses were used, (4) completely automatic heating and cooling systems were used throughout the run, and (5) pure O_2 fluidizing gas was used during the main burning portion of the run. All of these improvements lived up to expectation, yielding a very smooth, stable run with final product containing <0.1% burnable carbon.

The feed for Run 49 was a 14-kg batch of TRISO fertile particles crushed through a double-roll particle crusher system to yield product with a size distribution as shown in Fig. 4-21. Other physical properties of the material are included in Fig. 4-21.

The burner tube was preheated to 900°C using a completely automatic temperature control system. This system modulates the induction coil power output to control the susceptor, burner wall, and fluid-bed temperatures within preset limits (in this case 1100°, 900°, and 900°C respectively, with 15°C dead bands).

With a 40 SLPM purge of CO_2 passing through the burner tube, the feeder was actuated to introduce the crushed particle bed to the burner. The feeder is identical in both type and size to the one specified for the prototype secondary burner (as described in Ref. 4-6). This feeder performed well and will be used in all future runs.

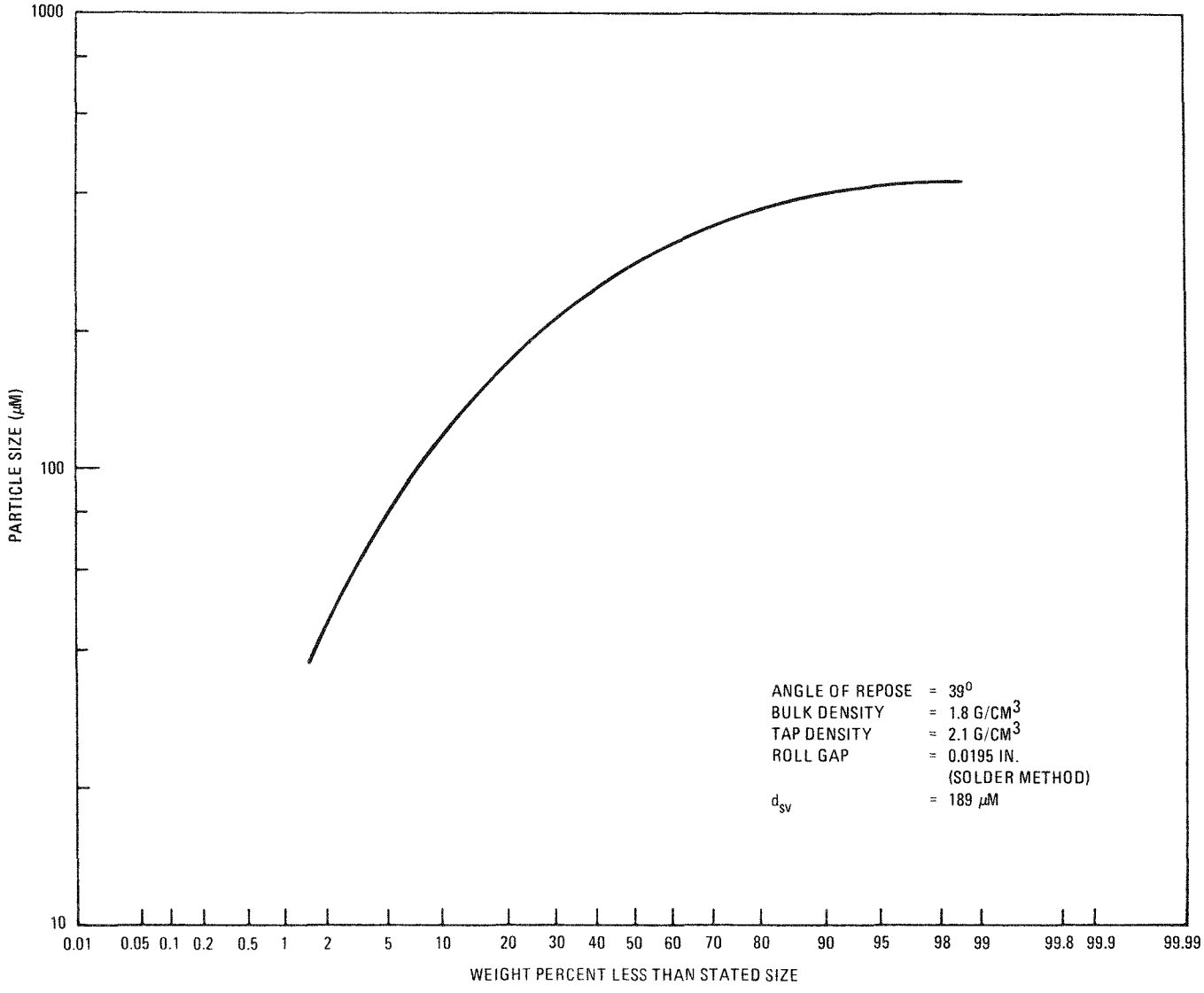

Fig. 4-21. Size distribution for Run 49 feed

The bed was then heated to 700°C followed by ignition. The O_2 flow was automatically ramped to 100 SLPM over a 6-min period. The burner cooling-air rate was automatically controlled to maintain the bed temperature at 900°C. Twenty minutes after ignition, the CO_2 flow through the burner was terminated, leaving only a pure O_2 flow at the inlet. This mode of operation was continued throughout the main burning portion of the run.

No significant change was noticed as a result of the switch to pure O_2 flow. The filter cooled slightly due to the decreased superficial velocity. The filter pressure drop also decreased for the same reason. These are normal indications of lower velocity. There was no O_2 in the off-gas and no bed temperature transients occurred. All of these findings indicate that there is no problem with the use of pure O_2 inlet gas during the main burning portion of the run.

The filters were blown-back every 10 sec with a 1-sec pulse of 50-psig CO_2. This is in accordance with the recommendations made in Section 4.2.1.2 for the reduction of filter pressure drop (increased filter chamber length 18 in., increased blow-back frequency, and decreased superficial velocity). The observed filter pressure drop during the main burning portion was 10 in. H_2O when the total flow was 140 SLPM and 4 in. H_2O when the total flow was 100 SLPM. These values are about one-half the pressure drops encountered in previous runs at these same flows. The recommendations for reducing pressure drop that were incorporated in this run will therefore be used in the future to keep the filter pressure drop at these low levels.

The tail burning portion of the run was begun when the off-gas CO content fell to 2%. Inlet gas flows were then changed to 60 SLPM O_2 and 40 SLPM CO_2. Filter chamber vibrators were actuated every minute to help return fines to the bed. The heating system was again used to automatically control the temperature. Just before shutdown, with the burner wall controlled at 900°C, the fluid bed was 775°C.

The bed was transported after cooling to 500°C. Bed removal and burner cleanout were accomplished in 5 min.

The size distribution of the product is shown in Fig. 4-22. Other physical properties are included in Fig. 4-22. No burnable carbon could be detected by a tray burning technique, which indicates that the carbon level was less than ∿0.1%.

As indicated above, all of the changes made in this run yielded favorable results. Future runs will concentrate on gathering Hastelloy-X off-gas filter operating data, running heat transients to support the primary design effort, and finalizing the overall control system.

4.3.2. 20-cm Prototype Secondary Burner

Detailed drawings of the main burner system, including the induction heating and cooling system, have been completed and are being reviewed for structural considerations prior to final approval. The burner support system and the remote handling design are near completion.

Efforts have been made during the quarter to verify the design concept in the 10-cm secondary burner. The expanded top section has been shown to significantly reduce the filter chamber temperature without greatly affecting the bed temperature or the process. The internal heat-transfer coefficient measurement was highly successful and provided a firm ground for the heating and cooling system design.

An automatic burner control schematic has been studied using an integrated heating and cooling control by the bed temperature. Preliminary process flow and piping and instrumentation diagrams were drawn for this system (Section 4.1).

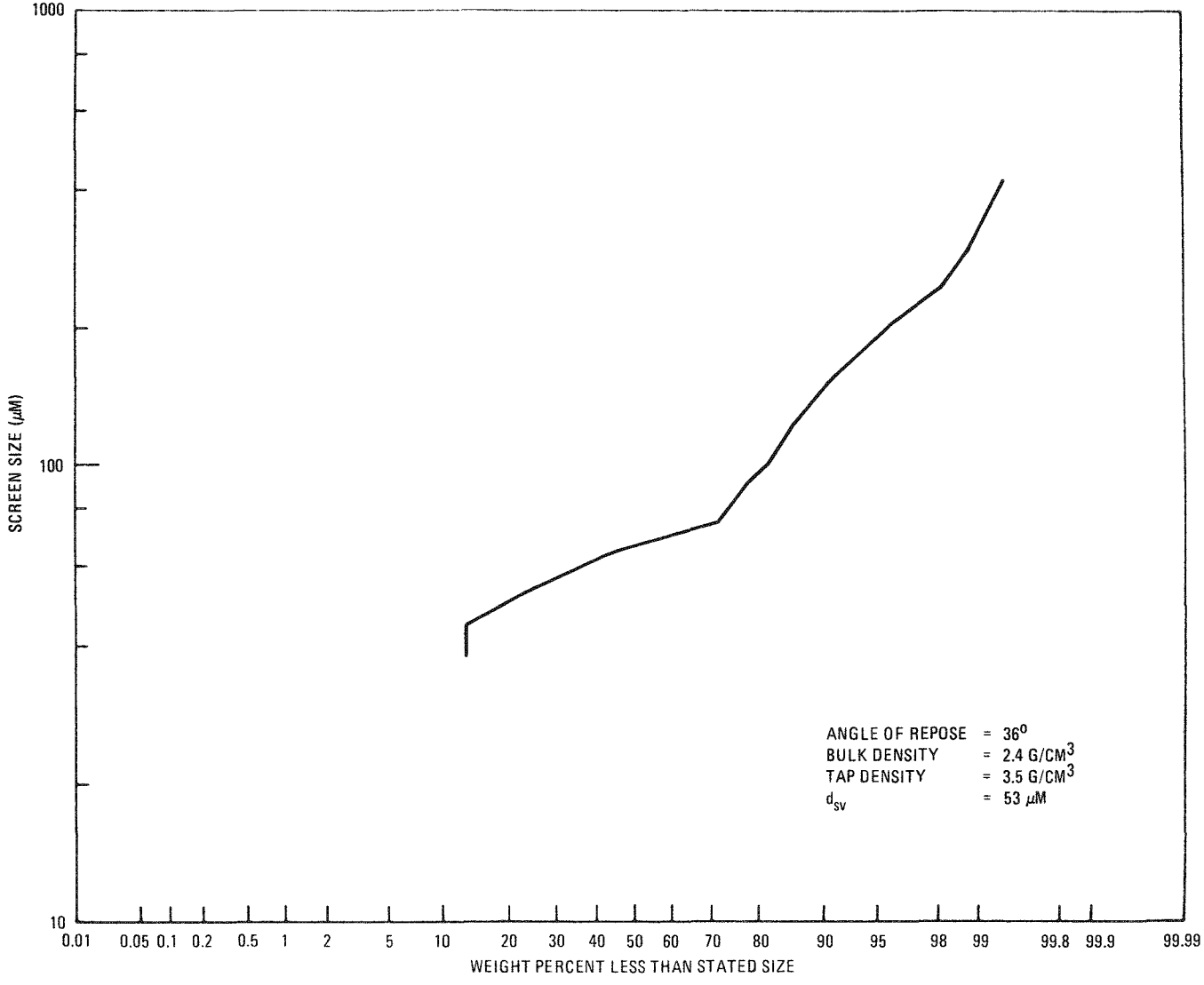

Fig. 4-22. Size distribution for Run 49 product

4.3.2.1. System Design

The detailed design of the main burner system and the heating and cooling system, including the following, has been completed:

1. Burner vessel and semiremote flange assemblies
2. Gravity-pneumatic feeder
3. Product removal valve
4. Induction heating system
5. Forced air-cooling system
6. In-vessel filters and blow-back system
7. System insulation
8. Burner support frames

The detailed design drawings are being checked for process, material, and structural (thermal stress) adequacy prior to final approval.

The overall burner assembly is shown in Fig. 4-23. The burner tubes have been received and the remote flange and in-vessel filters are on order (due June 30, 1975).

The detailed drawing for the gravity-pneumatic feeder and the test results were included in the previous quarterly report (Ref. 4-1). This item has been fabricated and tested in-house and is ready for installation.

The principle and basic design of the high-temperature product removal valve was previously described in Refs. 4-1 and 4-7. A bed cleaning Piccolo tube (Ref. 4-8) has been added to the system for "sweepdown." The valve assembly, located in the burner tube, is shown in Fig. 4-24. This figure also shows the inlet gas and product transport lines, as well as the Piccolo tube assembly.

The induction heating system design has been completed. The design parameters and procedures have been discussed previously in Refs. 4-1, 4-7,

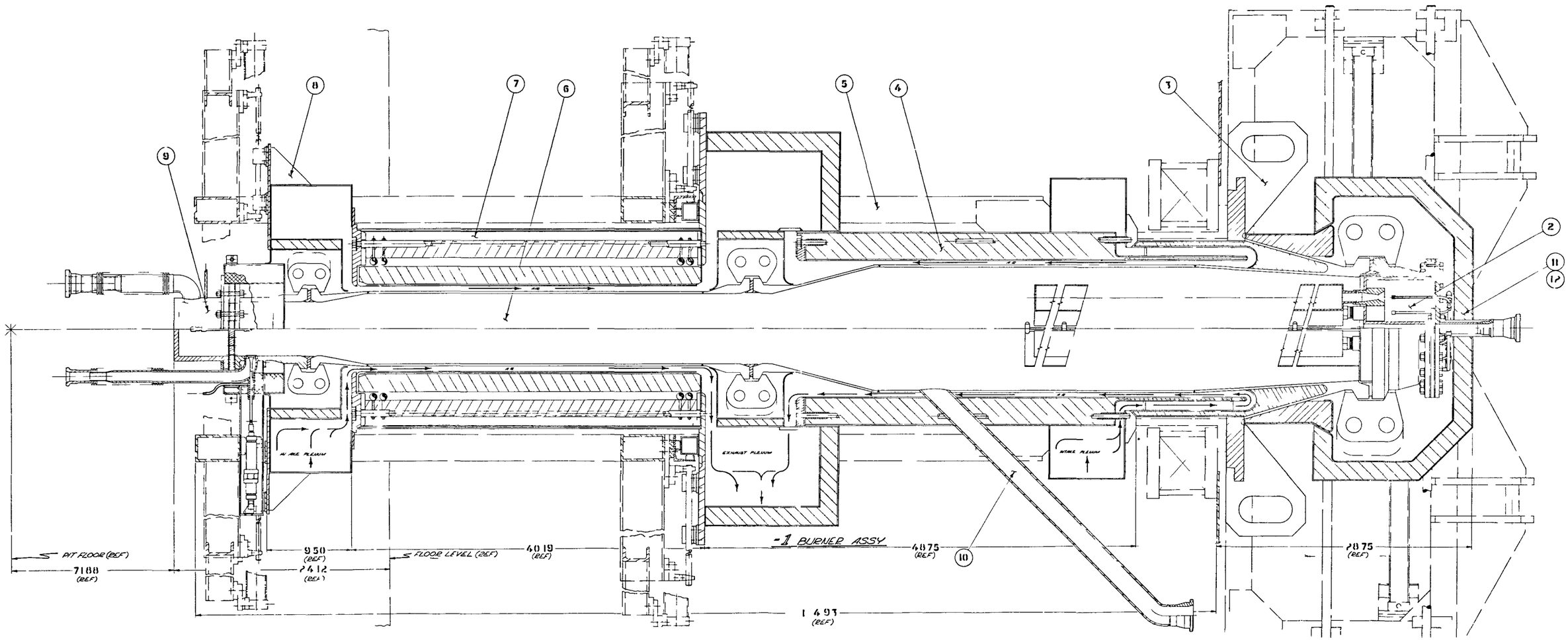

Fig. 4-23. Secondary burner assembly

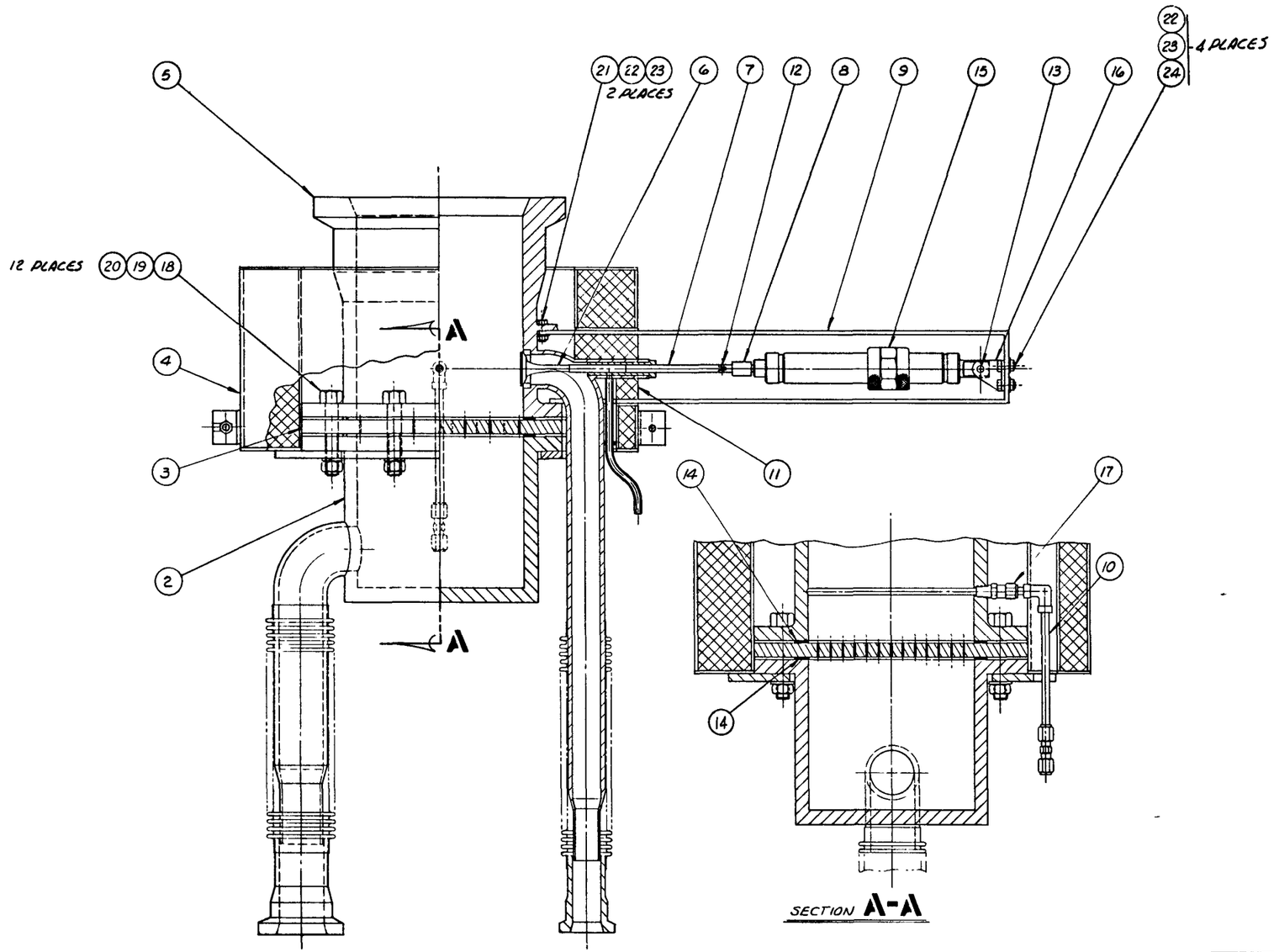

-1 SPOOL HUB ASSY

NOTES:

1. SOURCE:
2. SOURCE: BIMBA MFG. CO. MONEE, ILL. 60449
3. SOURCE: CRAWFORD FITTING CO. 29500 SOLON RD. SOLON, OHIO 44139

REQD/ASSEMBLY	ITEM	PART NO	DESCRIPTION	MATL	SPEC
			LIST OF MATERIAL		
-1					
4	24		HEX HD. CAP SCR 1/4-20 x 5/8	SS	COMC
6	23		LOCK WASHER 1/4 I.D. (NOM)	SS	COMC
6	22		HEX NUT 1/4-20	SS	COMC
2	21		HEX HD CAP SCR 1/4-20 x 7/8	SS	COMC
12	20		FLAT WASHER 1/2 I.D. (NOM)	HASTELLOY "X"	AMS 5536
12	19		HEX NUT 1/2-13	HASTELLOY "X"	AMS 5754
12	18		HEX HD CAP SCR 1/2-13 x 2 3/4	HASTELLOY "X"	AMS 5754
1	17	400-1-4	MALE CONNECTOR	HASTELLOY "X"	3
1	16	D167	PIVOT BRACKET		2
1	15	C-2016-A	AIR CYLINDER 'A' STROKE .25 'B' STROKE 1.75		2
2	14		SEAL		1
1	13		ROLL PIN 1/4 DIA. x 5/8		
1	12		ROLL PIN 3/32 DIA. x 5/16		
1	11	5247091-1	INSULATOR BLOCK		
1	10	5247083-1	PICCOLO TUBE ASSY		
1	9	5247082-1	CYLINDER SUPPORT BRACKET		
1	8	5247079-3	CLEVIS		
1	7	5247079-2	EXTENSION		
1	6	5247079-1	VALVE		
1	5	5247078-1	SPOOL HUB & VALVE GUIDE ASSY		
1	4	5247077-1	SPOOL SHROUD ASSY		
1	3	5247012-1	DISTRIBUTOR PLATE		
1	2	5247076-1	LOWER HUB ASSY		
	1	5247075-1	SPOOL HUB ASSY		

Fig. 4-24. Spool hub assembly

and 4-9. The design incorporates a 1/8-in.-thick susceptor plate and two magnetic field cutting coils at both ends of the coil. The susceptor provides better heating efficiency than occurs with direct heating of the vessel. The magnetic field cutting coils prevent the support plates from overheating due to a magnetic susception. The coil assembly, with structural support and the magnetic field cutting coil arrangement, is shown in Fig. 4-25. The overall coil, the insulation, and the susceptor plate assembly are shown in Fig. 4-26.

The coil and the work station for the induction heating are under fabrication by the vendor and are due in June 1975.

Detailed drawings for the forced air cooling system are in the final review stage prior to approval for fabrication. The burner temperature during the main burning stage is controlled by air cooling. The cooling air is admitted to the top and bottom air plenum for the upper and lower cooling jacket, respectively (see Fig. 4-23). Air plenums are provided at both the inlet and exhaust air lines to equally distribute the cooling air around the tube. The two exhaust plenums at the center are combined into one large plenum for easier fabrication and to minimize the number of vessel nozzles.

The filters and the blow-back orifice tubes and nozzles are shown at the top of Fig. 4-23. Three baffle plates divide the six filters into three groups; each group of two filters is blown-back sequentially. The baffle plates will prevent the fines from shifting from one set of filters to another and will aid in returning the fines to the bed (Ref. 4-10). The filters, which will be constructed of Hastelloy-X, have been received. The blow-back system design is complete and ready for final approval prior to fabrication.

A ceramic (fused silica, Foam 50) insulation material will be used to reduce the heat loss from the susceptor plate to the induction coil. A moldable ceramic (WRP-X-AQ, alumina-silica base insulation material) will

be used for all other insulation applications. The insulation has been designed to maintain the burner skin temperature below 150°F, which is the maximum allowable hot cell temperature.

Originally, the burner was to be supported by ring-stiffened gussets. This design has been changed to a circumferential skirt support, which has better thermal stress characteristics. The advantages of this new design are:

1. Increased cooling surface area.
2. Reduced thermal stress and fatigue.
3. Less stringent insulation requirements on the support.
4. Better thermal transient response.
5. Better mechanical stability.

The skirt design is shown in Fig. 4-27; the assembly is shown in Fig. 4-23.

The burner system (including the heating and cooling system) is supported by a framework as shown in Fig. 4-28. The framework has been designed in such a way that disassembly of the burner and heating and cooling system, or removal of the whole burner assembly with the framework, is possible.

4.3.2.2. System Design Verification

Some of the prototype burner design parameters and concepts are being tested in the 10-cm secondary burner. The preliminary results of the analysis are summarized in the following sections.

4.3.2.2.1. Minimum Fluidization Velocity. The minimum fluidization velocity of the secondary burner product particles was determined for two temperatures, 20° and 700°C. The results are shown in Fig. 4-29. Ideally,

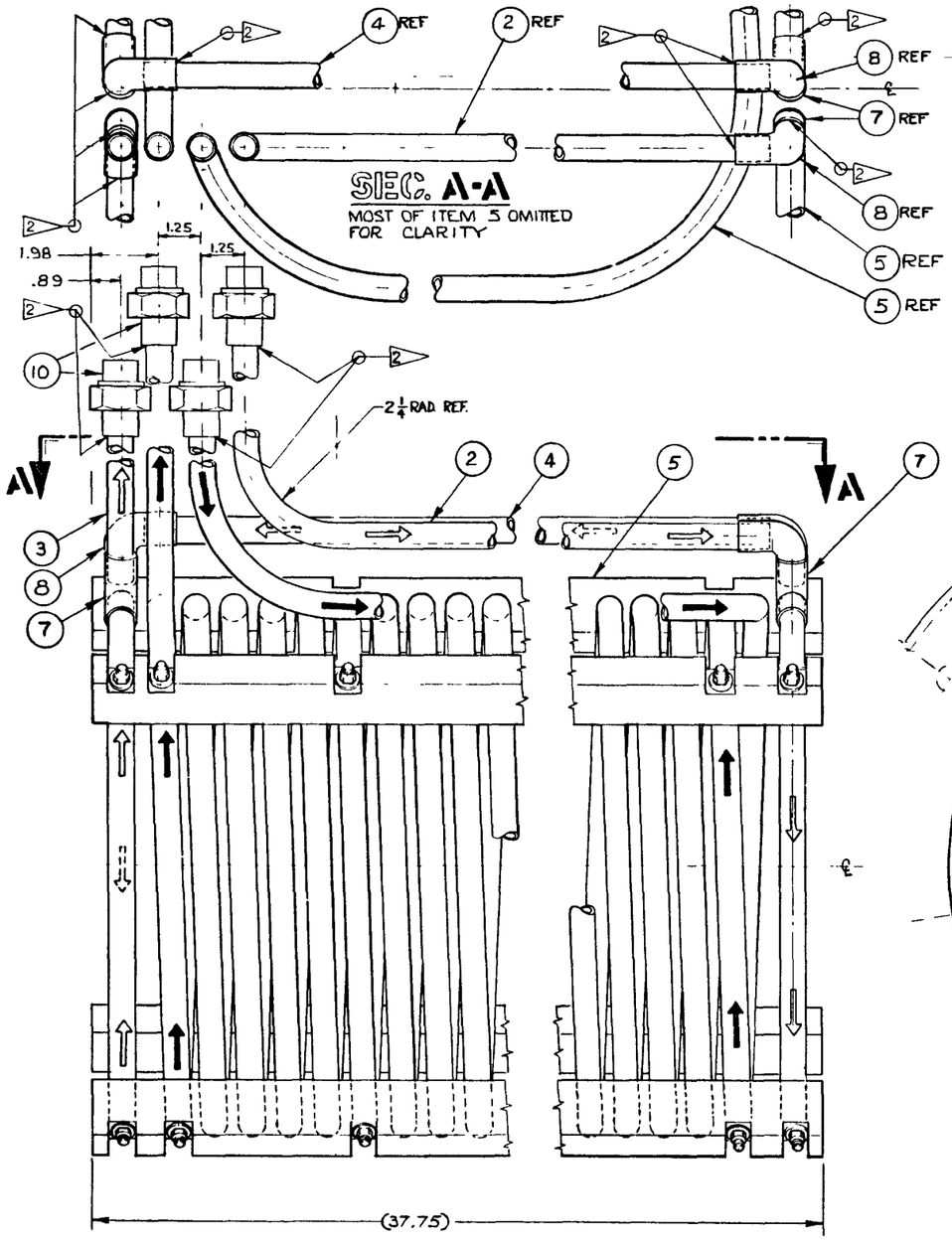

(-1) INDUCTION HEATER COIL ASSY
(VIEW ROTATED 10° FROM ITS TRUE PROJECTION FROM THE TOP VIEW)

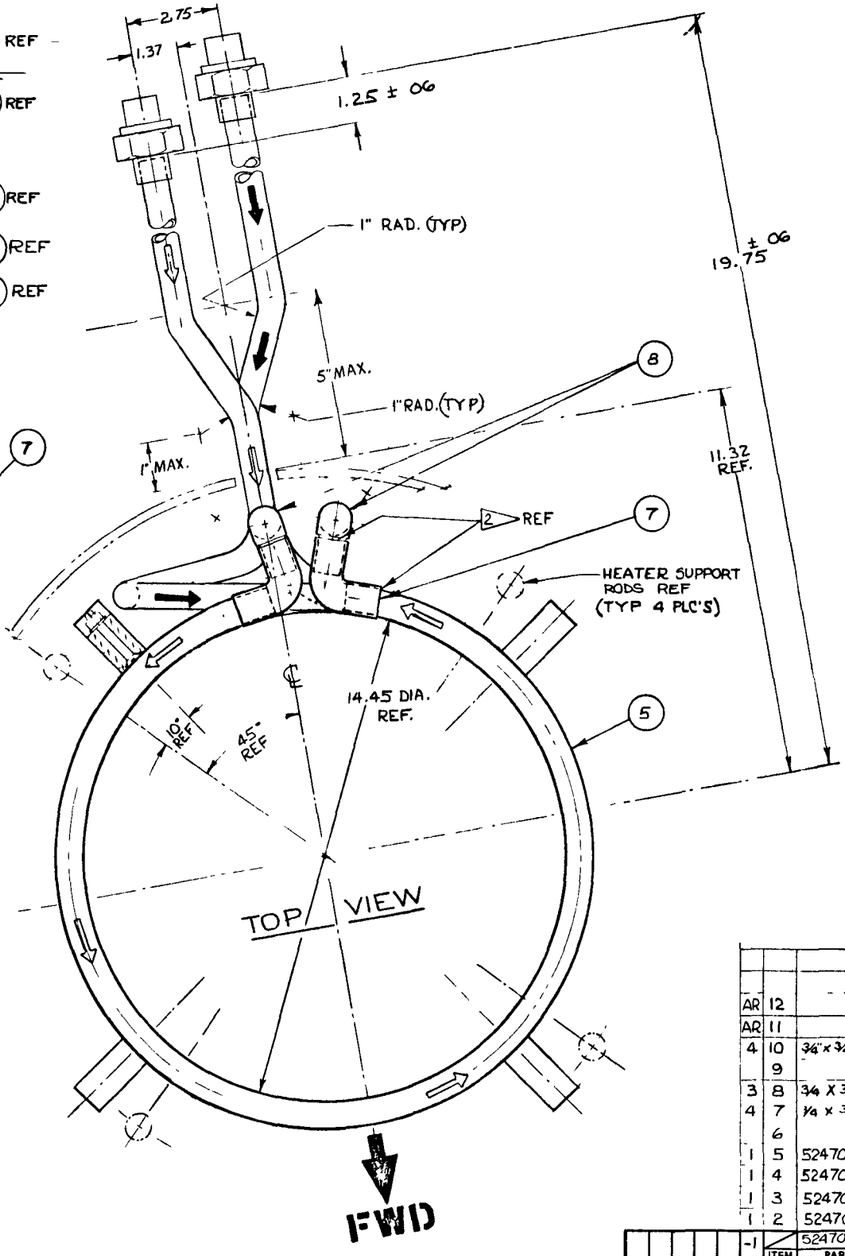

NOTES

1. DIMENSIONS AND TOLERANCES PER ANSI Y 14.5
2. SILVER SOLDER ALL SLIP JOINTS PER ACCEPTABLE COMMERCIAL STANDARDS
3. HYDROTEST COMPLETED ASSEMBLY AT 150 PSI, AMBIENT TEMP. FOR 6 HRS.
4. ARROWS INDICATE THE FOLLOWING FLOWS:
   - ⇨ MAGNETIC FIELD CUTTING COIL
   - ➡ INDUCTION HEATING COIL
5. OFFSET INDUCTION COIL SUPPLY AND RETURN TUBES AS INDICATED

REQD/ASSEMBLY	ITEM	PART NO.	DESCRIPTION	MATL	
			LIST OF MATERIAL		
	-1	5247036-1	INDUCTION HEATER COIL ASSY		
AR	12		SIL-FOS BRAZING ALLOY	15% SILVER	COM'L
AR	11		FLUX, BRAZING, NON-FERROUS	1100°F to 1600°F	COM'L
4	10	3/4" x 3/4"	UNION-GND JOINT, S.J.	COPPER	COM'L
	9				
3	8	3/4 X 3/4"	ELBOW 90°-STREET, S.J.	COPPER	COM'L
4	7	1/4 x 3/4"	ELBOW 90°-SLIP JOINT	COPPER	COM'L
	6				
1	5	5247031-1	INDUCTION COIL SPEC. COUT. DWG		
1	4	5247037-1	TUBE-CROSSOVER		
1	3	5247037-3	TUBE-OUTLET		
1	2	5247037-2	TUBE-INLET		

Fig. 4-25. Induction heater coil assembly

NOTES

1. ASSEMBLE IN AN INVERTED POSITION WITH THE SUPPLIES BEING AT THE TOP.

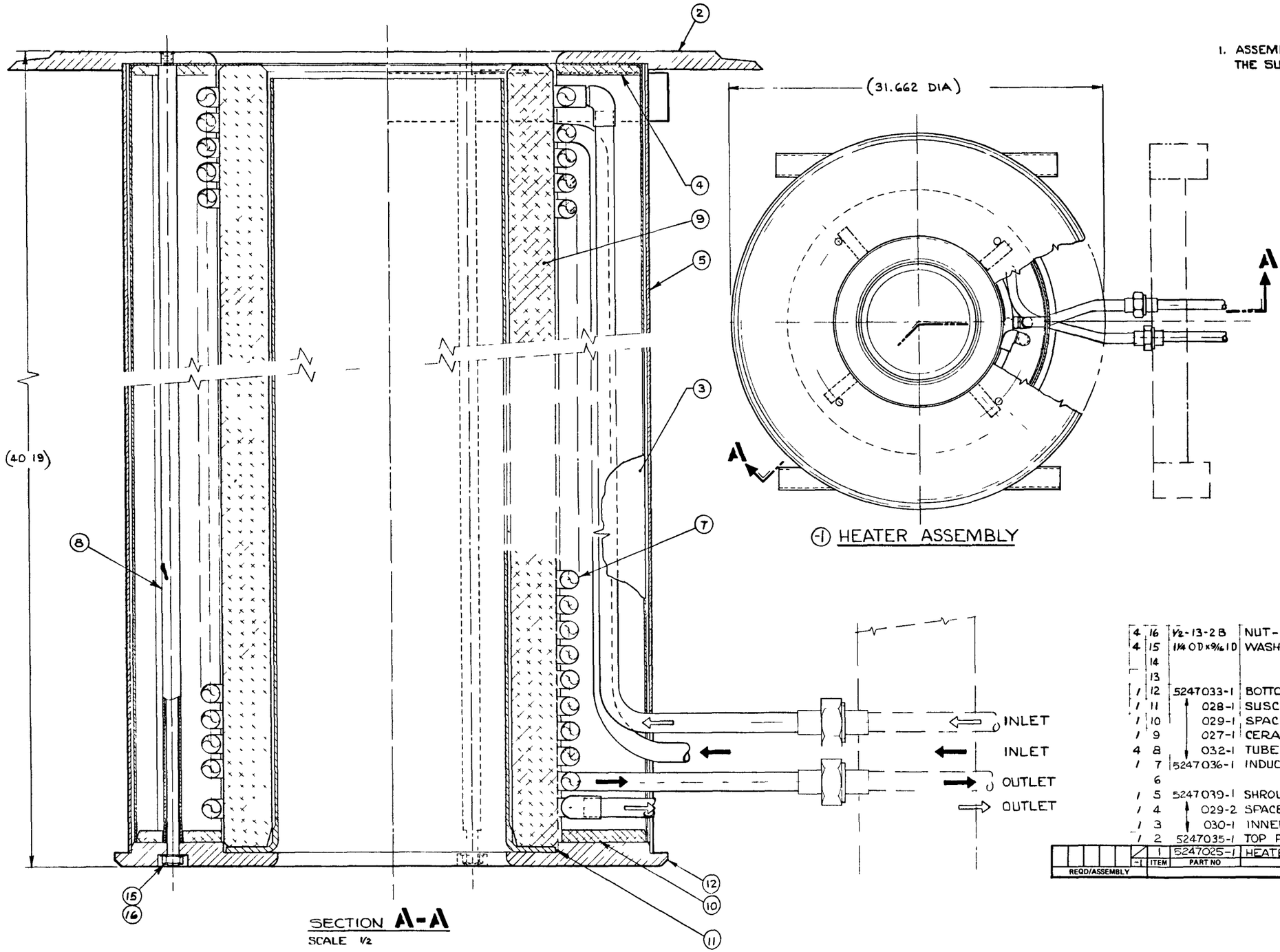

SECTION A-A
SCALE 1/2

-1 HEATER ASSEMBLY

REQD/ASSEMBLY	ITEM	PART NO	DESCRIPTION	MATL
			LIST OF MATERIAL	
4	16	1/2-13-2B	NUT-JAM, SELFLOCKING	SS -18-8
4	15	1/4 OD x 9/16 ID	WASHER-FLAT	SS -18-8
	14			
	13			
1	12	5247033-1	BOTTOM PLATE	
1	11	028-1	SUSCEPTOR TUBE	
1	10	029-1	SPACER, BOTTOM	
1	9	027-1	CERAMIC INSULATION	
4	8	032-1	TUBE, SUPPORT ROD	
1	7	5247036-1	INDUCTION COIL	
	6			
1	5	5247039-1	SHROUD, OUTER	
1	4	029-2	SPACER, TOP	
1	3	030-1	INNER SHROUD	
1	2	5247035-1	TOP PLATE	
1	1	5247025-1	HEATER ASSEMBLY	
-1	ITEM	PART NO	DESCRIPTION	MATL

Fig. 4-26. Heater assembly

NOTES:

1. REMOVE ALL BURRS & SHARP EDGES
2. DIMENSIONS & TOLERANCES PER ANSI-Y14.5
3. WELD FILLER METAL TO BE HASTELLOY X
4. SURFACE CONTOUR ON WELD JOINT TO BE SMOOTH & FREE OF UNDERCUTS, OVERLAPS, ABRUPT RIDGES OR VALLEYS
5. RADIOGRAPH INSPECT WELD PER ASTM E94

(6) .25 CORNER RADIUS OPTIONAL (TYP)

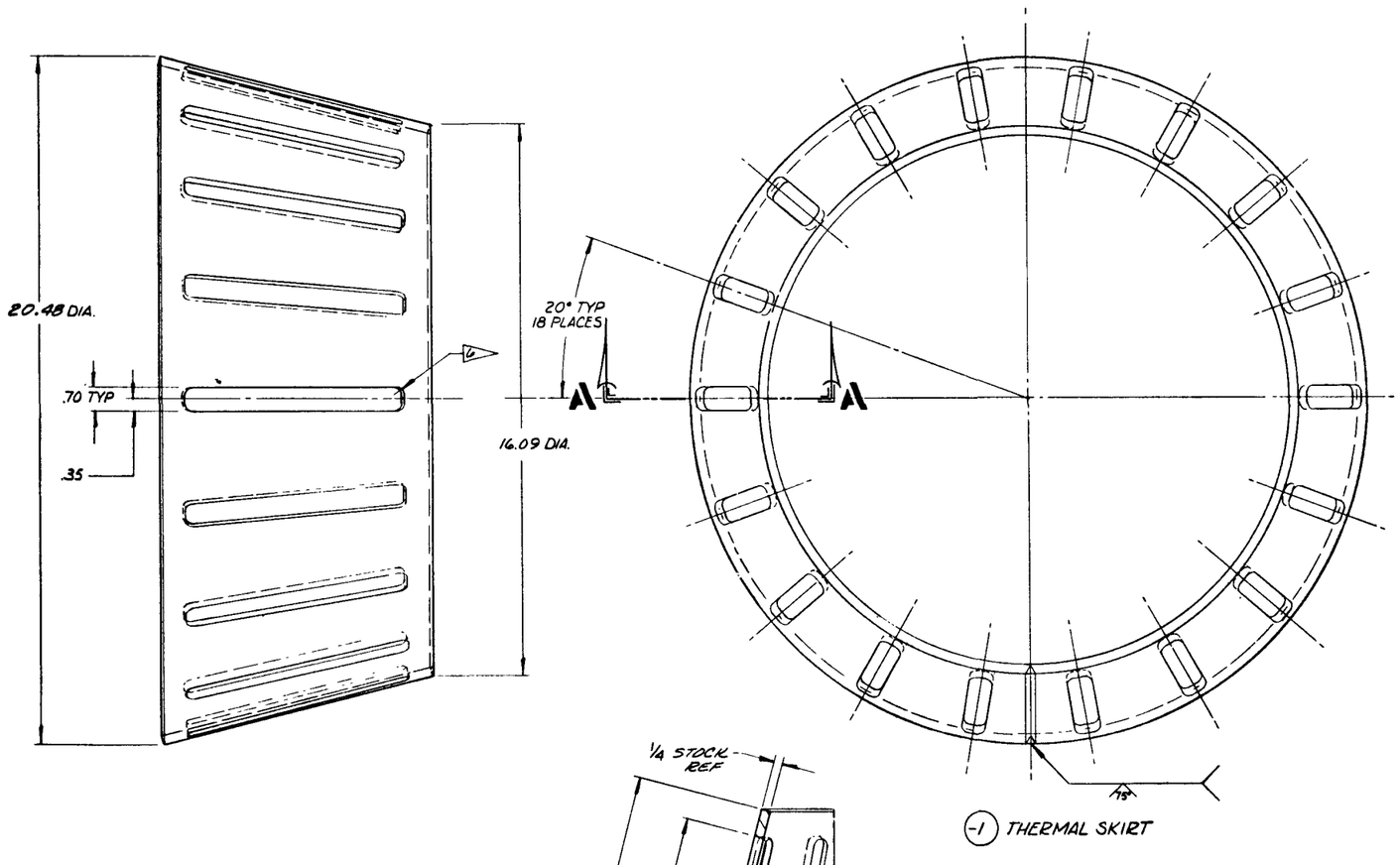

(-1) THERMAL SKIRT

	1	5247024-1	THERMAL SKIRT	1/4 PLATE	HASTELLOY X	AMS 5754

Fig. 4-27. Thermal skirt

NOTES

1. DIMENSIONS & TOLERANCES PER ANSI Y14.5.
2. REMOVE ALL BURRS & SHARP EDGES.
3. WELD FILLER METAL TO BE
4. LIQUID PENETRANT INSPECT ALL WELDS PER ASTM E165
5. FINAL THICKNESS OF PADS, ITEMS 30 THRU 39, TO BE WHAT IS REQUIRED TO MAINTAIN .250 TOTAL PROFILE ZONE & THICKNESS TOLERANCE OF $\pm .\frac{25}{13}$

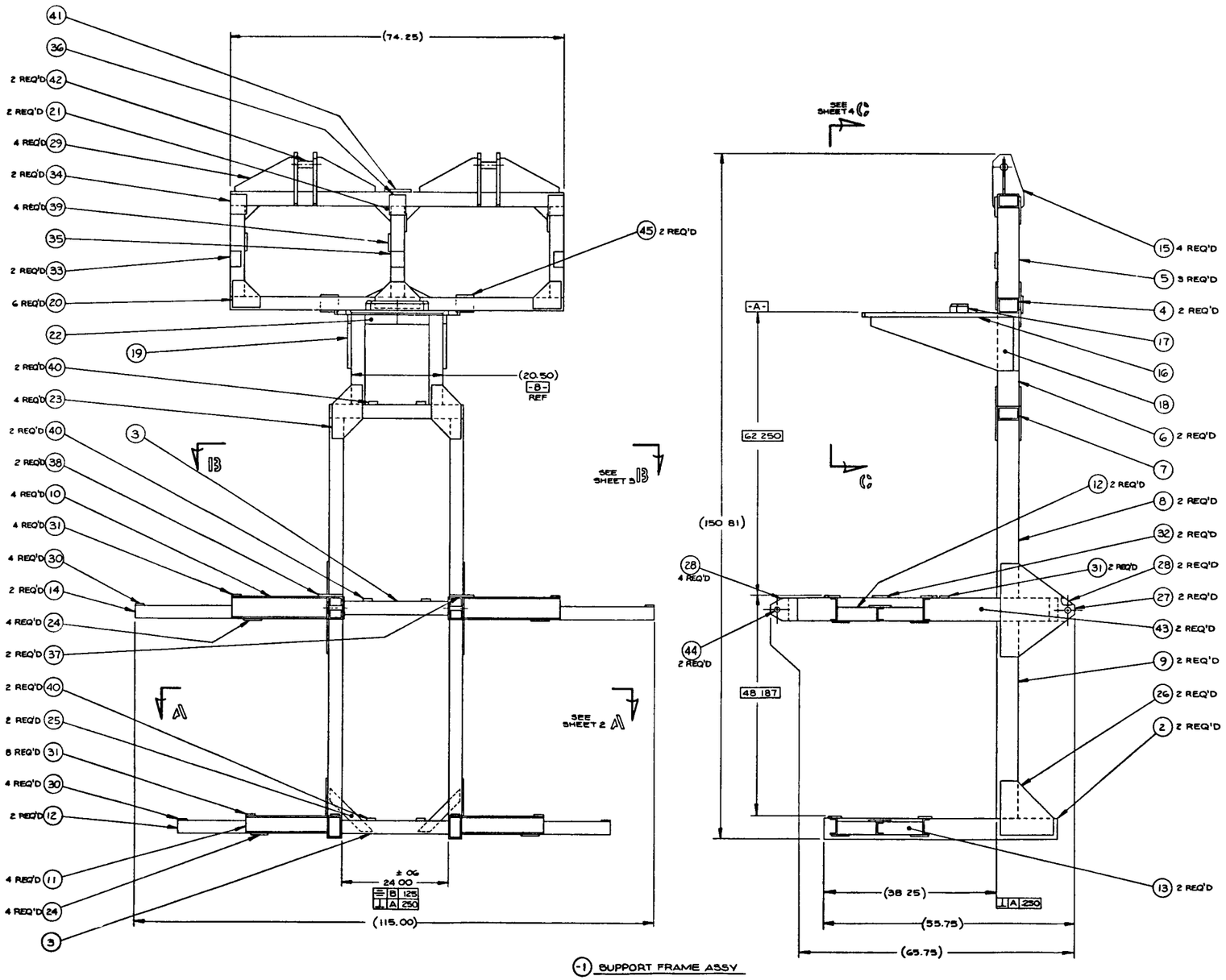

-1 SUPPORT FRAME ASSY

2	45	5247101-2	STOP BRACKET		
2	44	5247096-44	ROD, 1" DIA	STEEL	M1020
2	43	5247096-43	TUBE, 3 x 5 x ¼ WALL	STEEL	ASTM A501
2	42	5247096-42	ROD, 1½ DIA	STEEL	M1020
1	41	-41	PAD, ½ THK		ASTM A 105
6	40	-40		½	
4	39	-39		5	
2	38	-38			
2	37	-37			
1	36	-36			
1	35	-35			
2	34	-34			
2	33	-33			
2	32	-32			
14	31	-31			
8	30	-30	PAD, 5 THK		ASTM A 105
4	29	-29	GUSSET, ½ PLATE		ASTM-A36
6	28	-28		¼	
2	27	-27			
2	26	-26			
2	25	-25			
8	24	-24			
4	23	-23			
1	22	-22			
2	21	-21			
6	20	-20		⅛	
1	19	-19		¾	
1	18	-18	GUSSET, ¾ PLATE		ASTM-A36
1	17	-17	BLOCK		ASTM A-108
1	16	-16	PLATE, 1" PLATE		ASTM A36
4	15	-15	SUPPORT, ¾ PLATE		
2	14	-14	CHANNEL, 3 x 4.1 LBS		
2	13	-13	3 x 4.1 LBS		
4	12	-12	3 x 4.1 LBS		
4	11	-11	4 x 5.4 LBS		
4	10	-10	CHANNEL, 5 x 6.7 LBS		ASTM A36
2	9	-9	TUBE, 3 x 5 x ¼ WALL		ASTM A500
2	8	-8			
1	7	-7			
2	6	-6			
3	5	-5			
2	4	-4			
2	3	-3			
2	2	-2	TUBE, 3 x 5 x ¼ WALL	STEEL	ASTM A500
	1	5247096-1	SUPPORT FRAME ASSY		

Fig. 4-28. Support frame assembly

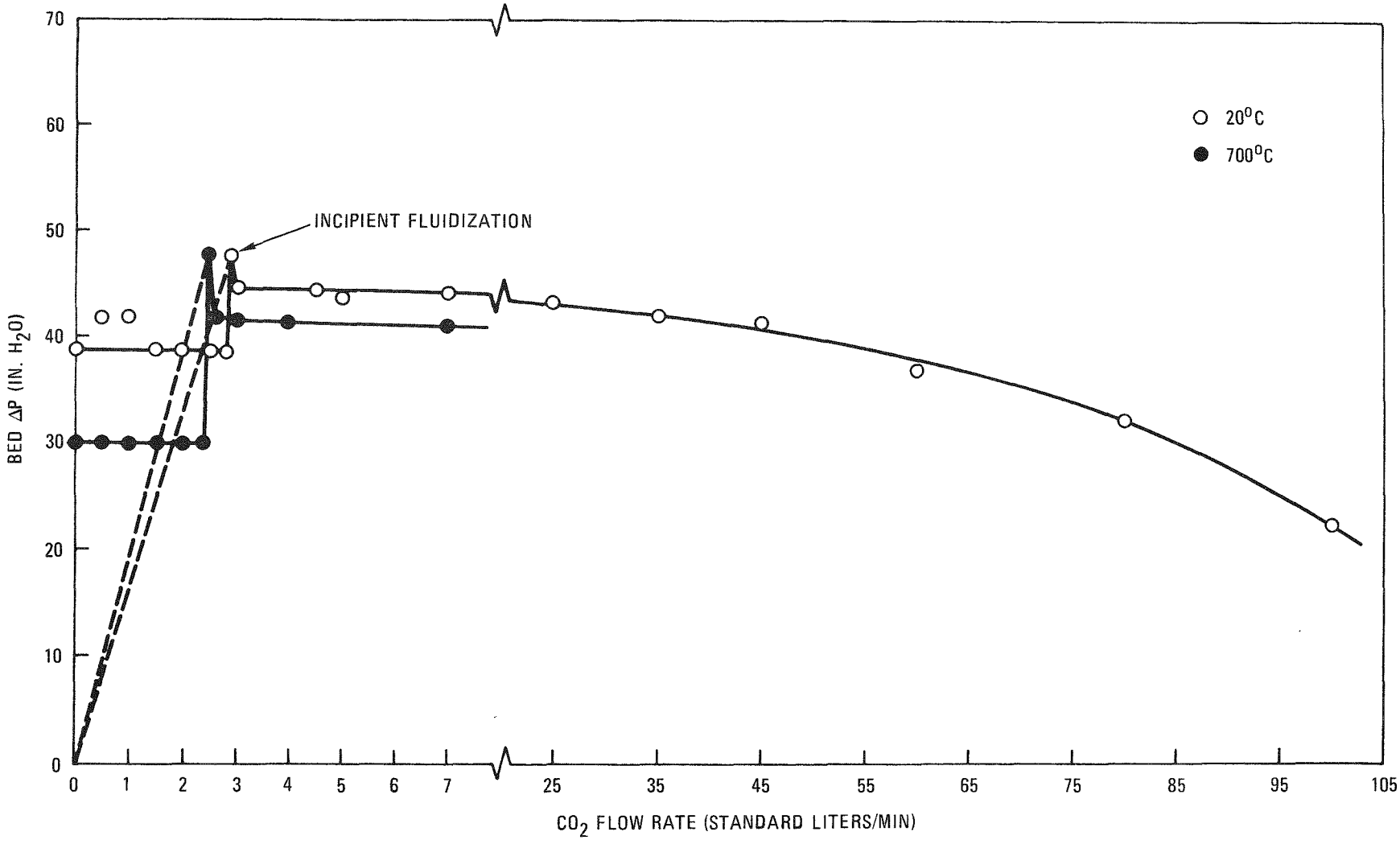

Fig. 4-29. Secondary burner incipient fluidization

the pressure drop should increase almost linearly from zero to the maximum value, as shown by the dashed line in Fig. 4-29. The actual measurement, however, shows a pressurization of the inlet plenum below the incipient fluidization, indicating that there is no flow due to the very fine particle size of this material. This no-flow condition at low flows was further evidenced by the fluctuation of the turbine flowmeter indication.

The result strongly implies a defluidization tendency for secondary burner product at low flows. The minimum (or, more correctly, incipient) fluidization velocities at 20° and 700°C were 0.7 and 1.8 cm/sec, respectively, based upon the 314 cm^2 cross-sectional area of the burner tube. The higher value at a higher temperature is contradictory to theory. However, the flow at 20°C was very erratic at incipient fluidization (3 SLPM) and was stabilized only at a higher flow rate (∿7 SLPM), while the flow rate or ΔP measurement at 700°C was quite stable at the incipient fluidization point. Therefore, the minimum fluidization velocity for this material is believed to be in the region from 1 to 2 cm/sec, which agrees well with previous predictions (Refs. 4-7, 4-11).

4.3.2.2.2. Internal Heat Transfer Coefficient. The bed-to-wall heat transfer coefficient is the most important rate-determining parameter in the heating and cooling process. The coefficient was measured for secondary burner product material with induction heating as the only heat source. The results are shown in Figs. 4-30 and 4-31.

Figure 4-30 shows a strong dependence of the heat transfer coefficient on temperature. This is probably due to increased radiation heat transfer at high temperature, as evidenced by the higher heat transfer coefficient at the upper section where the bed voidage is higher (Ref. 4-12). Although the correct mechanisms for the linear dependence of the heat transfer coefficient are not known, such a dependency has been widely observed (Ref. 4-13). The data points, therefore, are fitted by a linear regression method. From Fig. 4-30, the heat transfer coefficient ranges between

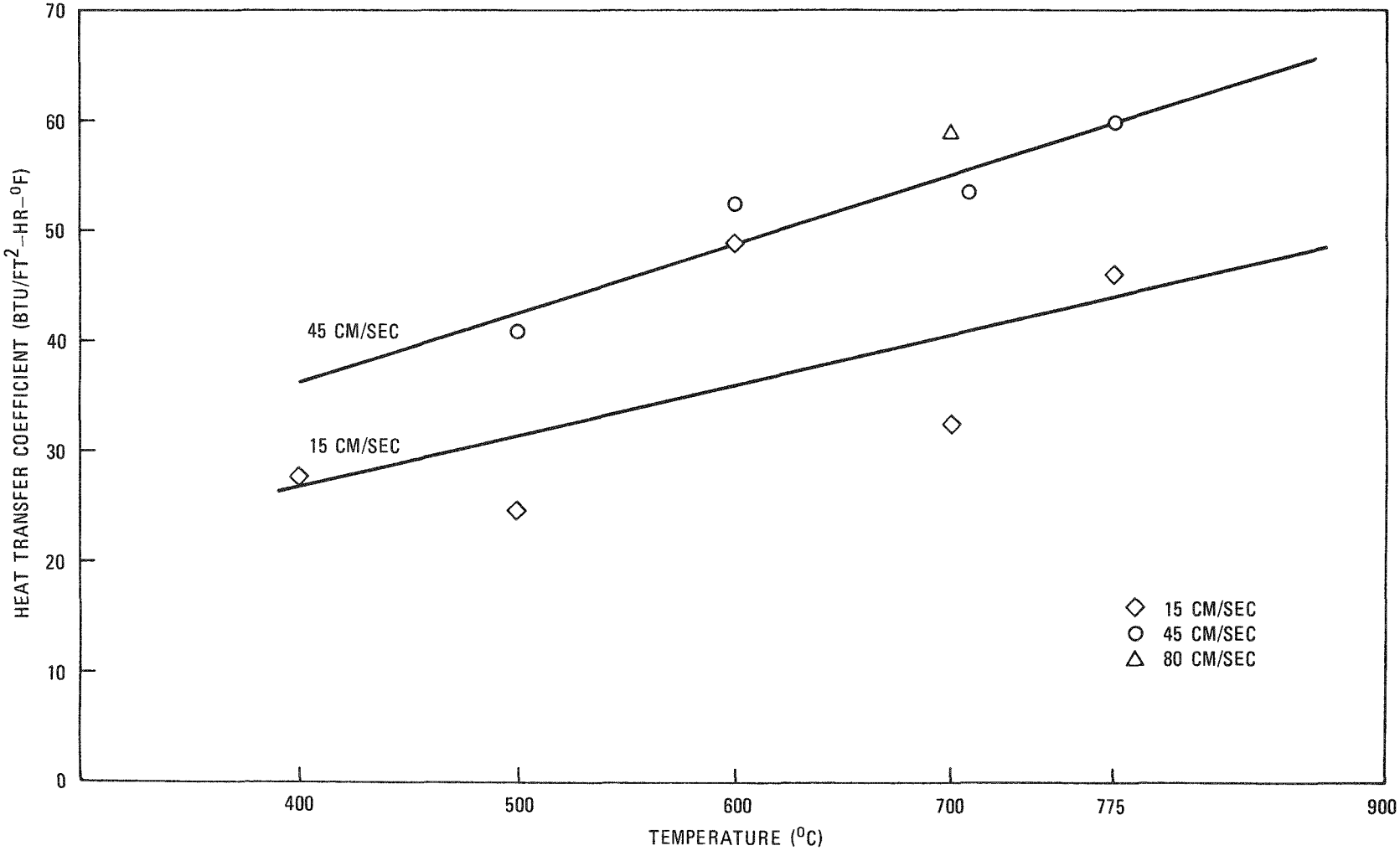

Fig. 4-30. Heat transfer coefficient versus temperature

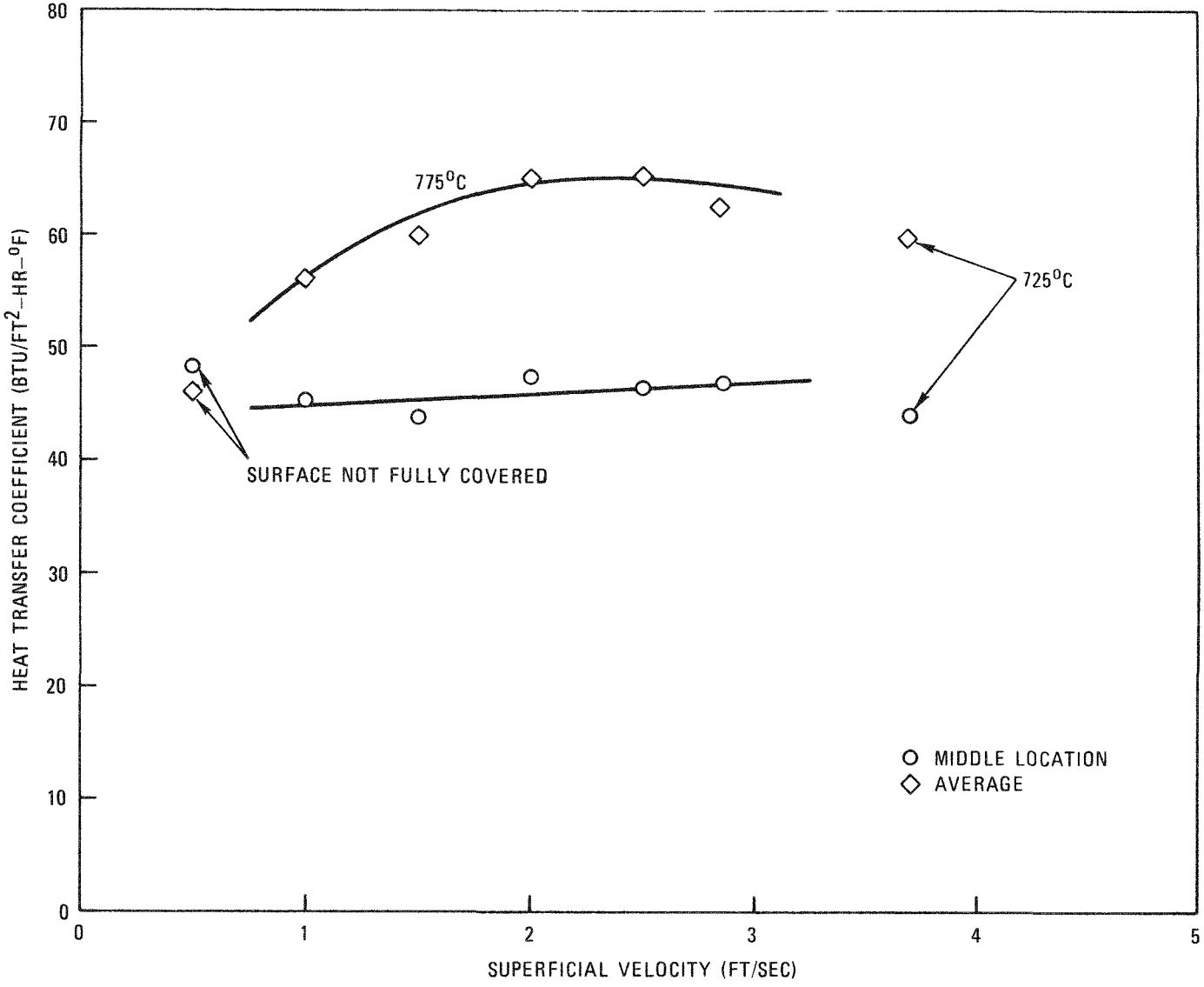

Fig. 4-31. Heat transfer coefficient versus superficial velocity

60 and 70 Btu/ft^2-hr-°F at 900°C at 1.5 ft/sec (45 cm/sec) superficial velocity.

Figure 4-31 also shows the dependency of the heat transfer coefficient on the superficial velocity. The average heat transfer coefficient peaks at a velocity around 2 ft/sec (60 cm/sec), while the coefficient at the middle section remains almost constant. Radiation heat transfer at high voidage fraction accounts for the higher transfer in the top section. Note also that h_{max} occurs at a much higher velocity than the theoretically predicted U_{opt} for heat transfer (Ref. 4-7), which does not take the radiation heat transfer into account.

From the above two observations the following important conclusions can be drawn:

1. The heat transfer coefficient is expected to be about 70 Btu/hr-ft^2-°F at the normal burner operating velocity ($\sim$2 ft/sec).

2. The maximum heat transfer coefficient occurs at a much higher velocity than the theoretical U_{opt}.

3. From the heat transfer point of view, the velocity range from 1 to 2 ft/sec during tail burning appears to be adequate.

From the same experiment the combined emissivity x geometric factor, εF, has been estimated to be on the order of 0.6.

A similar experiment on the feed particles will be performed during the next quarter.

4.3.2.2.3. Induction Heating System. While the heat transfer coefficient measurement was being made, the induction heating system was continuously used for about 18 hr at varying power levels (3 to 24 kW, equivalent

to 10 to 80% capacity). The system has proven to be reliable and the performance of the system is predictable. Power and temperature control has proved to be extremely easy, indicating that this system is an excellent choice for a fully automatic operation.

The coil loss has been checked at various power levels and the coil efficiency agrees well with theoretical predictions (Ref. 4-14).

4.3.2.2.4. Expanded Upper Filter Chamber. The expanded upper section in the 20-cm secondary burner was designed to reduce the filter temperature while also reducing elutriation; this should help to maintain higher bed temperatures during tail-burning.

The concept was tested in the 10-cm secondary burner by modifying the top section. The experimental results show that the filter chamber temperature was substantially lower during the main burning portion of the run, as well as during tail-burning.

4.3.2.3. Automatic Process Control

The burner temperature can be controlled, in principle, by two control variables, i.e., the oxygen supply or the forced air cooling rate. Both control modes have been tested in the 10-cm secondary burner; the latter was preferred for secondary burner control for the following reasons:

1. With air-cooling control, fully automatic control is very easy.

2. Temperature control by air cooling is not dependent on the fluidization.

3. For the secondary burner, the response to air cooling is fast enough to control the bed temperature, due to a high internal heat transfer coefficient and a relatively large heat transfer area per unit bed volume.

The schematic of the burner control is shown in Fig. 4-32. Details of the piping and instrumentation, together with the process flow diagram, are given in Section 4.1. The advantage of this control scheme is the integrated heating and cooling control.

REFERENCES

4-1. "Thorium Utilization Program Quarterly Progress Report for the Period Ending February 28, 1975," ERDA Report GA-A13366, General Atomic Company, May 30, 1975.

4-2. Petersen, J. F., "TAC2D, A General Purpose Two-Dimensional Heat Transfer Computer Code," USAEC Report GA-8868, Gulf General Atomic, September 6, 1969.

4-3. Kunii, D., and O. Levenspiel, Fluidization Engineering, J. Wiley & Sons, Inc., New York, 1969.

4-4. Zimmerman, R. D., "Burner Off-Gas Filter Pore Size," General Atomic unpublished data, March 3, 1975.

4-5. Carls, E. L., and N. M. Levitz, "Blowback of Sintered-Metal Filters: A Review of Tests and Operating Experience," USAEC Report ANL-7392, Argonne National Laboratories, January 1968.

4-6. Rickman, R. S.,"Evaluation of a Gravity Pneumatic Feeder System for Secondary Burners," General Atomic unpublished data, January 31, 1975.

4-7. "Thorium Utilization Program Quarterly Progress Report for the Period Ending November 30, 1974," USAEC Report GA-A13255, General Atomic Company, February 15, 1975.

4-8. Rickman, R. S., "Evaluation of a High-Temperature Bed Removal System Integrated with a Pneumatic Transport System for Use on Secondary Burners," General Atomic unpublished data, April 7, 1975.

4-9. Park, U., "Induction Heating Coil Design," General Atomic unpublished data, February 18, 1975.

4-10. Schmitt, E. S., Jr. (Pall Trinity Micro Corp.) to U. Park (General Atomic), private communication.

4-11. "Thorium Utilization Program Quarterly Progress Report for the Period Ending August 31, 1974," USAEC Report GA-A13178, General Atomic Company, October 3, 1974.

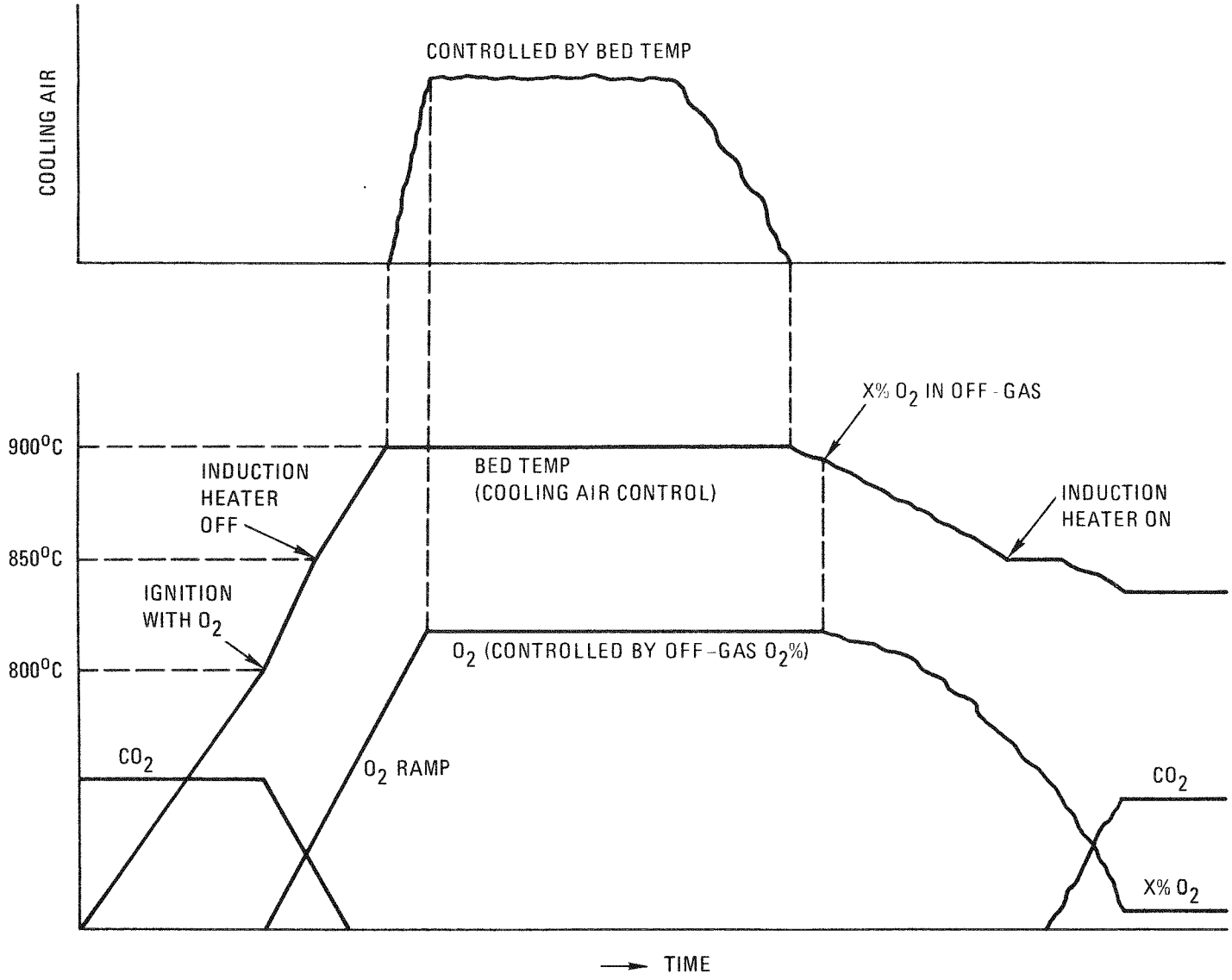

Fig. 4-32. Automatic control scheme of 20-cm secondary burner

4-12. Park, U., "Internal Heat Transfer Coefficient in the Secondary Burner," General Atomic unpublished data.

4-13. Zabrodsky, S. S., Int. J. Heat Mass Transfer 16, 241 (1973).

4-14. Park, U., "10-cm Secondary Burner Induction Heating Coil Design with a Susceptor Plate," General Atomic unpublished data, October 17, 1974.

5. AQUEOUS SEPARATION

5.1. LEACHING

5.1.1. Leacher Modifications

Modifications were made to both the 13-cm and 20-cm leachers during the quarter, as described below.

In order to obtain more efficient data acquisition, an air-lift sampling system has been installed on each leacher. The hot leachate is air lifted out of the leacher and cooled by passing it through a heat exchanger. With this system a large number of dissolution rate samples can be obtained during each run.

A steam heating jacket was installed on the outside of the bottom core of the 13-cm leacher. This jacket aids in heating the leacher and provides boiling action at the bottom of the leacher to increase agitation of the slurry.

The ring spargers have been removed from the interior of the leachers. All sparging is now done through the ball valve on the bottom of the 13-cm leacher. A new sparge tube has been installed in the 20-cm leacher to simulate the sparging configuration expected in commercial-scale leachers. This sparge tube is a 3/8-in. tube with the end cut at a 45° angle. The end is in the center of the leacher about 1/4 in. from the bottom of the core.

A steam jet product removal system has been installed on the 20-cm leacher to obtain transfer data during leaching conditions. The suction leg is a 1/2-in. tube cut at a 45° angle like the sparge tube. The end

is in the center of the leacher about 1/4 in. from the bottom of the core. The suction leg and the sparge tube are located side by side with the 45° openings facing away from each other. The steam jet is identical to the special jet described in Section 5.2.

Other minor modifications included replacing the 1/4-in. dip tubes for level and specific gravity measurements with 3/8-in. dip tubes to avoid plugging the tubes, increasing the distance between the dip tube ends to 10 in., installing a manometer for level and specific gravity readings from the dip tubes, making new feed hoppers, installing a 3/4-in. Clayton ball valve on the bottom of the 13-cm leacher, and replacing the electrical heaters on the 13-cm leacher.

5.1.2. Leaching Runs

Ten leaching runs were made during the quarter. Runs 97 and 98 were shakedown runs of the leaching equipment after all equipment in the leaching room was rearranged as a result of installation of the evaporator stripper and the insols dryer. Runs 99 and 100 were made to check out the air-lift sampling system. The results obtained from these runs were inconclusive but pointed out the need to filter the samples to prevent undissolved thorium from dissolving in the sample before analysis. Equipment problems led to the termination of Run 101 without data collection. Analytical data on runs 102, 103, 104, 105, and 106 are not complete; the results will be included in the next quarterly report.

5.2. LEACHER PRODUCT REMOVAL USING STEAM JET TRANSFER

A series of tests has been started to determine the feasibility and characteristics of using steam jet ejectors as a method of removing the product slurry from experimental and commercial dissolvers. The effect of the sparge rate on the transfer characteristics has been determined in this first set of runs.

The equipment arrangement used for the runs is shown in Fig. 5-1. The method of sparging and the location of the suction tube are shown in Fig. 5-2. The jet used was a special Penberthy Houdaille jet, which was designed for the purpose of transporting slurries similar to those expected from the leacher. The jet has a 0.20-in. I.D. throat and 1/2-in. NPT suction and discharge connections.

The liquid used for these initial runs was 50 liters of 38 wt % $NaNO_3$ solution having a specific gravity of 1.30. The specific gravity of the dissolver product is expected to be about 1.5 to 1.6. The slurry contained 5 wt % solids. In Runs 1 and 2, the solids consisted of 3.166 kg of SiC hulls and 0.260 kg of whole particles. After Run 2, the solids were air classified and the whole particles were removed. The solids in each of the remaining runs consisted of 3.426 kg of SiC hulls. The size distribution of the hulls is given in Fig. 5-3. The slurry temperature was initially about 20°C. A steam pressure of 90 psig was used for the motive force.

In all runs the solids were added to the liquid and then sparged to provide mixing similar to the mixing action in a leacher. The sparge was turned off, the solids were allowed to settle for 10 min, and the tank level readings were taken. After the desired sparge rate was set, the test run was made. In the case of zero sparge rate, there was no additional mixing after the 10-min settling period. The results of Runs 1 through 6 and 8 are given in Table 5-1.

As the sparge rate increased, the temperature rise of the slurry during transport increased (Fig. 5-4) and the flow rate of the slurry decreased (Fig. 5-5). It is quite likely that the sparge nitrogen introduced below the suction tube interferes with the transfer of the slurry. Sputtering of the flow, particularly at the start of the runs, was evident at sparge rates above 10 SCFH. These results indicate that sparge air using the configuration shown in Fig. 5-2 is detrimental to steam jet transfers.

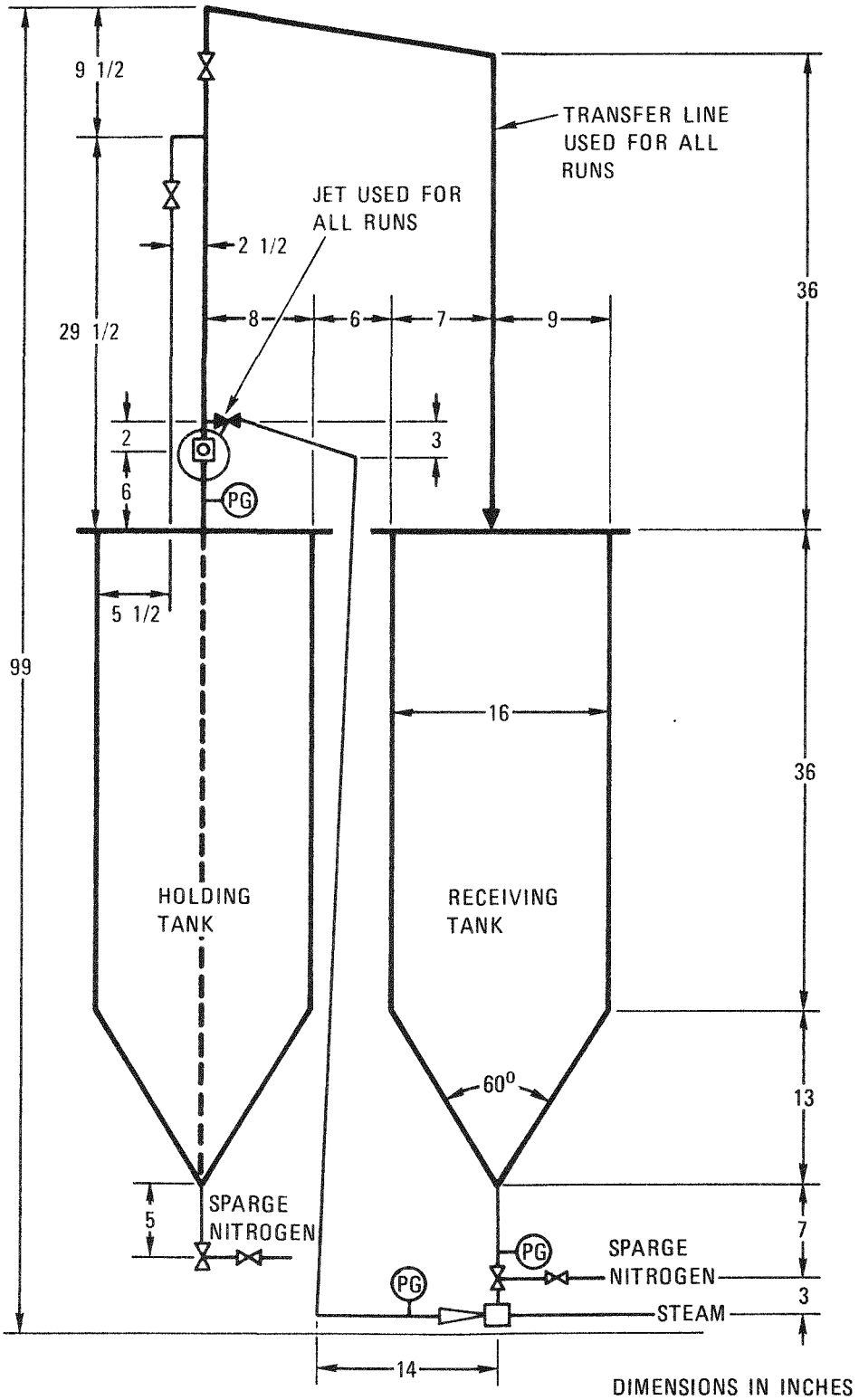

Fig. 5-1. Steam-jet transfer apparatus

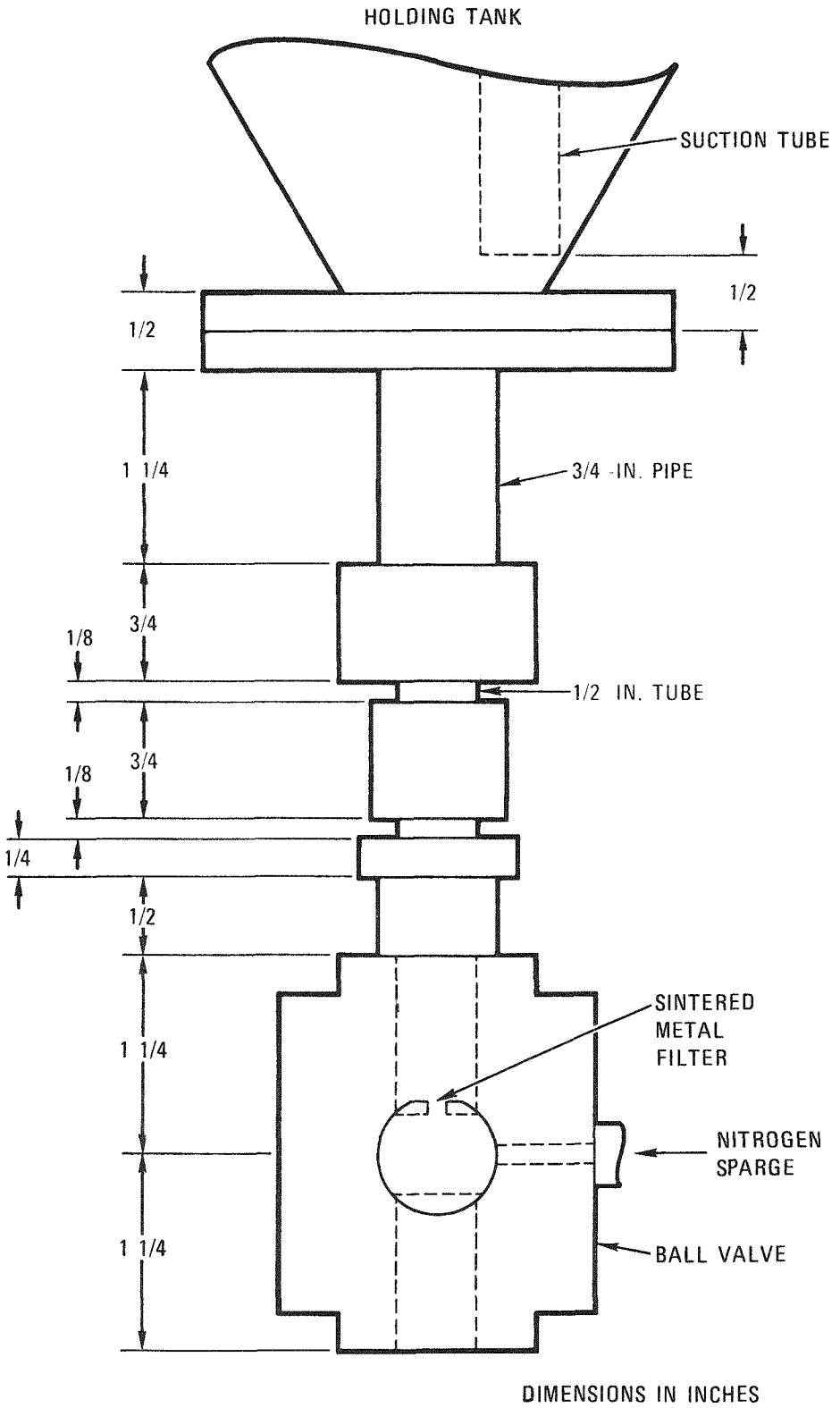

Fig. 5-2. Arrangement of sparge and jet suction tube

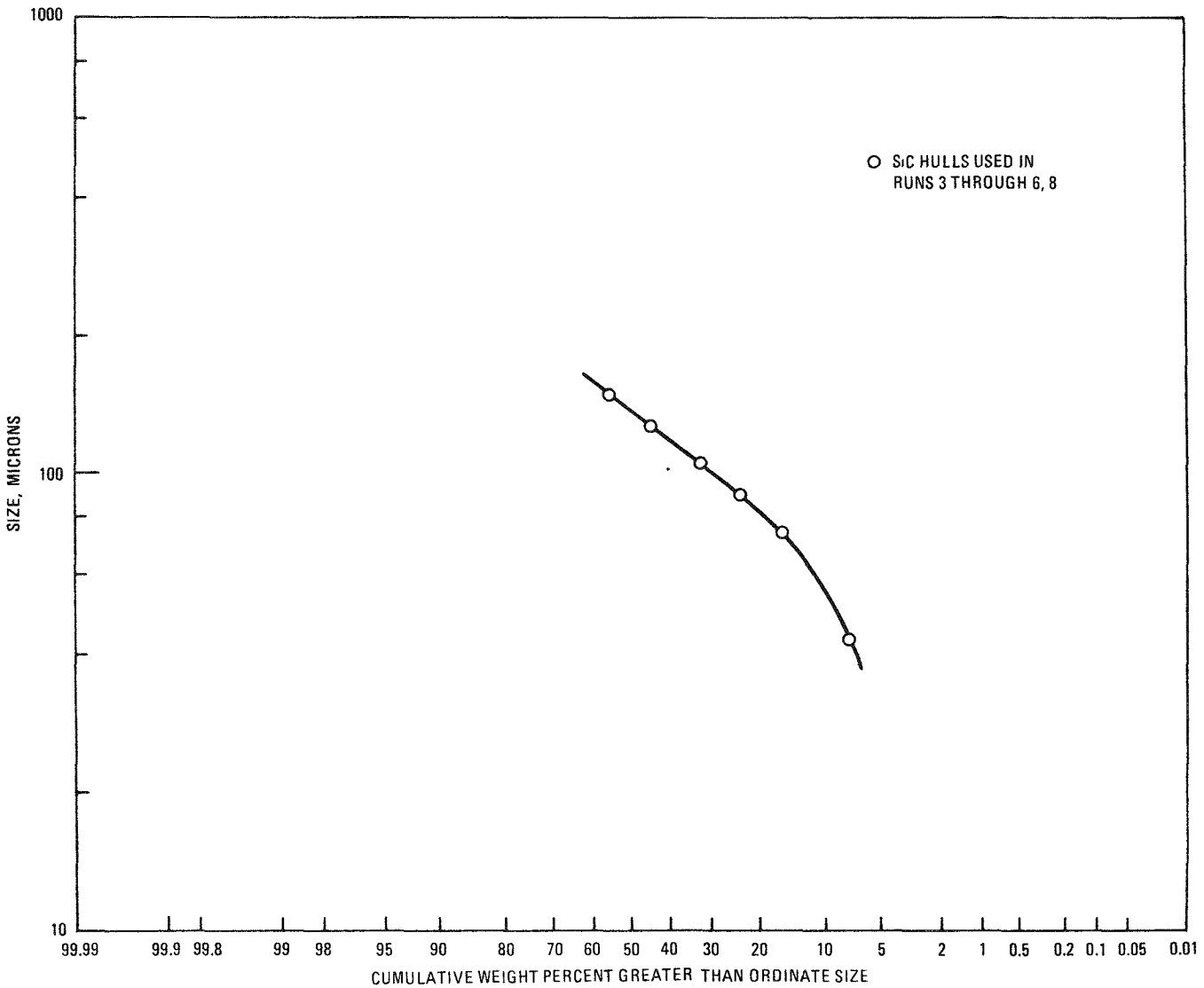

Fig. 5-3. Size distribution of SiC hulls

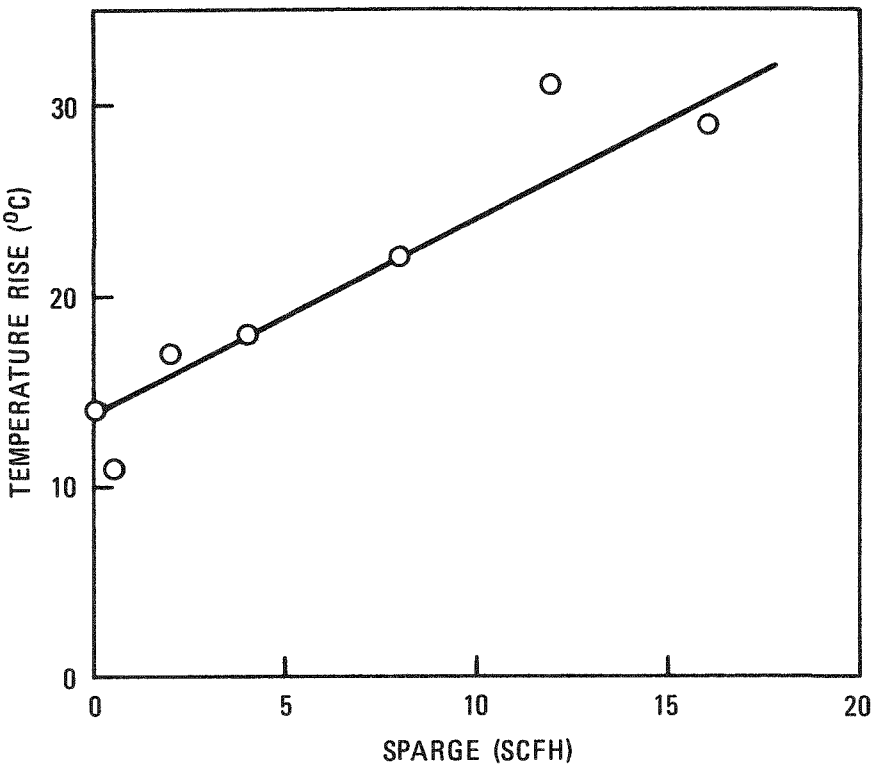

Fig. 5-4. Detrimental effect of sparge on temperature rise

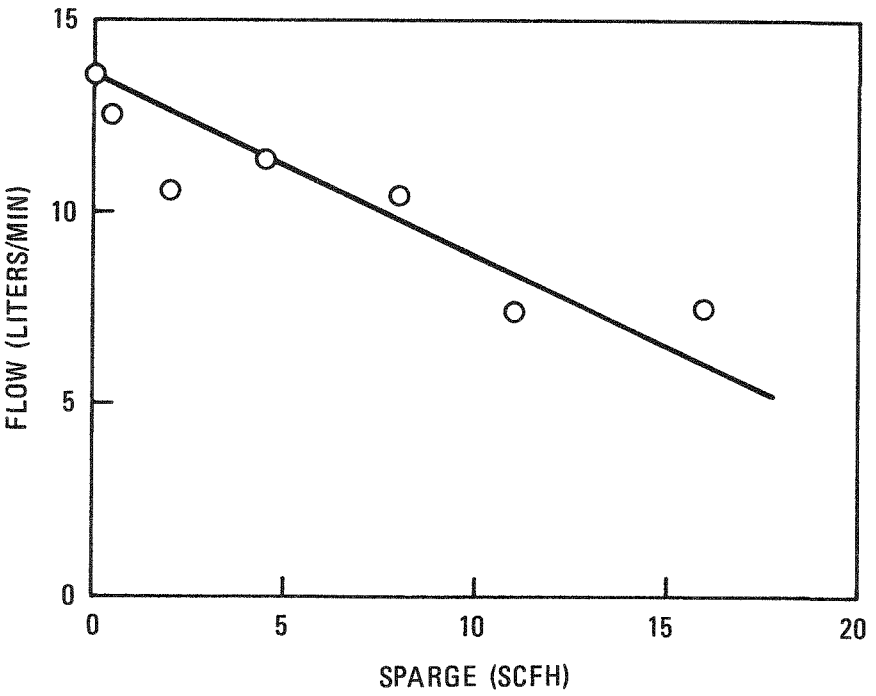

Fig. 5-5. Detrimental effect of sparge on flow rate

TABLE 5-1
DATA FROM RUNS 1 THROUGH 6 AND 8

Run	Sparge (SCFH)	ΔT[(a)] (°C)	Time[(b)] (min)	Liquid Holdup[(c)] (%)	Solid Holdup[(d)] (%)
8	0	14	3.7	0.091	1.33
1	0.5	11	4.0	0.100	0.073
2	2	17	4.7	0.154	0.71
3	4	18	4.4	0.028	0.32
4	8	22	4.8	--	--
5	12	31	6.8	0.025	1.34
6	16	29	6.7	0.011	0.47

(a) Temperature rise of slurry after steam jet transfer.

(b) Time to transfer 50 liters of slurry.

(c) Percent of initial liquid remaining in tank after trnasfer.

(d) Percent of initial solids remaining in tank after transfer.

As shown in Table 5-1, the liquid held up in the tank after the transfer decreases with increasing sparge rate. Two possible reasons for this decrease are (1) the air bubbles displace liquid out of the bottom of the tank and into the upper regions where it can be jetted with the suction leg, and (2) the violent bubbling action may splash liquid from the bottom of the tank into the suction leg.

There is no definite trend relating the amount of solids held up in the tank to the sparge rate. It is felt that the quantity of material held up in a dissolver is mainly dependent on the particular geometry of a given vessel and on its internals. The location of the suction leg in relation to the bottom of the tank is particularly important. These tests show, however, that less than 0.2% of the total liquid and less than 1.5% of the total solids are held up in this geometry.

These steam jet transfer tests indicate this method of product removal from the leachers is feasible. Additional testing will include variation in the length of the suction leg, steam pressure, slurry percentage, and slurry type.

5.3. BATCH CENTRIFUGE TESTS

Nine runs were made with the 12-in. solid-bowl centrifuge to determine the separation efficiency as a function of the feed rate and the rpm of the centrifuge for SiC hulls from a 1.3 specific gravity $NaNO_3$ solution. Analysis of data from the first six runs indicates that better than 99% separation efficiency is obtained when the centrifuge is operated between 1400 and 3200 rpm, the flow rate is between 9 and 13 liters/min, and the SiC content of the $NaNO_3$ solution does not exceed 10 wt %.

5.4. INSOLS DRYER

Eleven insols dryer runs were conducted during the quarter. The objective of these runs was shakedown testing of the insols dryer system, as well as initial data acquisition. The information obtained in the eleven runs is summarized as follows:

1. The concept of fluid-bed drying appears to be an acceptable method for handling the Fort St. Vrain type of insoluble solids resulting after dissolution of the fuels and separation by continuous centrifuge.

2. The fluid-bed unit operated satisfactorily under a relatively broad range of moisture content of the solids feed (from $\sim$2 to 25 wt %).

3. In all but one instance the dried product was well broken up and no clumps formed. In the one case where clumps formed and the lower portion of the bed solidified in the cone, the cause was attributed to a plugged distributor, which prevented sufficient agitation of the solids.

4. Visual observation has shown that large slugs of the wet solids are suspended within the vessel until dry enough to collapse. Therefore, the drying rate for identical inlet gas conditions may vary considerable depending on the local agitation within the solids bed. This is a result of the lower drying efficiency of the hot gas due to a smaller available surface area for drying.

5. There is, generally, evidence of a constant drying rate period and a falling drying rate period as indicated by the relative humidity of the exit gas.

6. In Run 4, the solids were completely saturated with water. A rathole formed early in the run, but no slugs formed. The exit gas relative humidity dropped throughout the run, with no noticeable constant drying rate. The end product was well broken up despite the excessive channeling at the onset.

Results of the drying runs conducted to date are presented in Table 5-2. These results were obtained during runs aimed primarily at the development of a standardized operating procedure for the insols drying system rather than data collection.

5.5. FEED ADJUSTMENT

Five feed adjustment runs were conducted using the batchwise mode of operation. The equipment used is shown in Fig. 5-6. The primary objectives of these runs were shakedown testing of the newly installed system and initial data acquisition. These runs provide the basis for developing an operating procedure as well as sampling techniques and methods.

Information gained from the five feed adjustment runs has led to some modifications in the equipment. The observations from these five runs and the resulting modifications are summarized as follows:

1. Initial runs (1 and 2) indicated pressurization of the evaporator-stripper vessel prior to any condensate being collected. This

TABLE 5-2
OPERATING DATA FROM INSOLS DRYER RUNS 1 THROUGH 11[a]

Run No.	Moisture Content of Solids Charge (wt %)	Total Drying Time (hr)	Relative Humidity (RH) of Exiting Nitrogen	
1	16.1	2.1	70-95	Definite peak when slug dropped
2	4.0	1.2	70-98	Definite peak when slug dropped
3	13.3	1.6	70-98	Definite peak when slug dropped
4	26.4	4.2	0-98	RH dropped gradually throughout run
5[b]				
6[c]				
7	10.8[d]	0.9	50-70	Lower RH than usual
8	1.6[d]	0.7	50-70	Lower RH than usual
9	1.1[d]	0.7	50-70	Lower RH than usual
10	9.0[d]	1.7	70-95	
11	14.2[d]	2.5	60-90	

[a] Drying gas - nitrogen, inlet gas temperature = 100°C, inlet gas velocity at STP = 2 ft/sec, and dry weight of solids charge = 2000 g.

[b] Run abandoned - loss of nitrogen.

[c] Run abandoned - plugged distributor.

[d] Moisture content estimated - balance out of service.

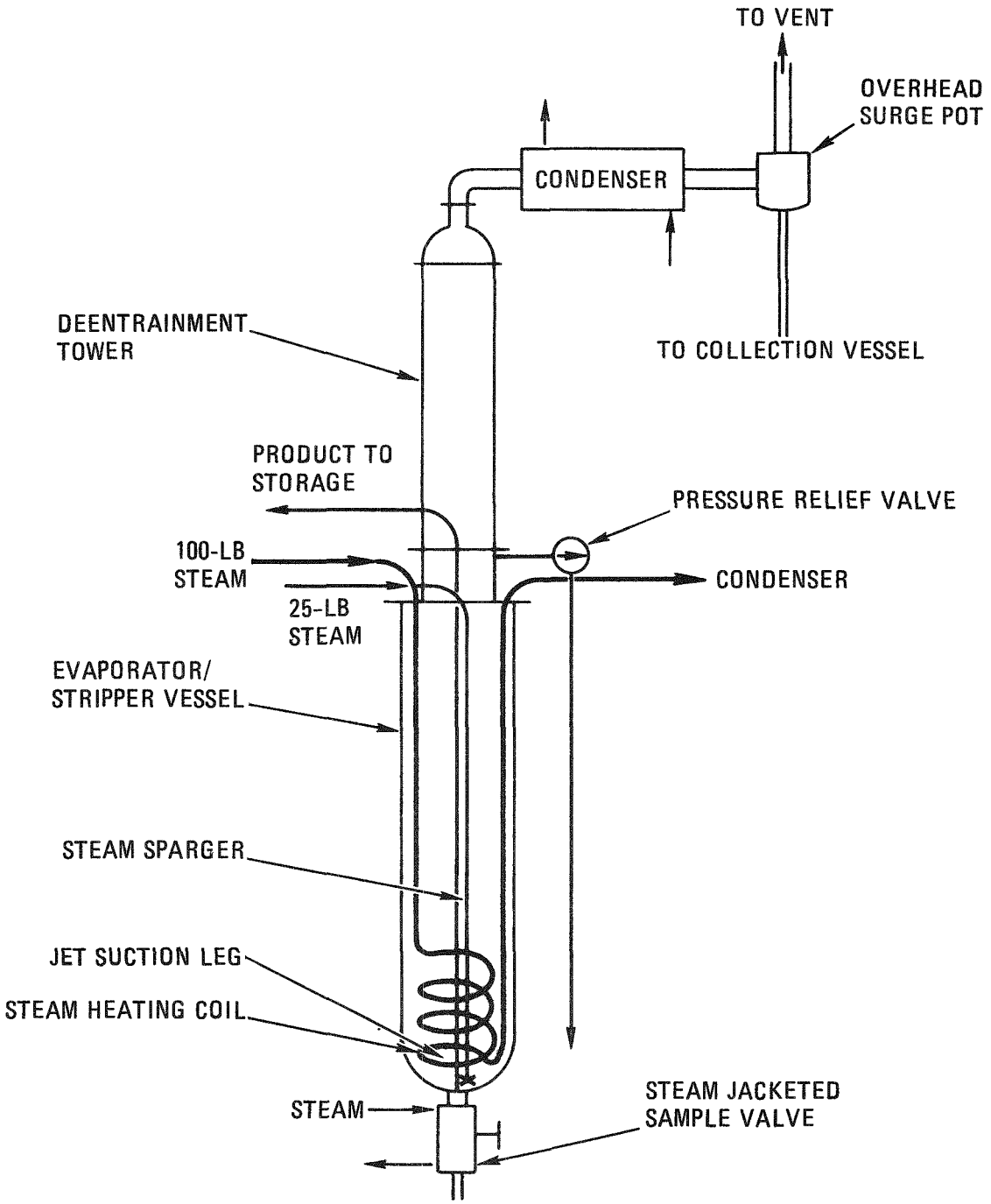

Fig. 5-6. Solvent extraction feed adjustment system equipment schematic - batchwise mode of operation

effect was attributed to tower flooding and insufficient venting downstream of the condenser. Condensation within the tower during heatup is believed to be the cause of the tower flooding. Early modifications included the addition of a condensate flash pot for venting and removal of half of the tower packing (1/2-in. Intalox saddles). Subsequent runs continued to result in flooding in the packed tower and pressurization of the evaporator-stripper vessel. Therefore, the remaining portion of the tower packing was removed and a safety relief valve was installed on the evaporator-stripper vessel. These modifications appear to have solved the problems of flooding and pressurization. A different type and size of tower packing or a demister pad will be installed at a later date.

2. The initial runs also indicated the need for a sampling system to obtain samples of the concentrated product during the run. Final modification of the system resulted in installing a steam jacketed valve at the base of the vessel to allow sample acquisition.

3. In two of the five runs, excessive boilup rates were encountered that resulted in a portion of the evaporator-stripper contents going overhead into the condenser and the condensate receiver. To alleviate this problem, the smaller of the two steam heating coils originally installed was removed, which led to a lower available surface area for heating and thus a lower maximum boilup rate.

4. The high concentration of the boil-down liquid resulted in plugging of the originally installed steam sparger as well as the suction leg of the steam jet. To alleviate further problems of plugging, the jet leg and steam sparger will be purged with nitrogen when not in use. The steam sparger was also modified from a porous distributor to a four-way open-ended tube.

5. There is some problem in direct measurement of the steam sparge rate with the current instrumentation. This problem is being investigated and until its resolution, the rate will be determined by mass balance.

Analytical data obtained from successfully completed runs indicate that the system produces an acid deficient product. Typical analytical data (from Run 3) are given in Table 5-3.

The first series of runs to be conducted for data acquisition will be started by mid-May. This series is intended to determine the effect of the steam stripping rate at a constant boiling point (135°C) on the acidity of the final product.

TABLE 5-3
ANALYTICAL RESULTS OF RUN 3

	Feed	BP = 125°C		BP = 135°C		SS[d] = 20 min		SS = 40 min		SS = 60 min		SS = 80 min		SS = 100 min		Diluted Product
		OH[a,b]	BD[c]	OH	BD	OH	BD	OH	BD	OH	BD	OH	BD	OH	BD	
Specific gravity at 25°C	1.450	--		--		--		--		--		--				1.518
Acidity (H^+), M	7.70	4.41	9.22	13.1	1.09	3.30	0.24	1.27	-0.18	0.80	-0.40	0.66	-0.67			-0.21
Fluoride concentration (F^-), M x 10^2	4.1	0.077	4.6	0.013	18.1	0.006	22.1	0.005	17.8	0.004	19.3	0.003	21.8			8.3
Aluminum concentration (Al^{+3}), M x 10^2	7.8	--	11.8	--	40.8	--	45.7	--	40.1	--	42.2	--	43.6			16.0
Thorium concentration (Th), g/l	137	3.56	164.5	0.004	662.6	0.005	942	0.012	685	0.010	729	0.005	774			273

(a) High results due to boilover at startup.

(b) OH = overhead.

(c) BD = boildown residue.

(d) SS = steam sparge.

6. SOLVENT EXTRACTION

Eight solvent extraction runs were completed during the quarter. The flowsheets investigated relate to HTGR fuel reprocessing and the Idaho HTGR fuel reprocessing pilot plant. The data are complete for Runs 17, 18, 24, and 25 and the results of these runs are reported here. The data on the other four runs are not complete as yet. The runs reported here were the first made in the expanded solvent extraction system of the pilot plant. Each of the runs used the extraction and partition flowsheet. Solvent degradation simulation studies were begun in this run series.

6.1. RUNS 17 AND 18

Runs 17 and 18 consisted of uranium and thorium extraction, partition, partition-scrub, uranium strip, and solvent wash operations in the five-column system. The flowsheet tested was the first cycle of Fig. 6-1.

Table 6-1 shows the stream analyses and flow for each operation. Table 6-2 shows the percent loss data and height equivalent to a theoretical stage (HETS) at the indicated percentage of flooding frequency. The cartridge details for each column are also contained in Table 6-2.

Run 17 served as the shakedown run for the five-column system. All of the columns were 2 in. in diameter except the partition column, which was 3 in. in diameter. The hardware for Run 18 was the same as that used for Run 17. The equipment functioned well for both runs.

The significant changes between the runs consisted of: (1) the reduction in flow rates in Run 18, and (2) the addition of dibutyl phosphate (DBP) in the 1AX stream in Run 18. The DBP was added to simulate the maximum solvent degradation expected due to radiolysis during the processing

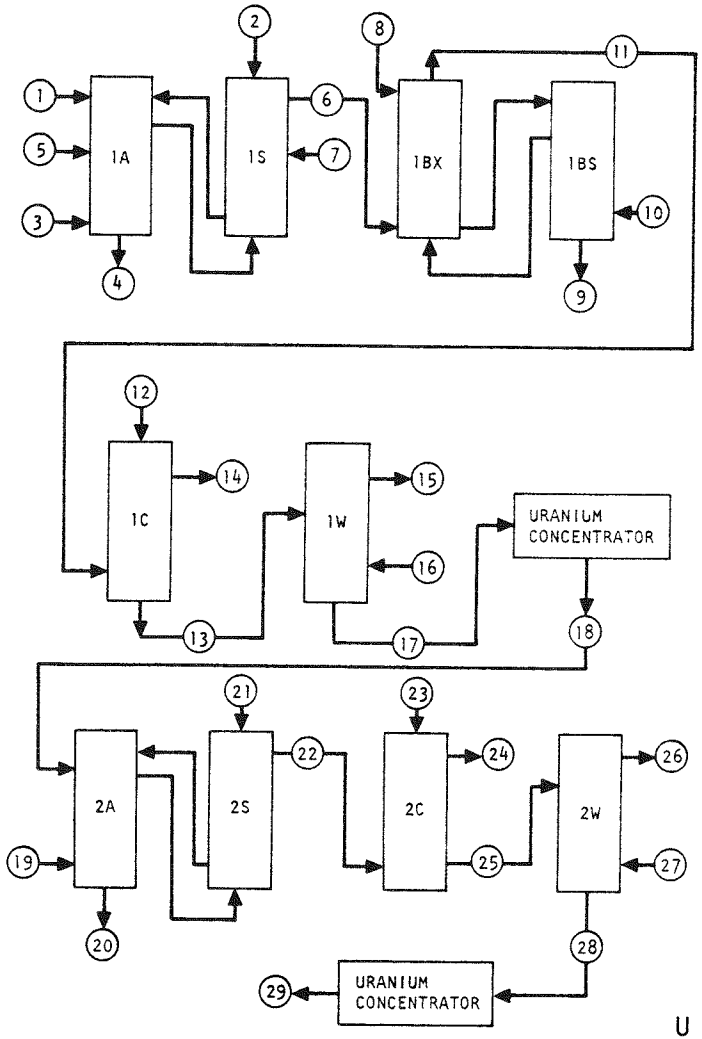

STREAM	STREAM NO.	FLOW (L/DAY)	COMPOSITION U (G/L)	Th (G/L)	HNO_3 (M)
1AF	1	725	14	348	<1.0
1AS	2	754			0.01
1AX	3	7250		(30% TBP)	
1AW	4	1903		(FISSION PRODUCTS)	
1AA	5	234			13.0
1AP	6	7250	1.4	35	
1AIS	7	190			5.0
1BX	8	4350			0.2
1BT	9	4350	Trace	102	
1BS	10	1300		(30% TBP)	
1BU	11	8550	1.19		
1CX	12	4300			0.01
1CU	13	4300	2.37		
1CW	14	8550		(30% TBP)	TO 10
1WS	15	430		(NPH)	SOLVENT WASH
1WW	16	430		(NPH)	
1WU	17	4300	2.37		
2AF	18	43.6	233		
2AX	19	858		(5% TBP)	
2AW	20	294		(WASTE)	
2AS	21	243			2.0
2AP	22	858	11.8		
2CX	23	430			0.01
2CW	24	858		(ORGANIC)	
2CU	25	430	23.6		
2WW	26	43		(NPH)	
2WS	27	43		(NPH)	
2WU	28	430	27.5		
U PRODUCT	29	43.6	233		

Fig. 6-1. Partition flowsheet

TABLE 6-1
ANALYTICAL DATA AND STREAM FLOWS, RUNS 17 AND 18

Stream	Stream No.[a]	Run 17 Th (g/liter)	Run 17 U (g/liter)	Run 17 HNO_3 (M)	Run 17 Flow (ml/min)	Run 17 Relative Flow	Run 18 Th (g/liter)	Run 18 U (g/liter)	Run 18 HNO_3 (M)	Run 18 Flow (ml/min)
1AF	1	370	36	1.1	110	100	369	35.9	1.1	100
1AS	2			1.0	136	123			1.0	126
1AX	3			(30% TBP)	1075	977			(b)	916
1AIS	7			(c)	7	6.4			(c)	8.5
1AA	5			13	25	22.7			13	13.5
1AW	4	0.27	2.8×10^{-4}	2.29			0.87	1.1×10^{-4}	1.74	
1BXF (1AP+1BSU)	1AP-6	36.3	3.87	0.14			44.2	3.77	0.11	
1BX	8			0.24	654	595			0.2	565
1BXT		68.3	0.48	0.48			72.4	0.63	0.45	
1BU	11	0.01[d]	3.44	0.019			0.013	3.24		
1BS	10			(30% TBP)	185	168			(30% TBP)	170
1BT	9	55	3.6×10^{-4}	0.51			56.5	2.2×10^{-3}	0.45	
1BSU	30	30.5	2.15	0.08			30.8	1.88	0.08	
1CX	12			0.01	623	566			0.012	550
1CW	14	4.6×10^{-4}	1×10^{-4}	0.02			8.2×10^{-3}	6.4×10^{-3}	0.02	
1CU	13	0.018	6.53	0.05			0.014	5.9	0.047	
1OS				(e)	123	112			(e)	110
1OW		1.8×10^{-4}	4×10^{-3}				0.061	0.067		
1OO		1.2×10^{-3}	1×10^{-4}	(30% TBP)			9×10^{-4}	2.6×10^{-3}	(30% TBP)	

[a] See Fig. 6-1.

[b] 30% TBP, 0.08 g DBP per liter.

[c] 0.8M aluminum nitrate.

[d] Calculated by material balance.

[e] 0.214M Na_2CO_3.

TABLE 6-2
COLUMN HETS, LOSS, AND FLOODING DATA, RUNS 17 AND 18[a]

Column	Purpose	Volume Velocity (gal/hr/ft^2)	Flooding Frequency (cpm)	Continuous Phase	Aqueous to Organic Ratio	HETS (ft)	Loss (%)		Flooding Frequency (%)	Temp.
							Th	U		
				Run 17						
1A	Extraction	984	137	Organic	0.26	--	0.22	0.002	73	Ambient
1BX	Partition	618	55	Aqueous	0.52	3.1 (Th)	0.03	--	76	Ambient
1BS	Partition-scrub	610	75	Aqueous	3.54	1.9 (U)	--	0.007	∿80	Ambient
1C	Strip	1369	35	Aqueous	0.49	3.3 (U)	--	0.006	80	115°F
1O	Solvent wash	1005	117	Organic	0.10	--	--	--	70	97°F
				Run 18						
1A	Extraction	846	143	Organic	0.27	--	0.61	0.001	75	Ambient
1BX	Partition	533	58	Aqueous	0.52	3.1 (Th)	0.03	--	80	Ambient
1BS	Partition-scrub	534	78	Aqueous	3.32	2.7 (U)	--	0.04	70	Ambient
1C	Strip	1189	55	Aqueous	0.51	3.8 (U)	--	0.10	70	116°F
1O	Solvent wash	869	122	Organic	0.10	--	--	--	76	96°F

[a] Cartridge Descriptions

2-in. extraction column: 1/8-in.-diameter-hole nozzle plates, nozzles down, 23% free area, 2-in. plate spacing, 13-ft extraction section, 9-ft scrub, 1-in. amplitude.

3-in. partition column: 1/8-in.-diameter-hole nozzle plates, nozzles up, 23% free area, 15-ft cartridge, plate spacing - 8-1/2 ft of 4 in., 1-1/2 ft of 3 in., and 5 ft of 2 in., 1-in. amplitude.

2-in. partition-scrub column: 3/16-in.-diameter-hole nozzle plates, nozzles up, 23% free area, 17-ft cartridge, 2-in. plate spacing, 1-in. amplitude.

2-in. strip column: 3/16-in.-diameter-hole nozzle plates, nozzles up, 23% free area, 15-ft cartridge, plate spacing - 8-1/2 ft of 4 in., 1-1/2 ft of 3 in., and 5 ft of 2 in., 1-in. amplitude.

2-in. solvent wash column: 1/8-in.-diameter-hole nozzle plates, nozzles down, 23% free area, 18-ft cartridge, 2-in. plate spacing, 1-in. amplitude.

of fully irradiated HTGR fuel. The DBP concentration in the 1AX stream was 0.08 g/liter.

Run 18 differed operationally from Run 17 primarily in the 1A column. A higher thorium concentration in the 1A column resulted in an exaggerated production of a third phase (second organic phase) in the scrub section. The expected DBP effects in the 1C column did not develop (i.e., visible precipitation of thorium dibutyl phosphate). However, changes in the phase dispersion did indicate organic wetted surfaces in the column probably caused by thin films of thorium dibutyl phosphate deposited on the column internals. Cloudiness in the 1AW stream was noted and could have been related to the presence of DBP in the 1AX stream.

The analyses of the 1BXF and the 1CW streams for DBP indicate that most of the DBP which carried over from the 1A column to the 1C column precipitated there. Less than 20% of the DBP in the 1BXF stream was detected in the 1CW stream (19 ppm in the 1CW stream versus 105 ppm in the 1BXF stream).

Significant thorium losses via the 1AW stream in each run are attributed to the thorium concentration in the 1A column versus any DBP effect. The variation in thorium concentration in the 1A column is indicated by the 1AP stream values. The concentration was 37 g/liter in Run 17 and about 47 g/liter in Run 18.

Uranium losses were at low levels in the 1AW streams in both runs and in the 1BT stream in Run 17. However, in Run 18 higher uranium losses were detected in the 1BT stream. This loss is difficult to explain since all conditions in the column were similar except for a decrease in the aqueous-to-organic ratio. This ratio decrease (an increase in the relative organic flow) would normally be expected to decrease the uranium concentration in the 1BT stream. The relative 1BS column efficiencies may have been affected by the pulse frequencies since the frequency was at 80% of flooding in Run 17 versus 70% in Run 18. The HETS values for the 1BS column also show the lower efficiency of the column during Run 18.

6.2. RUNS 24 AND 25

Runs 24 and 25 consisted of uranium and thorium processing using the basic flowsheet of Runs 17 and 18 (see Section 6.1 and Fig. 6-1) in the five-column system. Runs 24 and 25 were also used to simulate solvent degradation operation of the columns, as in Run 18.

Tables 6-3 and 6-4 show the stream analyses and flow rates for each run. Table 6-5 shows the percent loss data and HETS at the indicated percentage of flooding frequency. The cartridge and column details are included in Table 6-5.

In Run 24, solvent degradation was simulated by the addition of DBP to the 1AX stream. In Run 25, the DBP was added via the 1AIS addition point. The DBP concentration in the 1AX stream in Run 24 was about 0.08 g/liter. In Run 25, the concentration of DBP in the special 1AIS stream was about 25 g of DPB per liter of 30% TBP solvent, which was added at a rate sufficient to give 0.66 g/liter DBP in the 1BXF stream. The 0.08 DBP per liter of solvent is the maximum expected by solvent radiolysis in processing high burnup HTGR fuel. The 0.66 g DBP per liter of solvent were added to decrease the time necessary to observe major effects from the addition of DBP.

The addition of DBP via the 1AX stream at the lower concentration in Run 24 produced no visual effects, except for a slight change in the 1C column phase dispersion. However, the addition of the DBP to the scrub section at the higher concentration in Run 25 induced pronounced dispersion changes in the 1C column. An organic wetted film formed on the plates and walls of the column. A higher pulse frequency was required to maintain efficient phase contact with the organic wetted plates.

No significant changes were noted in the operation of the 1A extraction column. Thorium losses were comparable in both runs.

TABLE 6-3
ANALYTICAL DATA AND STREAM FLOWS, RUN 24

Stream	Stream No.[a]	U (g/liter)	Th (g/liter)	HNO_3 (M)	DBP (ppm)	Flow (ml/min)	Relative Flow
1AF	1	35.9	369	1.1		93	100
1AS	2			1.04		125	134
1AX	3			(30% TBP)	38[b]	947	1018
1AIS	7			(c)		11	12
1AA	5			∿13		23	25
1AW	4	2.3×10^{-4}	2.6×10^{-3}	3.0	3.7		
1BXF (1AP+1BSU)	1AP-6	3.23	33.7	0.14	275		
1BX	8			0.2		567	610
1BXT		0.54	66.6	0.49			
1BU	11	2.88	7.9×10^{-3}	0.012			
1BS	10			(30% TBP)		180	194
1BT	9	7.5×10^{-4}	58.5	0.47			
1BSU	30	1.86	28.3	0.07	780		
1CX	12			0.006		514	553
1CW	14	1.39×10^{-3}	1.1×10^{-3}	0.01	27		
1CU	13	5.98	1.0×10^{-2}	0.035			
1OS				(d)		116	125
1OW		1.8×10^{-2}	<0.01				
1OO		6×10^{-5}	2.6×10^{-4}		2.4		

[a] See Fig. 6-1.

[b] About 0.08 g DBP were added per liter of 1AX.

[c] 0.8M aluminum nitrate.

[d] 0.25M Na_2CO_3.

TABLE 6-4
ANALYTICAL DATA AND STREAM FLOWS, RUN 25

Stream	Stream No.[a]	U (g/liter)	Th (g/liter)	HNO_3 (M)	DBP (ppm)	Flow (ml/min)	Relative Flow
1AF	1	35.3	353.4	1.27		90	100
1AS	2			1.05		117	130
1AX	3			(30% TBP)		932	1036
1AIS	7			(30% TBP)	(b)	29	32
1AA	5			∿13		33	37
1AW	4	2.6×10^{-3}	2.45×10^{-3}	2.5	3.4		
1BXF (1AP+1BSU)	1AP-6	3.15	29.5	0.19	1314		
1BX	8			0.12		671	746
1BXT		0.65	47.3	0.52	16		
1BU	11	2.49	0.249	0.014	978		
1BS	10			(30% TBP)		166	184
1BT	9	2.1×10^{-3}	43.4	0.50	1.4		
1BSU	30	2.67	19.5	0.079	960		
1CX	12			0.012		529	588
1CW	14	3.2×10^{-2}	0.316	0.013	256		
1CU	13	5.08	4.77×10^{-2}	0.046	14		
10S				(c)			
10W		0.248	1.11		1260		
10O		7.1×10^{-3}	6×10^{-2}		5.6		

[a] See Fig. 6-1.

[b] About 25 g of DBP were added per liter of 1AIS solvent.

[c] 0.25M Na_2CO_3.

TABLE 6-5
COLUMN HETS, LOSS, AND FLOODING DATA, RUNS 24 AND 25[a]

Column	Purpose	Volume Velocity (gal/hr/ft^2)	Flooding Frequency (cpm)	Continuous Phase	Aqueous to Organic Ratio	HETS (ft)	Loss (%) Th	Loss (%) U	Flooding Frequency (%)	Temp.
				Run 24						
1A	Extraction	872	142	Organic	0.27	--	2×10^{-3}	2×10^{-3}	78	Ambient
1BX	Partition	547	58	Aqueous	0.50	2.9 (Th)	0.023	--	76	Ambient
1BS	Partition-scrub	543	78	Aqueous	3.15	2 (U)	--	0.012	78	Ambient
1C	Strip	1204	50	Aqueous	0.46	3.9 (U)	--	0.043	80	118°F
1O	Solvent wash	904	120	Organic	0.10	--	--	--	80	99°F
				Run 25						
1A	Extraction	(924)[b] 954	140 140	Organic	(0.26) 0.29	--	(0.05) 0.002	(0.02) 0.02	(80) 80	Ambient
1BX	Partition	(574) 572	57 57	Aqueous	(0.62) 0.61	[3.5 (Th)] 5.0 (Th)	(0.006) 0.84	--	(80) 80	Ambient
1BS	Partition-scrub	(608) 608	86 86	Aqueous	(4.29) 4.04	-- 1.8 (U)	--	0.05	(70) 70	Ambient
1C	Strip	(1196) 1183	50 50	Aqueous	(0.50) 0.48	[4 (U)] 5 (U)	--	(0.02) 1.27	(80) 80[c]	118°F
1O	Solvent wash	(875) 875	122 122	Organic	(0.10) 0.10	--	--	--	(76) 60[d]	90°F

[a] Cartridge Descriptions

2-in. extraction column: 1.8-in.-diameter-hole nozzle plates, nozzles down, 23% free area, 2-in. plate spacing, 13-ft extraction section, 9-ft scrub, 1-in. amplitude.

3-in. partition column: 1/8-in.-diameter-hole nozzle plates, nozzles up, 23% free area, 15-ft cartridge, plate spacing - 8-1/2 ft of 4 in., 1-1/2 ft of 3 in., and 5 ft of 2 in., 1-in. amplitude.

2-in. partition-scrub column: 3/16-in.-diameter-hole nozzle plates, nozzles up, 23% free area, 17-ft cartridge, 2-in. plate spacing, 1-in. amplitude.

2-in. strip column: 3/16-in.-diameter-hole nozzle plates, nozzles up, 23% free area, 15-ft cartridge, plate spacing - 8-1/2 ft of 4 in., 1-1/2 ft of 3 in., and 5 ft of 2 in., 1-in. amplitude.

2-in. solvent wash column: 1/8-in.-diameter-hole nozzle plates, nozzles down, 23% free area, 18-ft cartridge, 2-in. plate spacing, 1-in. amplitude.

[b] Values in parentheses were obtained prior to starting DBP 1AIS flow.

[c] Based on previous run data; visual efficiency was reduced due to presence of DBP.

[d] Frequency reduced to curtail unexpected column flooding at normal flow conditions.

The 1BX thorium partition column was not affected by the DBP additions except for an increase in thorium in the 1BU stream. The parts thorium per million parts of uranium increased in the 1BU stream from (1) 1000 with no DBP added to (2) 2740 with 0.08 g/liter DBP to (3) 100,000 with 0.66 g/liter DBP.

The 1BS column operation and the thorium product purity were unaffected by the DBP additions. The 1BT stream ranged between 7 and 45 parts uranium per million parts of thorium throughout the run series.

The change in the 1C column phase dispersion in Run 25 occurred after about 20 g of DBP had been added to the system, or about 2.2 g of DBP per square foot of 1C column internal surface area. No further change in 1C column operation was noted at the end of Run 25 after 72 g of DBP (8 g per square foot of column internal surface area) had been added to the system. It is anticipated that the column capacity would eventually decrease as the thorium DBP solids build up within the column.

The low acidity in the 1C column lowers thorium dibutyl phosphate solubility, which is responsible for the film formation described above. This film formation causes a significant holdup of the DBP and thorium present in the 1BU stream. However, some thorium and DBP leave the column via the 1CW stream, as indicated by Run 25 analyses.

In Table 6-5, two values are given for the 1C column HETS for Run 25. The value in brackets (4 ft) represents the operation before the DBP addition to the scrub section of the 1A column was started. The increase of the HETS value to 5 ft after the DBP was added may be caused by the column inefficiency and/or the shift in uranium equilibrium distribution. Most of the thorium that reached the sodium carbonate solvent wash (10) column in Run 25 was precipitated as hydroxide, which accumulated at the bottom interface. The 10 column also flooded at normal flow rates and pulse frequency near the end of the run. The flooding may have resulted from a change in the wetting characteristics of the nozzle plates or from

the presence of the thorium hydroxide solids. An increase in the organic overflow rate from the 1C column to the 10 column due to 1C column instability is another likely cause of the 10 column flooding.

The DBP analyses included in Tables 6-3 and 6-4 are considered as an indication of relative versus absolute values, but are very useful in tracing the path of the DBP through the system. Improved analytical methods for DBP are under investigation. From the analyses of Run 25, the path of the DBP is through the 1A and 1BX columns with the solvent. Some thorium is complexed with the DBP, and hence follows the same path as the DBP. This is clearly indicated by the 1BU analyses, which indicates a much higher concentration of thorium despite the increase of the aqueous-to-organic ratio in the 1BX column from Run 24 to Run 25.

In conclusion, the main effects noted to date from the addition of DBP to the acid-Thorex partition cycle is in 1C column instability, precipitation of thorium hydroxide in the 10 column, and an increase of thorium in the uranium product. Of these effects, the increased thorium in the uranium product is less significant since additional thorium separation can be achieved in the final uranium solvent extraction cycles.

The HETS values were obtained from McCabe-Thiele diagrams using the best estimate for equilibrium lines. The HETS is an average number for the length of column used; additional column length will change the HETS value. All HETS values and associated equilibrium data will be re-evaluated with the Thorex SEPHIS code supplied by ORNL when it becomes fully operational and necessary corrections have been made in the program.

6.3. FACILITY ADDITIONS

The installation of the uranium product concentrator for the solvent extraction pilot plant is nearing completion. The installation of the steam generator for use with the concentrator will be made in conjunction with the prototype line expansion.

6.4. BENCH-SCALE INVESTIGATIONS

6.4.1. Volatilization of Soluble Neutron Poisons During Solvent Extraction Feed Adjustment

In a larger HTGR fuel reprocessing plant, it is very likely soluble neutron poisons will be required as a nuclear criticality control measure in the leaching step and perhaps in the feed adjustment step. Therefore, it is essential that the soluble neutron poison not volatilize from the solutions.

Bench-scale tests were undertaken to measure the extent of soluble neutron poison volatilization during the feed adjustment step. The neutron poisons boron and cadmium were studied separately. Cerium was added to the leacher solution to provide a measure of entrainment so that appropriate corrections could be made to the measured soluble poison concentrations in the distillate. Since cerium is chemically similar to gadolinium, another neutron poison, it provided a qualitative measure of gadolinium entrainment. Tests representing both batch and continuous feed adjustment were made.

Table 6-6 summarizes the results of neutron poison volatilization runs for both batch (evaporation to 135°C followed by steam strip) and continuous (continuous steam strip to acid deficiency) operations.

The boron loss was 10% during batch operation and 30% during continuous operation. During the batch run the greatest amount of poison, 8%, was lost during the steam stripping portion with only a 2% loss occurring during evaporation to 135°C. This 2% loss is in agreement with literature (Ref. 6-1), which reported a 2 to 3% boron loss to the distillate during evaporation to 135°C and a 6% loss if the solution was further evaporated to 181°C.

Cadmium was essentially nonvolatilized (<0.1%) during both batch and continuous feed adjustment.

TABLE 6-6
SOLUBLE NEUTRON POISON VOLATILIZED DURING FEED ADJUSTMENT

	Fraction Cerium Entrained[a]	Fraction Volatilized[b]	
		Boron[c]	Cadmium[c]
Batch operation			
During boil-down to 135°C	0.6×10^{-4}	2.4×10^{-2}	0.7×10^{-5}
During steam sparging	0.81×10^{-4}	7.9×10^{-2}	1.5×10^{-5}
Overall	1.4×10^{-4}	10.4×10^{-2}	2.2×10^{-5}
Continuous operation	5.2×10^{-4}	30.5×10^{-2}	8.0×10^{-5}

(a) $\frac{\text{Quantity of Ce in distillate}}{\text{Quantity of Ce in initial feed solution}}$.

(b) $\frac{\text{Quantity of B or Cd in distillate}}{\text{Quantity of B or Cd in initial feed solution}}$ - fraction Ce entrained.

(c) Initial solution: 1M Th, 0.1M Ce, 0.2M B (or 0.2M Cd), 0.1M Al, 0.05M F, 8 to 9M HNO_3.

These results indicate boron is not an acceptable soluble neutron poison, but either cadmium or gadolinium are potentially acceptable.

HTGR fuel contains B_4C particles as a burnable poison. Should these particles dissolve during the leaching step, an appreciable fraction of the dissolved boron would be volatilized during feed adjustment and perhaps in the subsequent processing steps of waste concentration and waste calcination. The path of boron through the various processing steps needs to be established.

6.4.2. Investigation of Continuous Solvent Extraction Feed Adjustment

Continuous feed adjustment appears to offer the potential of lower capital and operating costs in a commercial-scale reprocessing facility. In order to demonstrate if acid deficiency could be achieved on a continuous operational basis, bench-scale tests were made to adjust the feed rate, steam rate, and evaporation rate in order to overcome the inefficiency at low acidity of the steam stripping process (Ref. 6-2). The following operating criteria were established:

1. The boiler solution temperature during the entire process was to be maintained at 135°C for a given evaporation rate. Too high a steam rate or feed rate would cause the temperature to drop. Maintaining the boiler temperature at 135°C would theoretically ensure that the acidity of each feed drop would be immediately reduced to 1M or less because of the nitric acid vapor pressure under these conditions.

2. The average feed residence time (defined as the volume of boiler solution/feed rate) would be greater than the average batch residence time necessary to achieve acid deficiency. The average batch residence time is defined as the volume of boiler solution divided by the rate of stripping from 135°C to acid deficiency on a batch basis, with the rate of stripping being the time required to collect 167% of the boiled down solution in the

distillate for a given steam and evaporation rate. This standard served to ensure that the feed would, on the average, be exposed to the stripping steam for a time equivalent to that which would be required to strip to acid deficiency on a batch basis. In most cases the feed rate was set as low as possible to ensure maximum residence time and always to give an average feed residence time greater than the average batch residence time.

It was felt that by working within these two criteria, the efficiency could be improved at least to a point where acid deficiency could be demonstrated.

However, as Table 6-7 illustrates, the feed rate, steam rate, and evaporation rate had little effect on improving the approach to acid deficiency on a continuous basis. Basically, the steam and evaporation rate were set as high as possible with the feed rate being the principle variable, in accordance with the above criteria. There was no definitive effect on the acidity even though the average feed residence time, a function of the feed rate, varied over a wide range. This would imply that there is little that can be done to improve the efficiency of the stripping process. Nevertheless, continuous feed adjustment did produce acidity levels that were 0.5M or less. These results indicate design and operation of a continuous feed adjustment step will require either higher temperatures or a multistage design to achieve acid deficiency.

Further runs (Table 6-8) also verified that when the feed flow was terminated during continuous operation and the stripping allowed to proceed until 167% of the boiler solution had been collected in the distillate before product removal, the product solution was acid deficient. An amount less than 167% could probably be collected; however, no attempt was made to define this amount.

Continuous feed adjustment could be applied to a flowsheet employing two feed adjustment points (to avoid Zr precipitation) where a low acid feed, on the order of 1M, is desired for the initial adjustment. This

TABLE 6-7
SUMMARY OF FEED ADJUSTMENT RUNS 1 THROUGH 8

Run No.	Continuous Feed Adjustment Conditions for 1M Th/Thorex Solutions		Free Acid Concentration of Product (M) Randomly Sampled During the Course of a Run			Average Feed Residence Time[a] (min)	Average Batch Residence Time[b] (min)	Evaporation Rate (determined during initial batch feed adjustment) (ml/min)
	Steam Rate (ml/min)	Feed Rate (ml/min)						
1	6.2	7.1	0.18	0.28	--	4.2	2.4	7.8
2	4.1	5.0	0.05	0.10	0.23	4.0	3.3	5.0
3	4.1	3.3	0.14	0.30	0.20	9.1	3.3	5.0
4	4.1	2.1	0.16	0.11	--	14	3.3	5.0
5	4.1	1.2	0.23	0.16	0.32	25	3.3	5.0
6	4.1	1.2	0.14	0.36	--	25	5.7	1.2
7	4.1	0.37	0.31	--	--	81	5.7	1.2
8	2.0	0.37	0.51	0.30	--	81	9.4	1.2

[a] Volume of boiler solution (30 ml)/feed rate).

[b] In steam stripping from 135°C to acid deficiency on a batch basis, 50 ml was collected in the distillate. The time required to collect this amount determined the rate of stripping, and this rate divided into the volume of the boiler solution (30 ml) determined the average batch residence time. The feed rate was always set to give an average feed residence time greater than the average batch residence time.

TABLE 6-8
FREE ACID CONCENTRATION IN
FEED ADJUSTMENT RUNS 4 AND 7

Run No.	Free Acid Concentration of Product Under Semi-Continuous Operation (M)[a]
4	-0.13
7	-0.06

[a] Semicontinuous conditions: Feed flow terminated and 167% (50 ml) of the boiler solution allowed to collect in the distillate before sample collection. Negative sign indicates an acid deficient condition.

would be followed after a codecontamination solvent extraction cycle by adjustment of the feed to acid deficiency on a batch or semicontinuous basis for further processing. Care should be taken, however, to further define the extent of acid adjustment during continuous operation since Zr precipitation begins around 0.6M free acid.

REFERENCES

6-1. Moore, J. G., and R. H. Rainey, Nucl. Sci. Eng. 11, 278 (1961).

6-2. Bradley, R. F., and C. B. Goodlett, "Denitration of Nitric Acid Solutions by Formic Acid," USAEC Report DP-1299, Savannah River Laboratory, June 1972.

7. SYSTEMS DESIGN

7.1. PROTOTYPE SIZE REDUCTION SYSTEM

Detail drawings are being generated from the conceptual assembly drawing (see Fig. 2-1, Section 2) as presented and approved by ACC Idaho in a joint meeting with GA, ERDA, ACC, and the Ralph M. Parsons Co. on January 16, 1975. Final design layouts are in progress for the primary crusher jaw and cheek plates. Detail study is being made of the pitman jaw motion cycles for analysis of interface considerations. The UNIFRAME structure is being designed to accommodate a 40-in. roll crusher with a modified unit support frame. All components of the UNIFRAME assembly will be designed so that a simulated remote hot cell condition can be demonstrated. Conceptual designs of the remote handling fixtures for the crusher system are presented in Figs. 7-1 through 7-5. Detailed engineering design and fabrication of these fixtures will be performed during fiscal year 1976.

7.2. PROTOTYPE PRIMARY BURNER

Final remote installation and removal concepts are being incorporated in burner design. Drawings for the heating-cooling system and vessel assembly were completed and transmitted to ACC Idaho for review and to Purchasing for selection of vendors.

Layouts are being finalized and detail drawings are under way on the dolly system for the primary burner spool, core, and plenum (see semiremote removal assembly, Fig. 7-6). Design for remote removal of the shrouding is under way.

The electromechanical interlocking schematic diagram and operational description were prepared for the primary burner.

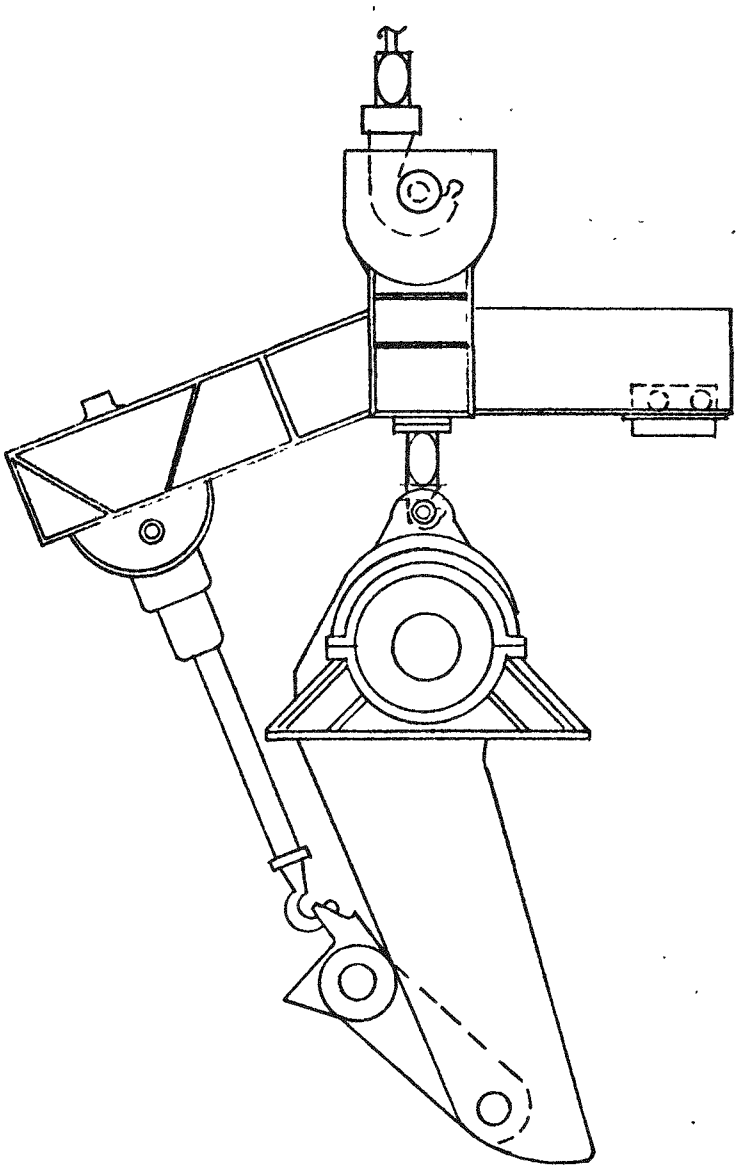

Fig. 7-1. Lift fixture for bottom movable jaw assembly

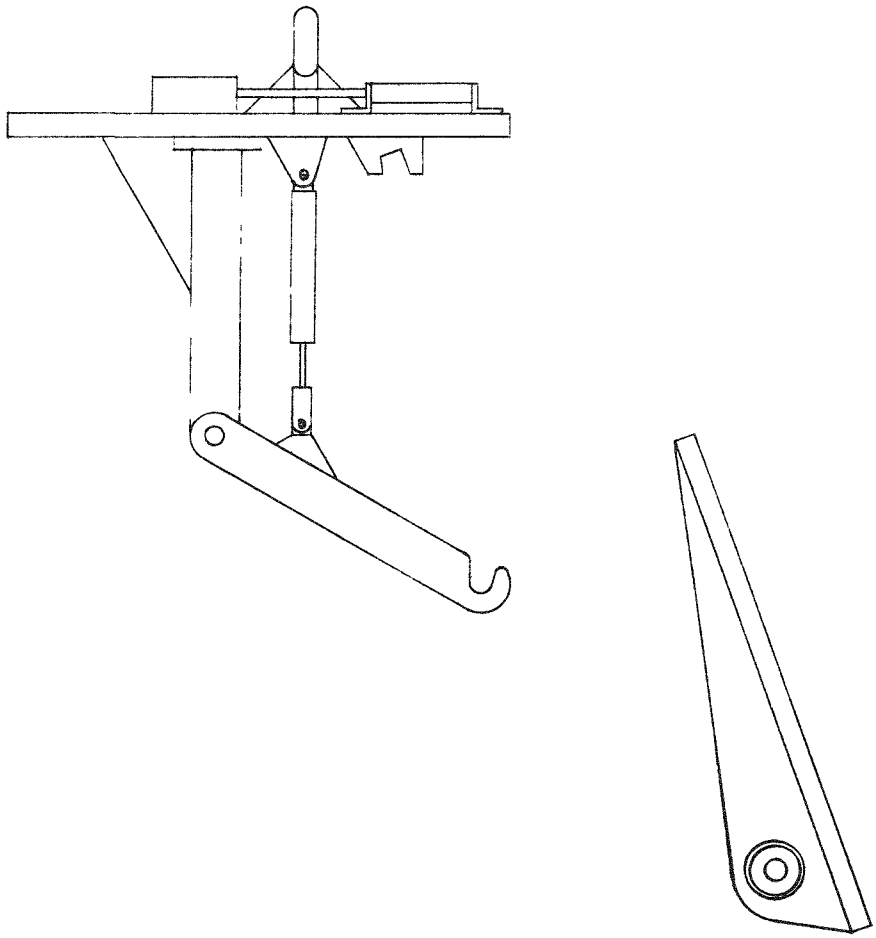

Fig. 7-2. Lift fixture for top stationary jaw

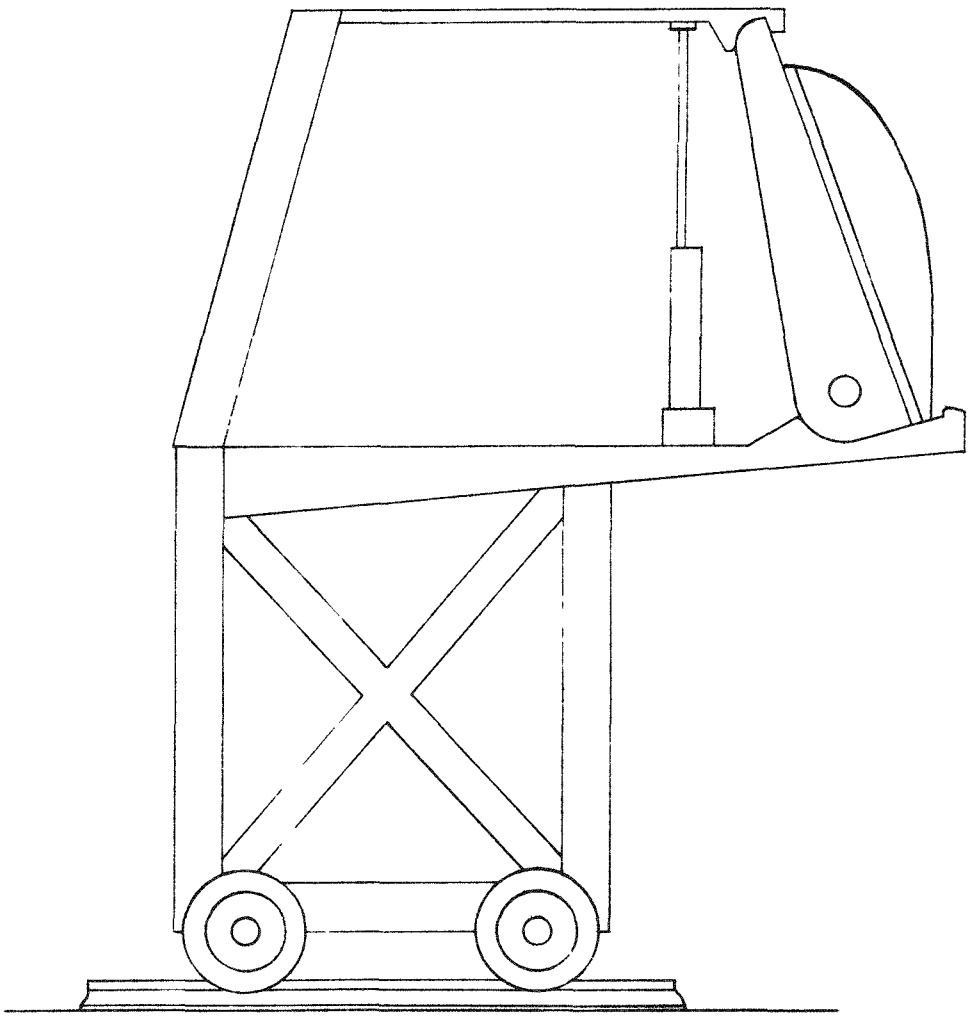

Fig. 7-3. Horizontal lift fixture for stationary jaw

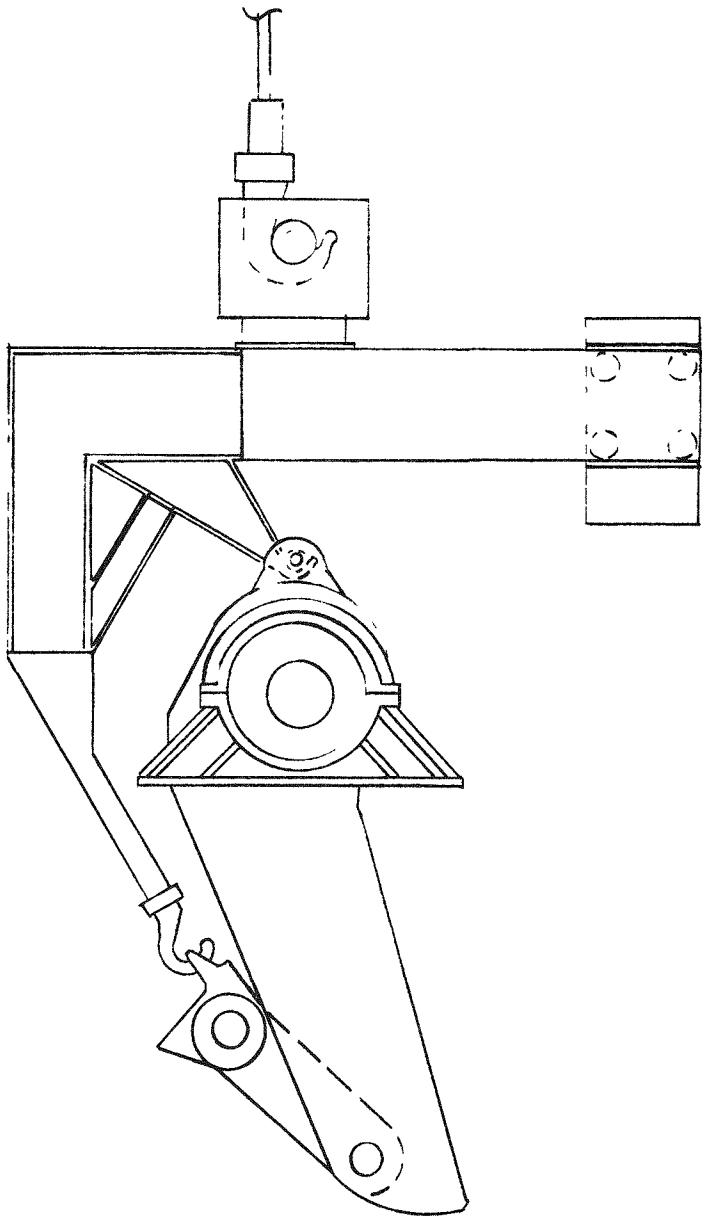

Fig. 7.4. Lift fixture for top movable jaw assembly

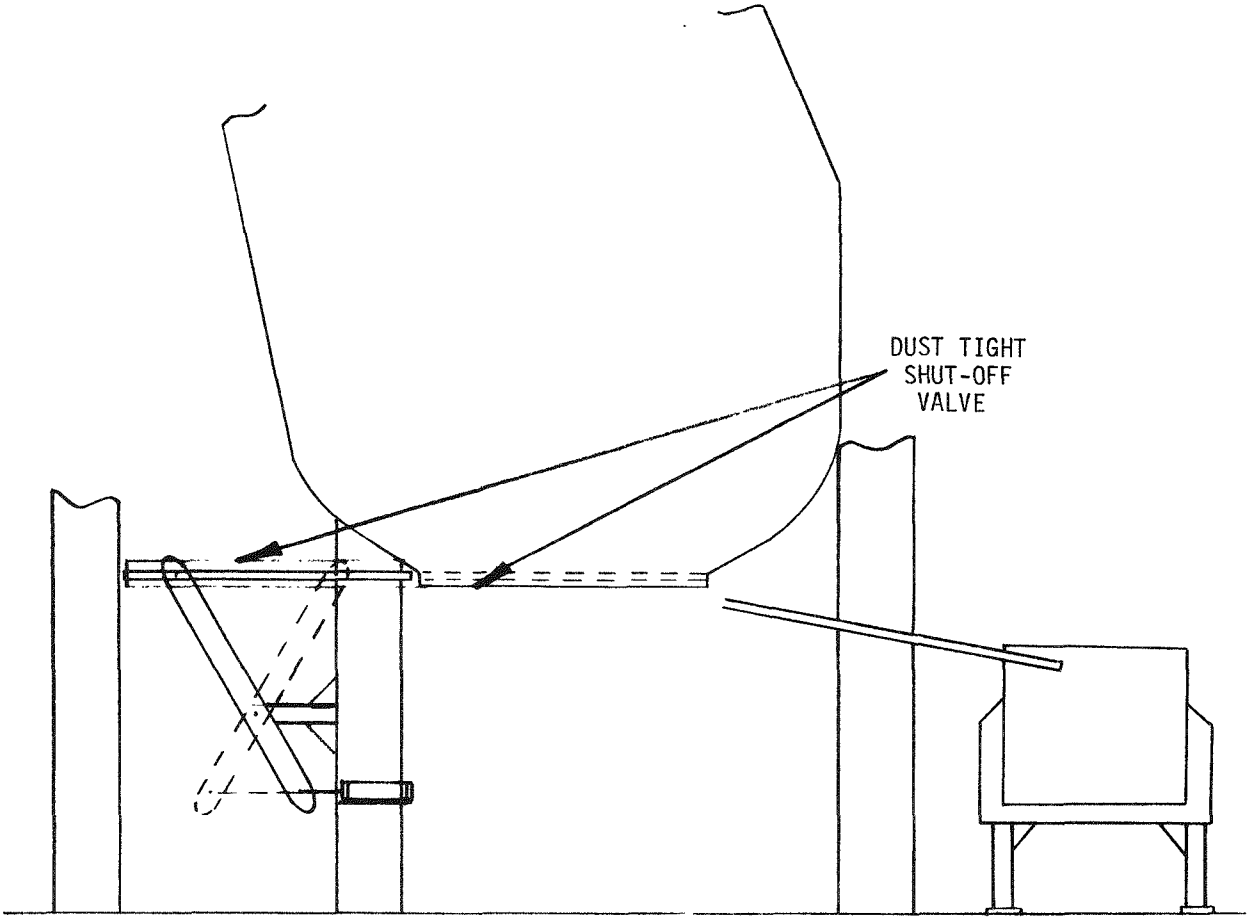

Fig. 7-5. Crusher shroud shut-off valve

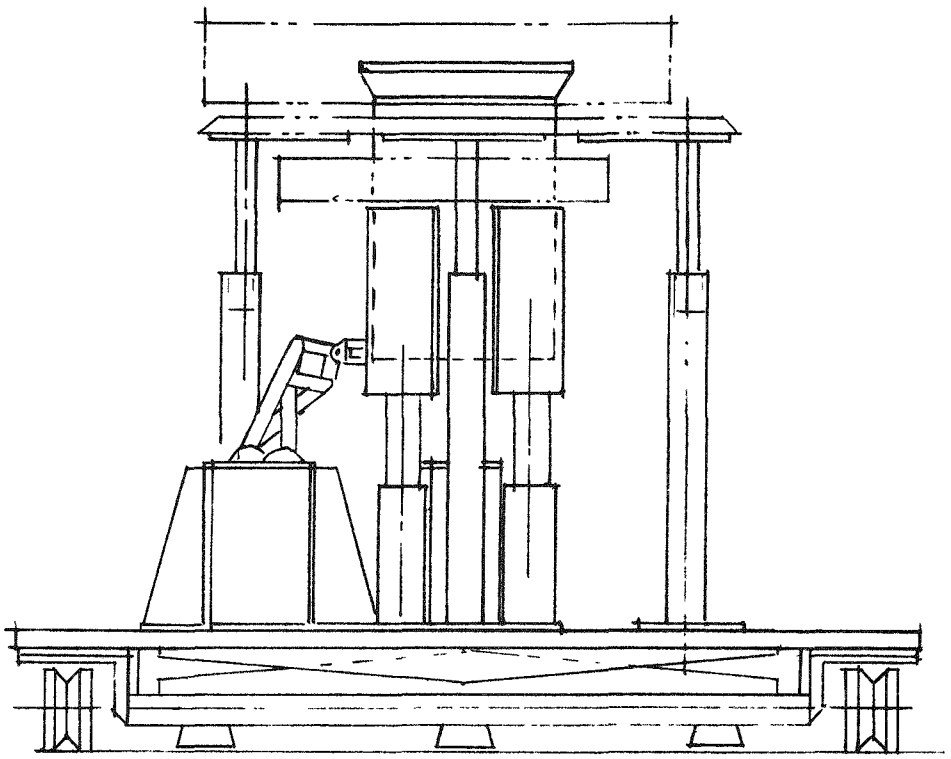

Fig. 7-6. Semiremote removal assembly

Conceptual designs of remote handling tools for the prototype burner system are illustrated in Figs. 7-7 through 7-10. Engineering design and fabrication of these components will be completed in fiscal year 1976.

7.3. PROTOTYPE SECONDARY BURNER

Remote installation and removal concepts are being incorporated in the secondary burner design. Detail drawings of the heating-cooling shroud, the bottom shroud, and the distributor plate and for product removal were completed and issued for review. An electromechanical interlocking schematic diagram and operating description have been completed for the secondary burner. Remote fixtures (Figs. 7-7, 7-11, and 7-12) were approved for engineering design and fabrication in fiscal year 1976.

7.4. PROTOTYPE PLANT SYSTEMS, GENERAL

Construction of the prototype line control room complex and adjacent platform extensions is complete. Control consoles are in place in the new control room and are ready for installation of instrumentation (Fig. 7-13).

The building space previously occupied by TRIGA Fuel Manufacturing was released to the Recycle Development Department on April 14. This area is the site for the crusher, primary burner, and secondary burner. Ground was broken on April 26 for the foundations for these units. The foundation for the burner support platform is complete; the foundation for the crusher is formed and ready for pouring, awaiting determination of anchor bolt arrangement. Figures 7-14 and 7-15 illustrate progress in construction during the quarter.

Construction of the support platform for the vent systems, along the east side of the east bay above the mezzanine floor level, is complete. All ventilation system components are on order.

Installation of three additional roof vents in the high-bay area is complete.

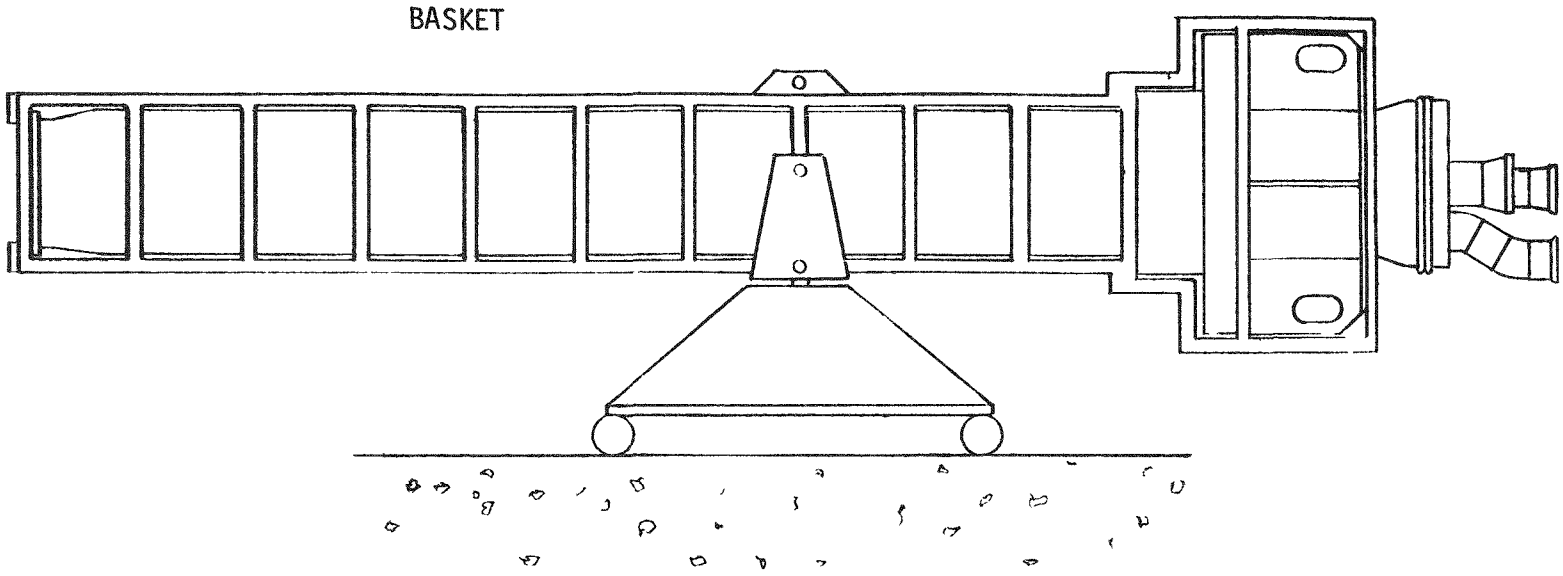

Fig. 7-7. Eight-inch and primary burner trunion fixture with baskets

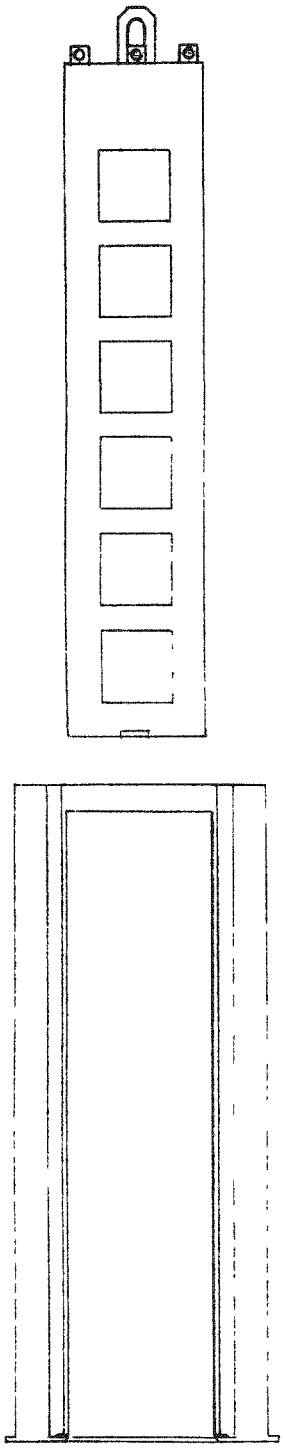

Fig. 7-8. Susceptor and ceramic removal fixture for primary burner

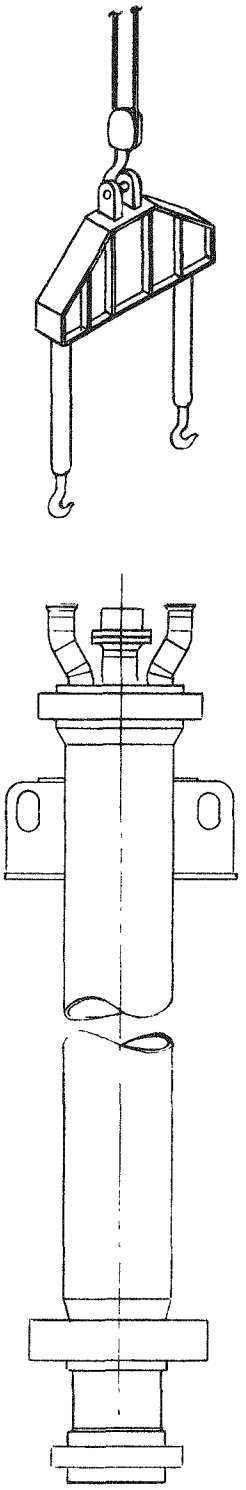

Fig. 7-9. Lift fixtures for primary burner

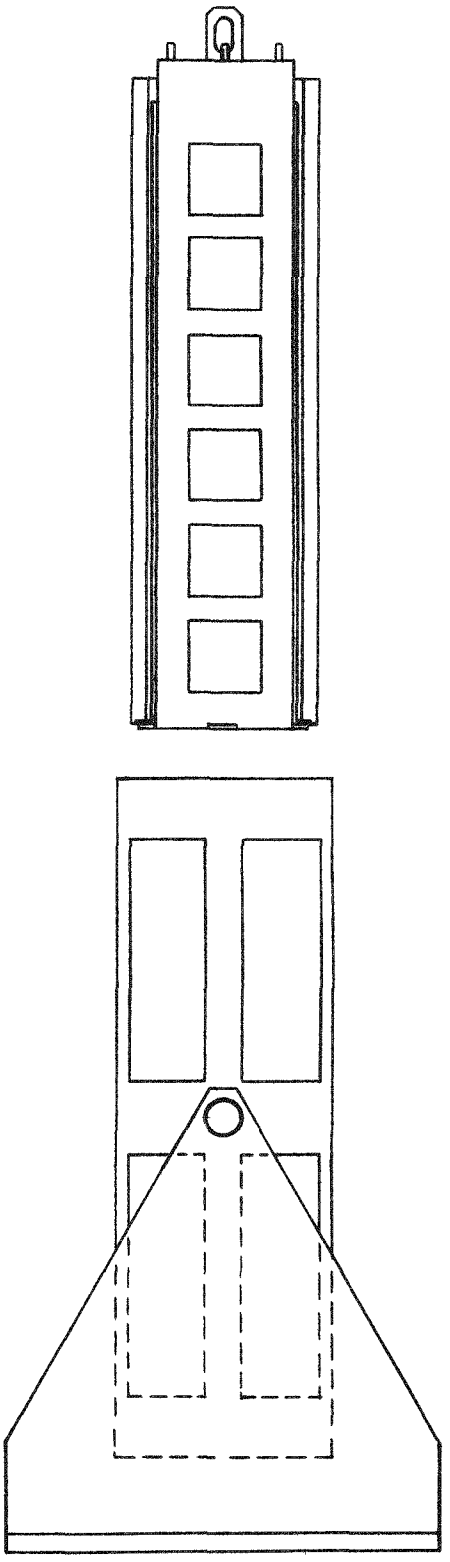

Fig. 7-10. Susceptor and ceramic trunion and holding fixtures for primary burner

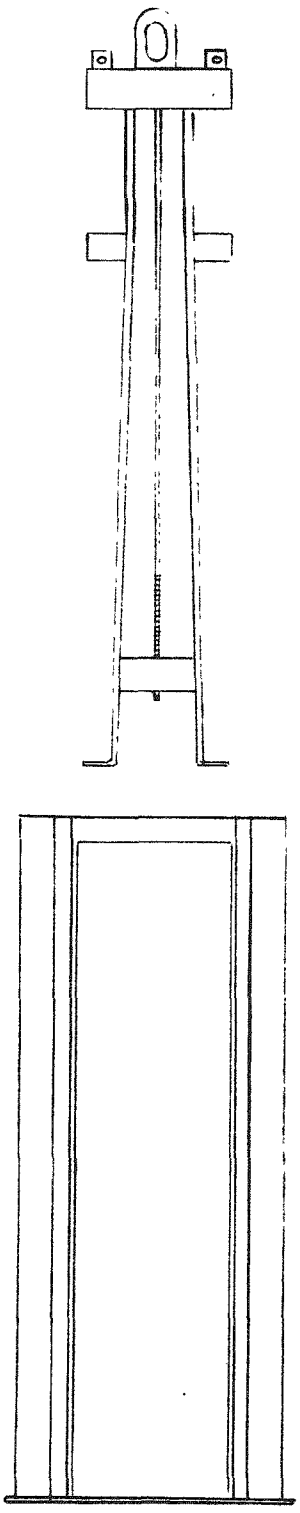

Fig. 7-11. Susceptor and ceramic removal fixture for 8-in. burner

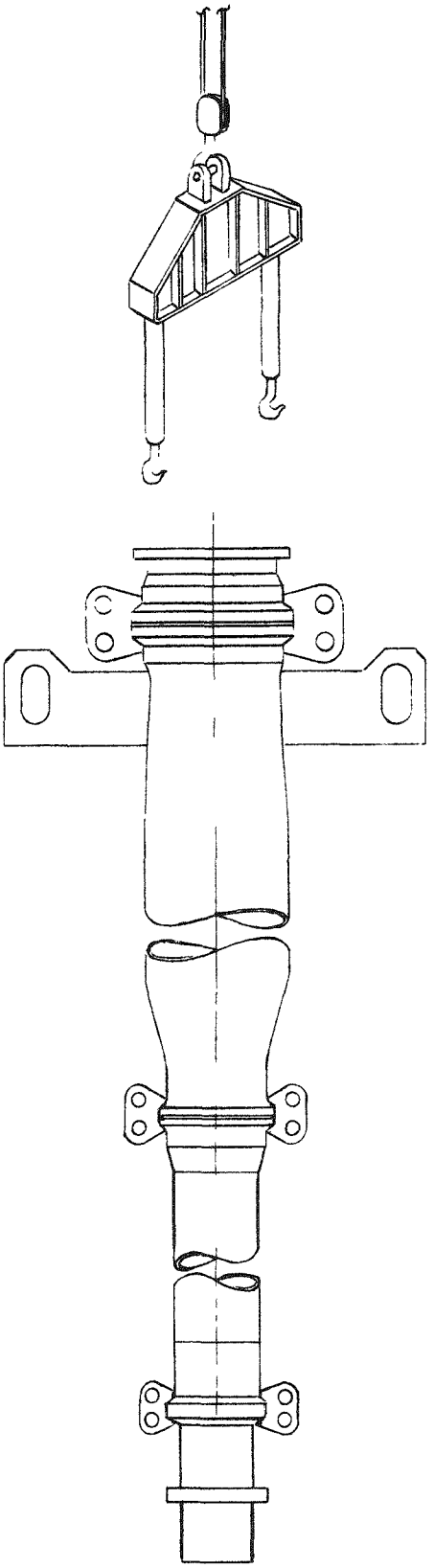

Fig. 7-12. Lift fixtures for 8-in. burner

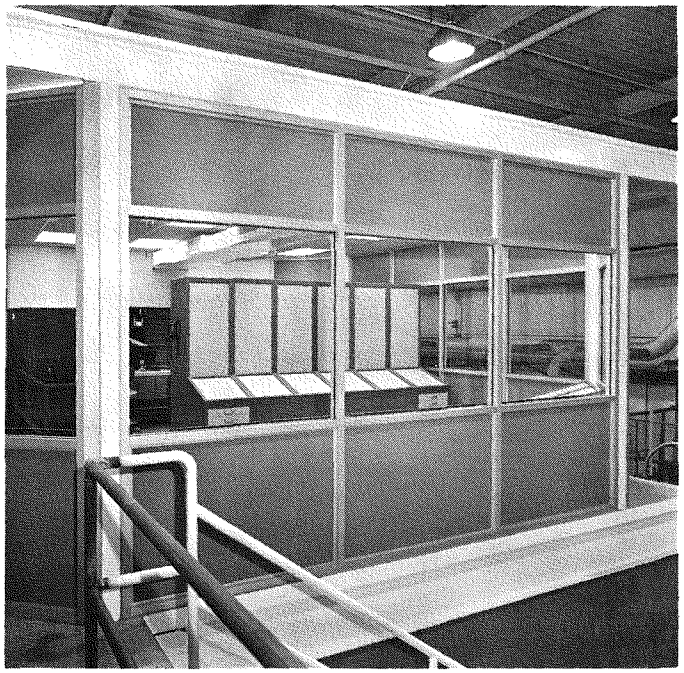

75FR1873

75FR1870

Fig. 7-13. Prototype pilot plant control room

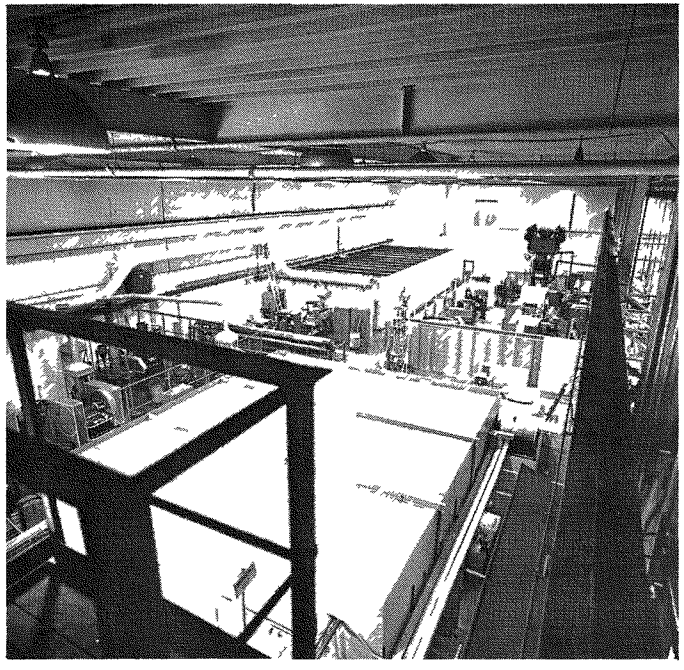

75S949 (a)

75S958 (b)

Fig. 7-14. E-Building prior to pilot plant construction: (a) north view and (b) south view

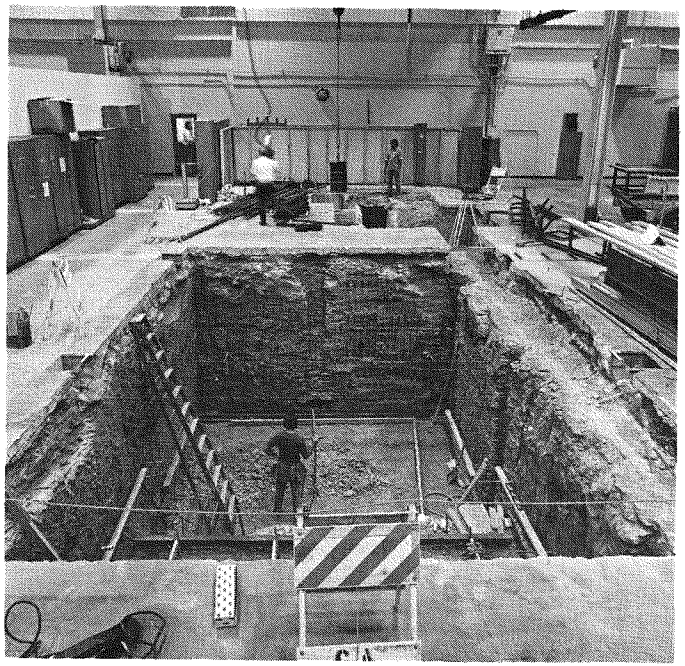

75S1636 (a)

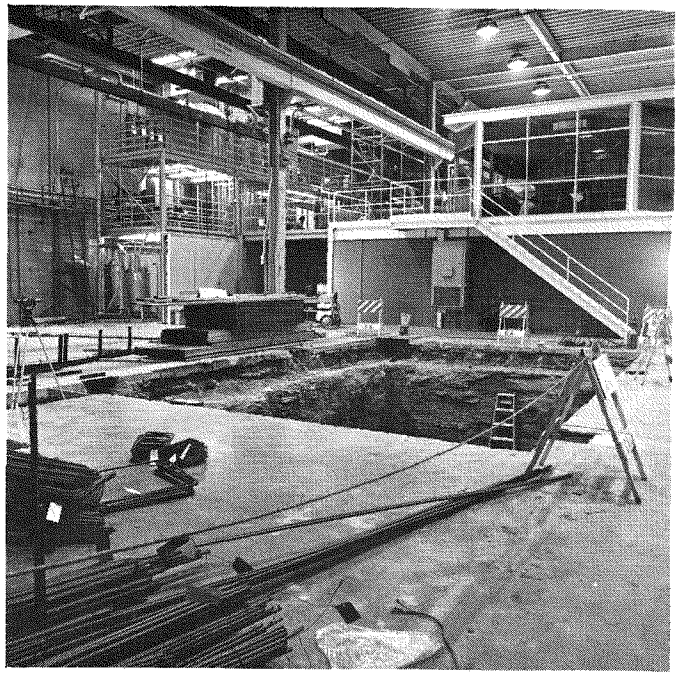

75S1637 (b)

Fig. 7-15. Excavation of prototype pilot plant: (a) north view and (b) south view

Extension of the 1-ton crane runway northward to the end of building is complete.

Design of an automatic-stop control system for the 20-ton crane is in process.

The facilities plan for the E-Building Reprocessing Development Program was distributed for comment to ERDA headquarters and site offices and to other contractors in the Thorium Utilization Program.

An isometric drawing of the reprocessing facility, including those items now planned in the crusher-burner prototype, were completed as shown in Fig. 7-16.

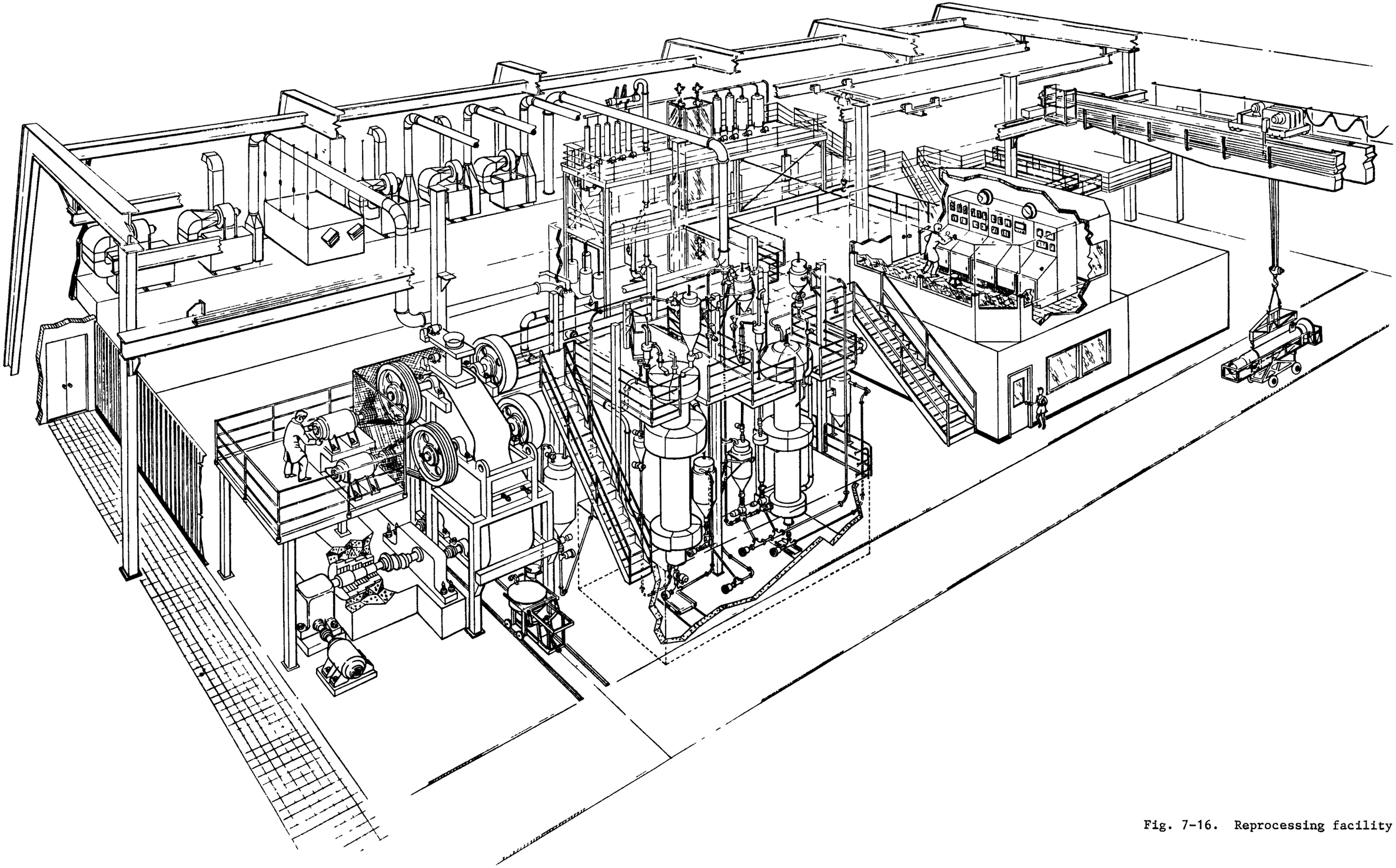

Fig. 7-16. Reprocessing facility

8. ALTERNATIVE HEAD-END REPROCESSING

The published literature as well as internal reports have been surveyed as a prelude to preparing a program for further study of alternative head-end reprocessing. The various alternative head-end processes described in the literature have been assessed by comparison with the reference process. Many mechanical, chemical, and electrochemical methods of disintegrating the spent fuel element have been described, and all but a few have serious shortcomings. There are two which appear to merit further process and economic evaluation; one is pressing of fuel rods from fuel element sections and the other is the disintegration of the fuel element with potassium.

Elements of a program to investigate these two approaches have been identified as:

1. Separation of fuel and graphite - preliminary process and economic evaluation.

    a. Pressing fuel rods from fuel element sections.

    b. Disintegration of fuel element with potassium.

2. Disposal of graphite - preliminary process and economic evaluation of burning separated chunk graphite from item 2b in a fuel-bed type boiler.

As an initial step in the above program, a preliminary process flow diagram with heat and material balances and approximate equipment sizes has been prepared for the disintegration of the spent fuel element with potassium.

9. CONCEPTUAL DESIGN OF AN HTGR FUEL TARGET RECYCLE PLANT

9.1. CONCEPTUAL DESIGN STUDY OF TARGET RECYCLE PLANT

A report covering the conceptual design study of a commercial-scale recycle plant for HTGR fuel has been issued. The design study, summarized in Ref. 9-1, was carried out by General Atomic in conjunction with the Ralph M. Parsons Company. The report includes summary design descriptions and supporting process flow diagrams and material balance data for the major process systems of an integrated recycle facility for reprocessing, waste processing, and refabrication of HTGR fuel. Design descriptions of support systems and architectural plans and sections covering all major systems of the integrated facility are also included in the report. Design qualifications and design technical areas of concern for a commercial-scale recycle plant are discussed.

9.2. TECHNICAL EVALUATION OF RESIN LOADING PROCESSES

An evaluation was carried out to compare the uranium loading of resins by the ammonium and amine processes. Preliminary studies indicate that a two-stage resin loading technique using the NH_4^+ form by the C-464 resin could be adapted to previously planned process requirements for the TURF demonstration at HNL. The studies further indicate that this process can provide about 30% savings in capital cost and space requirements over the current reference WAR (H^+) approach. However, the larger volume requirement for the NH_4^+ form of the resin could result in a minor economic penalty when this resin is used in the WAR (NH_4^+) process. A change in the WAR (H^+) reference resin loading technique would not require a major redesign effort; modifications would merely involve the removal or resizing of some equipment items and the rerouting of some plumbing lines.

9.3. PARTICIPATION IN ERDA THORIUM UTILIZATION PROGRAM TASK FORCE

General Atomic participated in an ERDA Task Force which evaluated and developed a detailed Summary Program Plan and estimate for an Alternate Program for HTGR Fuel Recycle. The proposed program includes development of HTGR fuel recycle technology, operation of cold and hot pilot facilities, and the design, construction, and operation of an intermediate-sized HTGR Recycle Facility (HRF) having a reprocessing capability for 20,000 spent fuel elements per year, along with a refabrication capability for 10,000 fuel elements per year.

9.4. REVIEW OF ALTERNATE HTGR RECYCLE FACILITY CONCEPTS

In support of further evaluation of technical and programmatic options for an intermediate-sized HTGR Recycle Facility (HRF), GA is participating with HNL in a review of alternate design concepts for a fuel recycle plant. plant.

REFERENCE

9-1. Jackson, D., "Conceptual Design Summary and Design Qualifications for HTGR Target Recycle Plant," ERDA Report GA-A13365, General Atomic Company, May 1975.